Horizon 2020

Project acronym:	**LASH FIRE**
Project full title:	**Legislative Assessment for Safety Hazard of Fire and Innovations in Ro-ro ship Environment**
Grant Agreement No:	**814975**
Coordinator:	**RISE Research Institutes of Sweden**

Deliverable D04.3

Simulation tool for consequence quantification

April 2022

Dissemination level: **Public**

Abstract

To address the lack of historical data, a simulation tool (hereafter referred to as STCQ) has been developed to quantify the consequences of ro-ro shipboard fires to people, ship, and cargo. The consequences of fires (except human consequences) will be converted into monetary units, which in turn will be used, as far as possible, as input data of the risk model to provide societal costs for different ro-ro space fire scenarios.

STCQ is the combination of three upgraded models:

- A CFD model, here the model SAFIR, to assess the fire consequences in the ro-ro space where the fire started, as well as in the other ro-ro spaces, embarkation stations, rescue stations and disembarkation routes out of the ship. More precisely, this involves evaluating the times after which given thresholds are exceeded. Heat and smoke detection times are also provided;
- A probabilistic network model to assess the consequences of fire and smoke in the accommodation spaces. The model estimates the level of damage by indicating the fire status (i.e., ignition, flashover, fully developed fire phase, or decay phase) and the position of the smoke interface over time in each accommodation compartment; and
- An evacuation model to evaluate fire consequences to persons on board.

This report briefly presents the numerical tools used and their extension to ro-ro ships, then the numerical results obtained by the STCQ for some selected worst credible scenarios over a duration of one hour of fire (the calculation time being too long to consider simulating all possible fire scenarios over 3 h of fire). Simulations of fire originating from closed and open ro-ro spaces, as well as on the weather decks of two generic ro-ro ships, namely the Stena Flavia and the Magnolia Seaways, have been performed by varying the location of the fire source and wind conditions (i.e., no wind and headwind). It was assumed that no firefighting action was taken and that the load capacity of vehicles in ro-ro spaces was 100%. Other scenarios have been added to study the influence on the fire consequences of accidental situations such as a loss of integrity of the insulation system, a loss of containment of the fire origin ro-ro space. Finally, simulations of evacuation (i.e., for both assembly and abandonment phases) during the selected fire scenarios have been performed.
Simulation results for two fire scenarios on the Stena Flavia are detailed and discussed.

To ensure consistency and ease of use of the expected results in the risk model, the results obtained for all selected fire scenarios are presented in the form of files indicating the times, or periods of time, when given thresholds, related to heat and smoke detection, safety of persons on board, and integrity of the ship's structure, cargo, and other targets, are exceeded, and compared with evacuation times (where relevant).

This project has received funding from the European Union's Horizon 2020 research and innovation programme under grant agreement No 814975

Document data

Document Title:	D04.3 – Simulation tool for consequence quantification		
Work Package:	WP04 – Formal Safety Assessment		
Related Task(s):	T04.5		
Dissemination level:	Public		
Deliverable type	R, Report		
Lead beneficiary:	21 – RS2N		
Responsible author:	Bernard Porterie		
Co-authors:	Yannick Pizzo		
Date of delivery:	2022-04-20		
References:			
Approved by[1]	Eric De Carvalho on 2022-04-04	Stina Andersson on 2022-04-19	Maria Hjohlman on 2022-04-14

Involved partners

No.	Short name	Full name of Partner	Name and contact info of persons involved
21	RS2N	SARL RS2N	Bernard Porterie - bernard.porterie@rs2n.eu Yannick Pizzo - yannick.pizzo@rs2n.eu
18	LUL	Universite de Lorraine	Anthony Collin - anthony.collin@univ-lorraine.fr

Document history

Version	Date	Prepared by	Description
01	2020-05-13	B. Porterie	Draft of structure
02	2021-11-10	B. Porterie	Draft of final report, circulated to reviewers
03	2022-01-18	A. Collin	Integration of the evacuation part in the report
04	2022-03-30	B. Porterie	Final report, circulated to reviewers
05	2022-04-20	B. Porterie	Final report

[1] Disclaimer: this approval is in the context of the quality management of LASH FIRE project and does not constitute any approval or review of the software in regards with the IMO regulations.

Contents

1 Executive summary

1.1 Problem definition

The problem to be solved is to estimate the consequences to people, cargo, and ship of fires originating from ro-ro spaces.
To do this, several challenges must be overcome:

- Develop a simulation tool capable of providing consistent and useful data to feed the risk model developed in WP04, and then to compute the societal costs associated with fire scenarios, after converting the consequences of fires (except for humans) into monetary costs (WP05 Life Cycle Cost (LCC) tool);
- Select a limited number of relevant fire scenarios. Due to the long computation times, fire scenarios corresponding to all branches of the risk model cannot be simulated;
- Identify critical fire scenarios; and
- Assess the impact of fire on the evacuation for the assembly and abandonment phases, depending on whether the persons on board are moving from their actual position to the assembly stations (AS) or from the AS to the embarkation stations and the location of the life-saving appliances (both grouped hereafter under the name of LSA).

1.2 Technical approach

Due to the lack of historical data, numerical simulations of fires in ro-ro spaces, as well as their consequences in the other spaces of the ro-ro ship (i.e., other ro-ro spaces, accommodations, embarkation stations, rescue stations, and disembarkation routes) were performed using a simulation tool for consequence quantification (STCQ) combining three upgraded models: a CFD (Computational Fluid Dynamics)-based model and a network model to simulate fire development and smoke transport in ro-ro spaces and accommodations respectively, and an evacuation model to assess life consequences.

For fire scenarios, partners involved in Action 4-A and ship operators have selected a limited number of accident scenarios to be modelled during a specific workshop. Accordingly, and based on the feedback from the FIRESAFE studies, priority was given to simulating severe fire scenarios (assuming no firefighting action and a 100% vehicle load in ro-ro spaces), which will challenge the fire containment from ro-ro spaces and then the evacuation. The fire scenarios were defined by varying the location of the fire source and wind conditions for two generic ro-ro ships, namely the Stena Flavia and the Magnolia Seaways (DFDS). Other scenarios have been added to study the influence on the fire consequences of accidental situations such as a loss of integrity of the insulation system, a loss of containment of the fire origin ro-ro space. Finally, evacuation scenarios (i.e., for both assembly and abandonment phases) were modelled.

To ensure consistency and ease of use of the expected results in the risk model, these results are presented in the form of files giving the times, or periods of time, when given thresholds, related to heat and smoke detection, safety of persons on board and the integrity of the ship's structure, cargo, and other targets, are exceeded, and compared with evacuation times (where relevant).

1.3 Results and achievements

For the selected fire scenarios of the Stena Flavia (generic ro-ro passenger ship) and Magnolia Seaways (generic ro-ro cargo ship), the simulation results provide data to feed the risk model, in the form of directly usable summary files (i.e., Excel or Word files).

It was found that the consequences of a fire on the cargo and structure of the ship are most severe when the fire originates in an open ro-ro space, as the oxygenation conditions of the fire are favourable to the ignition of all the cargo (here, vehicles) and potential targets, with significant thermal stresses on the hull. When the fire starts in a closed ro-ro space, the consequences are less

severe because of the under-oxygenation of the fire. This is also true for weather decks, but here because of the low level of containment which favours the escape of hot gases to the environment, limiting the heat flux to the cargo and the structure.

For the selected fire scenarios, fire consequences on humans increase with the level of confinement of the ro-ro space, due to smoke accumulation (closed ro-ro space) or external flame/smoke escape through openings (open ro-ro spaces). They were evaluated in the ro-ro spaces, embarkation stations, rescue stations, and disembarkation routes, as well as around the first truck on fire to estimate the available time for safe first response.

For all scenarios, the conventional smoke detectors detected the fire the fastest.

For fires in open ro-ro spaces, the predicted timelines were found to be qualitatively consistent with those extracted from the available accident investigation reports, whereas the predicted consequences of a fire started in a closed ro-ro space were underestimated. The simulation conditions (e.g., no mechanical ventilation, high level of confinement, no loss of integrity of the thermal insulation system, or steady environmental conditions) may explain the observed differences. It should be noted that the study of the influence of mechanical ventilation is out of the scope of WP04 and is addressed in WP11.

The results on the evacuation process show that the times required for the assembly phases are less than or equal to the propagation time of a major fire, limiting the risk of fatalities. For the abandonment phase, the results show that, in several scenarios, the thermal constraints at the location of LSA and along the disembarkation routes are too high to allow all passengers or crew members to safely leave the ship. Nevertheless, these consequences could be significantly reduced by emergency response procedures already implemented by ship operators (such as firefigthing, boundary cooling, etc.) or by external intervention (fire rescue team, tug boat, or helicopter).

Most of selected fire scenarios may be considered as worst credible scenarios since all the cargo in the ro-ro space where the fire broke out has burned, without any means of firefighting having been engaged. Lesser consequences of fire are expected if firefighting action is taken. Moreover, calculations of fire consequences were also very conservative due to the assumption of a 100% load capacity of vehicles in ro-ro spaces.

1.4 Contribution to LASH FIRE objectives

This deliverable contributes to the following WP04 objectives:

- To develop a simulation tool to determine the consequences of fires originating in ro-ro spaces;
- To provide consistent and usable risk model inputs to calculate the societal costs associated with each fire scenario (as far as possible); and
- To help identify critical scenarios.

1.5 Exploitation and implementation

As far as possible, the results will be used within LASH FIRE to feed the risk model with consistent and quantifiable data (refer to LASH FIRE deliverable D04.5 “Development of holistic risk model report”).

The simulation tool STCQ can also be used to estimate the impact of risk control measures in Action 4-B, by assessing the risk reduction compared to the safety level established for the reference cases.

In WP11, it can help evaluate the fire integrity to ensure safe evacuation in relation to the Safe Return to Port requirement or the orderly evacuation over a minimum of three hours, and thus determine new fire integrity requirements.

2 List of symbols and abbreviations

AMERIGO	Alternative Model for Evacuation Related to an Idealized conGestion Operation
ATSFR	Available Time for Safe First Response
CFD	Computational Fluid Dynamics
CO	Carbon monoxide
CO_2	Carbon dioxide
DR	Disembarkation route
DZ	Drencher Zone
FDS	Fire Dynamics Simulator
FSA	Formal Safety Assessment
FTP	Flux-Time Product
HGV	Heavy Goods Vehicle
HRR	Heat Release Rate
IMO	International Maritime Organization
LCC	Life Cycle Cost
LSA	Life-Saving Appliances
MS	Magnolia Seaways
MSC/Circ.	IMO Marine Safety Committee Circular
NIST	National Institute of Standards and Technology
O_2	Oxygen
pdf	Probability density function
PMMA	Polymethyl methacrylate
PS	Port Side of the ship
PU	Polyurethane
PVC	Polyvinyl chloride
RHF	Radiative Heat Flux
Ro-ro	Roll-on/roll-off
RS	Rescue Station
RTI	Response Time Index
SF	Stena Flavia
SOLAS	Safety Of Life At Sea International Convention
SS	Starboard Side of the ship
STCQ	Simulation Tool for Consequence Quantification
THF	Total Heat Flux

3 Introduction

Main authors of the chapter: Bernard Porterie and Yannick Pizzo, RS2N, and Anthony Collin, LUL.

3.1 Scope

The present deliverable focuses on Task T04.5 of Action 4-A (Figure 1) which is 1) to estimate the consequences of ro-ro ship fires to people, cargo, and the ship, not only in the ro-ro space where the fire originated, but also in other ro-ro spaces, assembly stations, evacuation and disembarkation routes, and accommodations spaces; and 2) to help identify critical fire scenarios. Fire consequences will be converted (except for humans) into monetary costs (WP5 LCC tool) before being used by the risk model to calculate societal cost associated to each fire scenario.

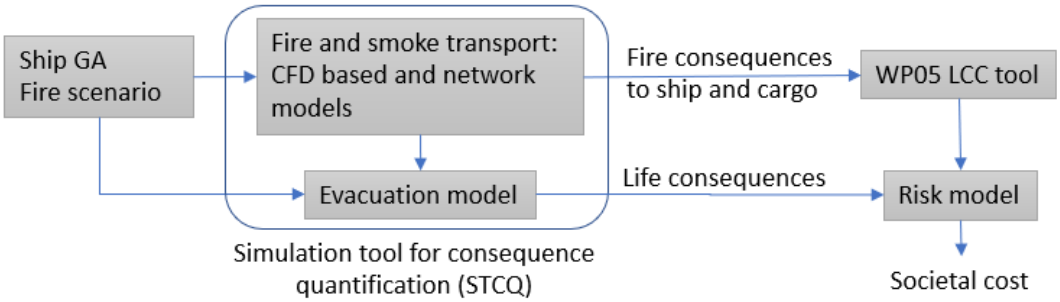

Figure 1: Flow chart of Action 4-A.

3.2 Background

3.2.1 Fire and smoke spread model

Fire risk assessment in multi-compartment enclosures is a major issue with consequences for life and property, as well as structures, human activities, and the environment. These consequences become even more critical when it comes to ro-ro ships. Historical data on the consequences of ro-ro ship fires are scarce and may be limited in their content. One way to overcome this issue is to use numerical models to simulate the transport of fire and smoke, as well as the evacuation of people, and thus the consequences of fires on board ro-ro ships.

Research and development on fire and smoke propagation models in multi-compartment enclosures have undergone several developments over the past decades. Unlike the prescriptive approach, the performance-based approach has a high degree of generality. It is a quantitative approach based on more or less fine modelling of fire and smoke transport. Currently, different approaches are used to address this challenge, either deterministic, such as CFD models (e.g., [1-5]) or zone models (e.g., [6]), or probabilistic, such as physics-based stochastic models (e.g., [7,8]) (the purely probabilistic models, because they do not contain any physics, are not able to properly model fire propagation in multi-compartment spaces [9]). While CFD models are accurate, they require considerable computational resources and a large amount of input data and parameters. In contrast, the physics involved in probabilistic models is less detailed, but these models are very fast. In between are the zone models. These have limitations, particularly in terms of the dimensions and aspect ratio of the fire compartment, which prevents their application to large spaces such as ro-ro spaces.

3.2.2 Evacuation model

From the viewpoint of pedestrian movement modelling, typically evacuation models are either microscopic or macroscopic. The microscopic evacuation models consider each evacuee as a discrete element or so-called agent of the simulation. Therefore, each evacuee is clearly distinguished from

the others and has unique physical features (e.g., walking speed). Correspondingly, an evacuee is considered as a Lagrangian particle, while its travel to a safe area through an emergency exit route is governed by several different forces (e.g., repulsive forces to avoid collision with other agents). This type of evacuation modelling is based on the theories of pedestrian movement introduced by Helbing [10] which have been implemented either through deterministic or stochastic approaches. The macroscopic models, on the other hand, consider all the evacuees as a single crowd in the form of a continuous fluid. In this case, it is not possible to distinguish one evacuee from another. Instead, the features of all the evacuees are averaged and ascribed to the crowd in the form of mean properties, such as mean density and mean velocity. The macroscopic models originate mainly from the pioneering works of Hughes [11] which described the concept of crowd movement via its density evolution through time using a scalar conservation law. For a global overview of the main evacuation tools developed over the past few decades, the reader is recommended to refer to the review of Kuligowski et al. [12].

The evacuation model of AMERIGO developed through the present project is a mesoscopic model, i.e., a model that considers the behaviour of the evacuees individually while only simulating their overall flow as a collective continuum. Mesoscopic models, unlike microscopic and macroscopic models, have only been a subject of very few studies [13]. The AMERIGO model essentially estimates the crowd density in each compartment over time using several balance equations, the theory of which is based on an extension of the work done by Togawa [14]. In the present work, the verification and validation of the mesoscopic model of AMERIGO are performed using the evacuation test cases of MSC.1/Circ.1533 as well as evacuation experiments performed at the University of Lorraine.

3.3 Objectives

To take advantage of the benefits of each approach, while considering their limitations, the proposed simulation tool is based on the combination of three improved models:

- The CFD-based model SAFIR, to simulate fire and smoke transport in ro-ro spaces, embarkation and rescue stations, and along evacuation and disembarkation routes;
- A network model to simulate fire and smoke transport in accommodation spaces, where fire growth and smoke production in each compartment of the accommodations are beforehand computed using a zone model; and
- The mesoscopic AMERIGO evacuation model.

This report presents first the components of the simulation tool STCQ.

STCQ was applied to determine the consequences of fires originating from open and closed ro-ro spaces and weather decks for selected fire scenarios on two generic ro-ro ships, namely the Stena Flavia and the Magnolia Seaways, varying the location of the fire source and the wind conditions.

The process of selecting the fire scenarios is based on the conclusions of a workshop organised for this purpose between the partners involved in Action 4-A and ship operators. The fire scenarios retained can be considered as worst credible scenarios since it was assumed that the ro-ro spaces were 100% loaded with vehicles and that no means of firefighting were engaged.

Then, the output data set obtained for each selected fire scenario regarding fire consequences in ro-ro spaces and accommodations, embarkation stations with life-saving appliances (LSA), rescue stations (RS), and disembarkation routes is detailed. To ensure consistency and ease of use of the expected results of the evacuation model to assess consequences on people first, and then in the risk

model developed in T04.4, these results are presented in the form of files giving the times, or periods of time, when given thresholds, related to heat and smoke detection, safety of persons on board and the integrity of the ship's structure, cargo, and targets, are exceeded, and compared with evacuation times (where relevant).

4 Damage criteria and threshold levels for exceeding acceptable exposure levels for humans

Main author of the chapter: Bernard Porterie, RS2N.

To calculate fire consequences and identify critical scenarios, a set of thresholds have been considered. Outputs are used to categorize the level of damage caused by fire to:

- People;
- The cargo, in terms of number of vehicles ignited over time;
- The ship, in terms of damage to the hull, specific targets and accommodation compartments;

The IMO MSC circular MSC/Circ.1002 on "Guidelines on Alternative Design and Arrangements for Fire Safety" [15], as amended by MSC.1/Circ.1552 [16], provides life safety performance criteria to be used when evaluating the elapsed time before the effects of fire and smoke directly impact occupant tenability. These are (see also [17, 18]):

- Maximum gas temperature: 60°C;
- Maximum radiant heat flux: 2.5 kW/m²;
- Minimum visibility: 10 m or 5m in spaces ≤ 100 m²; and
- Maximum CO concentration: 1200 ppm (instantaneous exposure) or
  500 ppm (for 20 minutes of cumulative exposure time).

Thus, visibility, radiant heat flux, temperature, and gas concentration are monitored as a function of time in the range [0-2m] above the deck in public spaces and in the range [0-1.8m] in all other areas of the accommodation spaces.
Although the criterion threshold of 500 ppm for a cumulative exposure duration of 20 minutes is considered, it cannot be used for evacuation of people because it depends on the route followed by each person on board when evacuating (which is not available by the evacuation model). Anyway, we will see that the 1200 ppm threshold is not a relevant criterion to smoke exposure.

For the cargo, the level of damage is estimated by calculating the number of vehicles ignited over time. Degradation level of vehicles before ignition is also available.

The impact of fire on potentially combustible targets is considered by monitoring the total incident heat flux over time at specific locations. Their eventual ignition can be predicted *a posteriori*, depending on the nature of the material constituting the target. The behaviour of Polyvinyl chloride (PVC) targets is given as an example.

It is assumed that the hull is damaged when its temperature exceeds a critical value at which mechanical deformation can occur. In the simulations, a temperature threshold of 500°C is chosen, in agreement with the partners involved in Action 4-A and [19, 20].

The accommodation spaces can be damaged by fire and/or smoke. The level of damage can be estimated by the network model, indicating the state of the fire (e.g., ignition, flashover, or fully developed fire) and the position of the smoke interface over time in each accommodation compartment.

5 Methodology

Main authors of the chapter: Bernard Porterie and Yannick Pizzo, RS2N, and Anthony Collin, LUL.

5.1 Numerical approach

In this section, we describe the components of the STCQ simulation tool used to assess the consequences of a fire originating from a ro-ro space, focusing primarily on the extensions made to meet the stated objectives.

CFD-based model SAFIR – Fire and smoke spread inside ro-ro spaces

The CFD-based model used to simulate fire and smoke spread in ro-ro spaces is derived from the open-source academic version of the code SAFIR. A detailed description of SAFIR is out of the scope of this report and the reader could find more details in [3]. As the fire-induced flow is a low-speed flow, the physical modelling used in SAFIR is based on the low-Mach number assumption, which removes the acoustic waves from the equations and only keeps thermodynamic pressure time variations. The gas phase is computed by solving the set of Favre-averaged conservation equations of mass, momentum, energy, and species, together with transport equations for the turbulent kinetic energy and its rate of dissipation. Turbulence is modelled using the standard k-ε model, with additional buoyancy-driven production/destruction and classical wall laws. Turbulent combustion is based on the Eddy Dissipation Model and the one-step irreversible chemistry is assumed. The radiation model is based on the grey assumption and requires the solution of the radiative transfer equation, where the gas absorption coefficient is calculated as the sum of the contributions from the soot and combustion products. The evolution of the soot volume fraction is described via one conservation equation by assuming that a certain amount of fuel is simply converted to soot with an empirical soot conversion factor. The three-dimensional conjugated heat and mass transfer problem at any gas-solid interface inside the computational domain (here, vehicles and bulkheads) is solved using a blocking-off region procedure [21, 22]. Wall conduction is considered through the one-dimensional Fourier's equation. The general resolution algorithm is totally implicit, the time step limitations being due to the unsteadiness of the fire-induced flow.

To meet the challenge of fire and smoke simulations in ro-ro spaces, the original version of SAFIR [3] has been extended in three ways.

Firstly, the spread of fire from one vehicle to another was considered. The FTP (Flux-Time Product) method was chosen to estimate the time required to ignite a vehicle exposed to fire. Originally defined by Smith and Satija [23], FTP is a concept which predicts the time to piloted ignition of a combustible material exposed to incident radiation. The concept was then extended by Smith and Green [24], Toal et al. [25], and Shields et al. [26]. The method was then further improved by Shields et al. [27] and Silcock et al. [28] to include materials (plastics and timber) of different thermal thicknesses.

The concept is that when a combustible material is exposed to an external heat flux, the FTP accumulates until it exceeds a critical value and the material ignites, thus giving the time to ignition. In terms of mathematical formulation, the accumulation of FTP is calculated at every time step such that:

$$FTP_i = \sum_{i=1}^{m} (\dot{q}''_i - \dot{q}''_{cr})^n \Delta t_i$$

where n is a power law exponent, Δt_i is the ith time increment, $\dot{q}''_i$ is the total heat flux (kW/m²) received by the vehicle at i^{th} time increment, and $\dot{q}''_{cr}$ is the critical heat flux (kW/m²) of the combustible material. Ignition occurs when FTP_i exceeds a critical value FTP_{cr}.
Thus, for this study, the FTP method is used to obtain the ignition time of a subsequent vehicle with respect to the ignition and burning of a preceding vehicle, as well as the ignition time of targets. The FTP method has the advantage of allowing ignition predictions to be more general than the classical thermal solutions by allowing the power law index to be chosen to provide the best fit to the experimental ignition data rather than forcing a solution based on the physical thickness of the sample [29].
In [29], FTP parameters are given for the components which are likely to be ignited first on a vehicle (Table 1).

Table 1: Power lax index, critical FTP and heat flux values for selected components (extracted from [29]).

Component	Power law index	FTP_{cr} $[s.(kW/m^2)^n]$	$\dot{q}''_{cr}$ (kW/m^2)
Mudflap	1.5	3258	5.7
Rubber tyre	1.5	9828	8.0
Bumper trim	2.0	21862	3.1
Wheel arch	2.0	50234	0.0

For this study, it is hypothesised that components which are made from rubber are likely to be ignited first as compared to other components.

For targets, the FTP parameters are known for a wide range of solid materials [30]. Targets made of PVC, representative of electrical panels or cable trays, are given as an example, but the damage of targets made of another material can be done *a posteriori*, the evolution of the received fluxes being recorded over time.

Secondly, the outputs of SAFIR have been extended to provide a complete set of data for the risk and evacuation models in terms of toxicity, visibility, and thermal constraints (temperature and heat flux) on cargo, ship structure and specific targets. This required to compute gas concentrations, temperature, soot volume fraction, radiative and total heat flux at specified locations.

Estimates of visibility through smoke can be made by using the equation $V = C/K$ where C =8 for a light-emitting sign and C =3 for a light-reflecting sign [31]. The light extinction coefficient K is defined as $K = \kappa_m \rho Y_s$, where κ_m = 8700 m²/kg [32] is the mass extinction coefficient, ρ_s the soot density, usually equal to 1800 kg/m³, and X_s the soot volume fraction. Therefore, the visibility can be written as

$$V = \frac{C}{\kappa_m \rho_s X_s}$$

Using C =3, as suggested in the present simulations, visibility values of 5 m and 10 m correspond to soot volume fractions of 0.03830 and 0.01915 ppm, respectively.

Thirdly, heat and smoke detector models have been implemented in SAFIR.
The model for the detector sensing element temperature is based on a convective heat transfer process. The first order differential equation that describes the rate of temperature increase of the sensing element is [33]:

$$\frac{dT_s}{dt} = \frac{u^{0.5}}{RTI}(T - T_s)$$

where T_s is the temperature of the sensing element, RTI its response time index, and u the gas speed at detector location. The value of RTI used in the simulations is that used in FIRESAFE II [34], i.e., 100 $m^{1/2}s^{1/2}$.
For smoke detectors, the model is slightly different. It is based on the change in the mass fraction of smoke in the sensing chamber that can be found by solving the following equation [34]:

$$\frac{dY_c}{dt} = \frac{(Y_e - Y_c)}{L/u}$$

where Y_e is the mass fraction of smoke in the free stream (kg/kg) and L the characteristic length of the detector geometry (m). The default detector parameters are for the Heskestad model with a characteristic length of 1.8 m. Then, the predicted mass fraction of smoke in the sensing chamber $Y_c(t)$ can be converted into an expression for the percent obscuration per unit length by computing [35]:

$$Obs = \left(1 - e^{-\kappa_m \rho Y_c l}\right) \times 100\% \; per \; length \; l$$

where ρ is the density of gas at detector location, and l is the length over which the light is attenuated (here, 1 m).

In accordance with EN 54:2001 and IEC 60092:504 (FSS Ch. 9 §2.3.1 and MSC/Circ.1035 [36]), the upper and lower limits of activation temperature have been chosen at 54 and 78°C respectively for heat detectors, and a percentage obscuration value of 12.5 %/m for the activation of smoke detectors.

Network model – Fire and smoke spread between compartments

A probabilistic network model is used for the accommodations. It is based on a polydisperse (i.e., compartments may differ in size) and amorphous (i.e., no geometrical regularity) network of ship compartments. The dynamic nature of the model is based on time-dependent normal probability density functions (pdf) of fire development (flashover, fully developed fire, and decay phase) and fire transmission between compartments through the walls and openings.
The network model is largely inspired by the one presented in [37]. However, extensions have been made to adapt the model to the specificities of ro-ro ships:

- At the compartment scale, the mean durations of the fire phases and fire transmission through the walls, used by the pdf, were determined by a zone model, considering the effects of fire load, compartment geometry, ventilation, and insulation systems.
- The zone model also provides the flow rate of smoke coming out of the fire compartment, as well as its temperature and density. To account for the decrease in smoke temperature as a function of distance from the fire source the correlation of Bailey et al. [37] was used:

$$log\left(\frac{T_f(x) - T_{amb}}{T_{f0} - T_{amb}}\right) \cong 0.003 - 0.018\,x$$

  where $T_f(x)$ is the smoke temperature at the distance x from the fire room, T_{f0} is the smoke temperature in the fire room (i.e., at $x = 0$), and T_{amb} the ambiant temperature.

Given the probabilistic nature of the network model, statistical averages of fire phases and transmission times are calculated from a large number of samples. Preliminary computations show that 100 samples are sufficient to achieve good statistical accuracy.
The network model is very fast (computational time of a few seconds), which allows a large number of fire scenarios to be simulated.

Evacuation model

The mesoscopic evacuation model developed in this project is called AMERIGO, standing for Alternative Model for Evacuation Related to an Idealized conGestion Operation. This evacuation model is based on an extension of the model proposed by Togawa [14] for the estimation of the evacuation time of a single room:

$$t_{evac} = \begin{cases} \dfrac{L_{max}}{V_{fw}} & \text{when } N_{people} = 1 \\ \dfrac{L_{max}}{V_{fw}} + \dfrac{N_{people}}{\varphi_{max} l} & \text{when } N_{people} > 1 \end{cases}$$

where t_{evac} is the total travel time of people exiting the room, L_{max} is the maximal distance inside the room to the exit, V_{fw} is the free walking speed, N_{people} is the total number of people inside the room, l is the width of the exit and φ_{max} is the maximal linear people flux. Note that in the configurations with more than one person in the room, a second term is added to account for the effect of congestion formation behind the doorway.

The evacuation model AMERIGO extends the single room evacuation model proposed by Togawa [10], such that it is adapted to the evacuation of an arbitrary number of interconnected rooms, while all the model parameters are set according to the guidelines of MSC.1/Circ.1533 [37]. The extended model makes the following assumptions:

- The escape route used by the evacuees is the shortest path possible, which is determined at the beginning of the evacuation process and cannot be modified during the simulation;
- Between two doorways, the evacuees travel at a fixed speed, denoted here by V_{fw};
- At every doorway, the flux of people leaving the room is limited by an upper bound, denoted here by φ_{max}.
- The stairs are considered as free circulation zones where the free walking speed is reduced to 0.59 m/s in accordance with MSC.1/Circ.1533, Annex 3 [37].

Based on the aforementioned principles and assumptions, AMERIGO considers a balance equation for each doorway in order to determine the flow of people through the doors, taking into account the size of congestion at each instant behind every door, as shown in Figure 2.

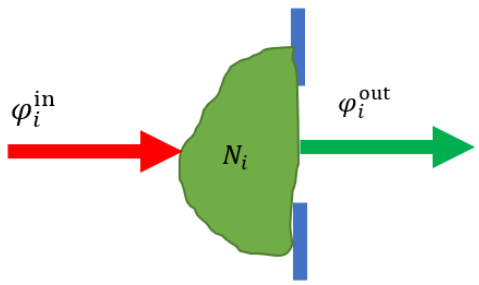

Figure 2: Schematic representation of the congestion behind a doorway.

The congestion behind door *i*, represented by N_i (total number of people waiting in the congestion zone behind the door) is fed by the incoming flux of people, named φ_i^{in}, and the outcoming flux of people, φ_i^{out} which represents the persons leaving the congestion. This last term is bounded by a maximal value, denoted by $\varphi_{i\,max}^{\text{out}}$, which mainly depends on the width of the doorway and varies between 0.9 and 1.2 pers./s/m according to the guidelines of MSC.1/Circ.1533 [37]. Here the term "doorway" can also consider locations where several people fluxes come together, such as corridors and stairs, with the aforementioned values being the average values calculated based on the flux data provided in MSC.1/Circ. 1533. Therefore, the balance equation for doorway *i* can be written as follows:

$$\frac{\mathrm{d}\ N_i\ (t)}{\mathrm{d\,t}} = \varphi_i^{\text{in}}(t) - \varphi_i^{\text{out}}(t)$$

where φ_i^{out} is bounded as previously mentioned, and its values depend on the flux φ_i^{in}. Depending on whether congestion is formed behind the doorway, φ_i^{out} is given by:

$$\varphi_i^{\text{out}}(t) = \begin{cases} \varphi_{i\,max}^{\text{out}} & \text{when} \quad N_i\ (t) > 0 \\ \min\left(\varphi_i^{\text{in}}(t), \varphi_{i\,max}^{\text{out}}\right) & \text{when} \quad N_i\ (t) = 0 \end{cases}$$

where φ_i^{in} is the influx of people feeding the congestion, including firstly people in the space immediately next to door *i* and secondly people from other rooms in transit through this space. Accordingly, φ_i^{in} can be expressed as:

$$\varphi_i^{\text{in}}(t) = \varphi_i^{\text{zone}\ i}(t) + \sum_{\substack{j=1 \\ j\neq i}}^{N_{\text{doorway}}} \alpha_{ij}\varphi_j^{\text{out}}\left(t - \Delta\tau_{ij}\right)$$

where $\varphi_i^{\text{zone}\ i}$ is the flux of people coming from the space immediately next to door *i*, while $\Delta\tau_{ij}$ is the transit time for an evacuee to reach door *i* from door *j*, and $\alpha_{ij} = 1$ if there is a connection between doors *i* and *j*, otherwise α_{ij} is equal to zero.

Considering the abovementioned principles, the simulation of a ship evacuation using AMERIGO involves the following:

1. Defining the geometry of the problem, e.g., the location of people, exits, stairs, etc.
2. Application of a pathfinding algorithm to determine the shortest escape path for every location inside the geometry
3. Time loop for each given doorway (or exit):
    a. Calculation of φ_i^{in}, i.e., the flux of people coming towards the door at discrete time t_i;
    b. Calculation of φ_i^{out}, i.e., the flux of people leaving through the door at time t_i;
    c. Calculation of N_i, i.e., the total number of people who are waiting in the congestion zone behind the door at time t_i.
4. Outputting the results of evacuation.

The main limitation of the AMERIGO is that it fixes the evacuation paths at the beginning of the simulation and only follows the shortest routes towards the final exits, such that the escape route used by an evacuee cannot be further adjusted according to the evolution of congestion or the development of fire hazards along the path later on.

The verification and validation (presented in Appendix 11.1) of these implementations in the AMERIGO model were performed in the present work using the evacuation test cases of MSC.1/Circ.1533 guidelines [49] from the International Maritime Organization (IMO) as well as evacuation experiments performed at the University of Lorraine. Accordingly, the corresponding comparisons suggest that AMERIGO can reasonably reproduce the tested evacuation scenarios, albeit within the limitation of its mesoscopic model.

5.2 Ship models

The simulation model geometries for the Stena Flavia and Magnolia Seaways are shown in Figure 3. They are extracted from the ship models available in WP05 and FDS data files. Information on the thermal insulation between decks and in the accommodations was also provided by WP05 partners and ship operators.

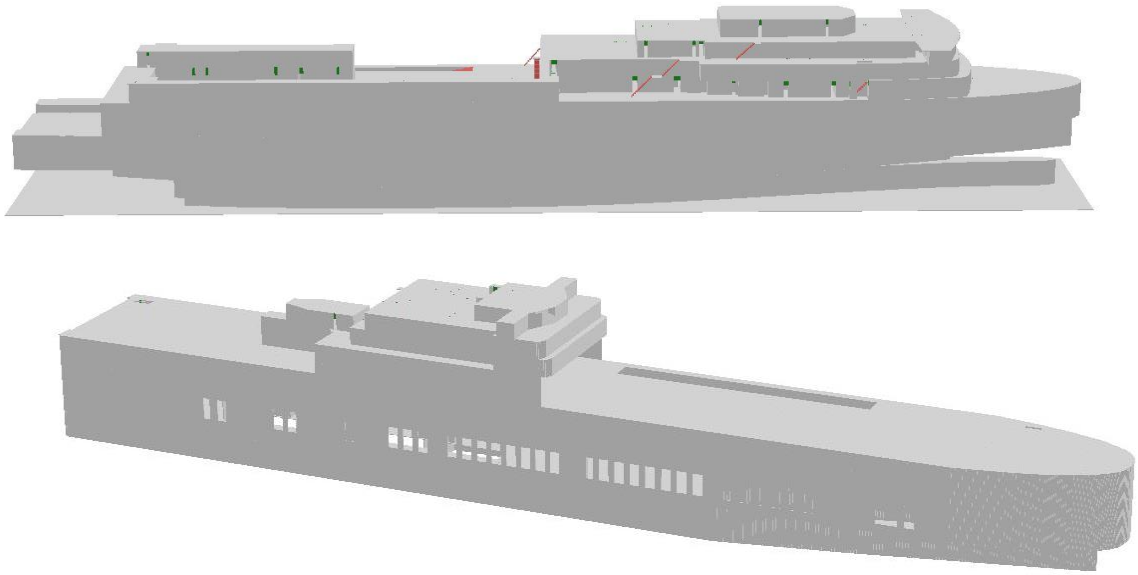

Figure 3: Stena Flavia (top) and Magnolia Seaways (bottom) ship models.

5.3 Fire scenarios

Each possible fire scenario represents a branch of the risk model event tree (refer to LASH FIRE deliverables D04.4 “Holistic risk model” and D04.5 “Development of holistic risk model report”). Due to the long calculation times (approx. one week CPU or process time for one hour of fire simulation), fire scenarios corresponding to all branches of the risk model cannot be simulated. Consequently, project partners and ship operators selected a limited number of accident scenarios to be modelled during a specific workshop [39]. As a result, and based on the feedback from the FIRESAFE studies, the emphasis was placed on simulating severe fire scenarios as a priority. The consequences of other fire scenarios will be assessed using a qualitative approach based on the examination of past accidents and expert judgements.

The selected scenarios for the fire and evacuation simulations aboard the Stena Flavia (SF) and the Magnolia Seaways (MS) are given in Table 2. They correspond to different locations of the fire origin (Figure 4 and Figure 5) and wind conditions for the fires originating in open ro-ro spaces. For all scenarios, we assumed that the doors were closed.

This study also includes for the Stena Flavia accidental scenarios influencing the transmission of fire and smoke from the ro-ro spaces to the assembly and evacuation areas, and thus fire integrity. These scenarios, derived from scenario SF3, were added to study the influence on fire consequences to people of accidental situations such as a loss of integrity of the insulation system or a loss of containment of the ro-ro space where the fire starts:

- Scenario SF3.1: the openings around the LSA on both sides of the ship were closed (Figure 6), which limits external flames and the transport of smoke to the upper decks.
- Scenario SF3.2: at time t_1, a large amount of smoke (here, 1 kg/s) coming from the fire on deck 4 enters in the accommodations at point E (Figure 7), due to a door defect.
- Scenario SF3.3: at time t_1, fire spreads from deck 4 to deck 5 at point B, due to an insulation defect (Figure 7).
- Scenario SF3.4: at time t_1, fire spreads from deck 4 to deck 5 at point G, due to an insulation defect (Figure 7).

For scenarios SF3.2 to SF3.4, the time t_1 was estimated from the CFD results of scenario SF3.

Note that the high CPU time also limited the simulation time to one hour of fire.

Table 2: Simulation scenarios.

Scenario	Ship	Fire location	Wind	Notes
SF1	SF	Open ro-ro space – Deck 4 - Centreline (Point A)	-	No loss of insulation system integrity or ro-ro space containment
SF2			18 knots headwind	
SF3		Open ro-ro space – Deck 4 - Centreline (Point B)	-	
SF3.1			-	No loss of insulation system integrity or ro-ro space containment Deck 4 openings around the LSA on both sides of the ship are closed
SF3.2			-	No loss of insulation system integrity At time t_1*, a large amount of smoke, here about 1 kg/s*, enters in the accommodations, at point E, due to a door defect
SF3.3			-	No loss of ro-ro space containment At time t_1*, fire spreads from deck 4 to deck 5 at point F*, due to insulation defect.
SF3.4			-	No loss of ro-ro space containment At time t_1*, fire spreads from deck 4 to deck 5 at point G*, due to insulation defect.
SF4			18 knots headwind	No loss of insulation system integrity or ro-ro space containment
SF5		Open ro-ro space – Deck 4 - Starboard side (Point C)	-	
SF6		Closed ro-ro space – Deck 3 - Centreline (Point D)	-	
MS7	MS	Weather deck - Centreline (Point A)	-	
MS8		Open ro-ro space (garage) - Centreline (Point B)	-	
MS9		Open ro-ro space – Upper deck - Port side (Point C)	-	
MS10			18 knots headwind	
MS11		Closed ro-ro space – Lower hold - Centreline (Point D)	-	

*deduced from CFD results

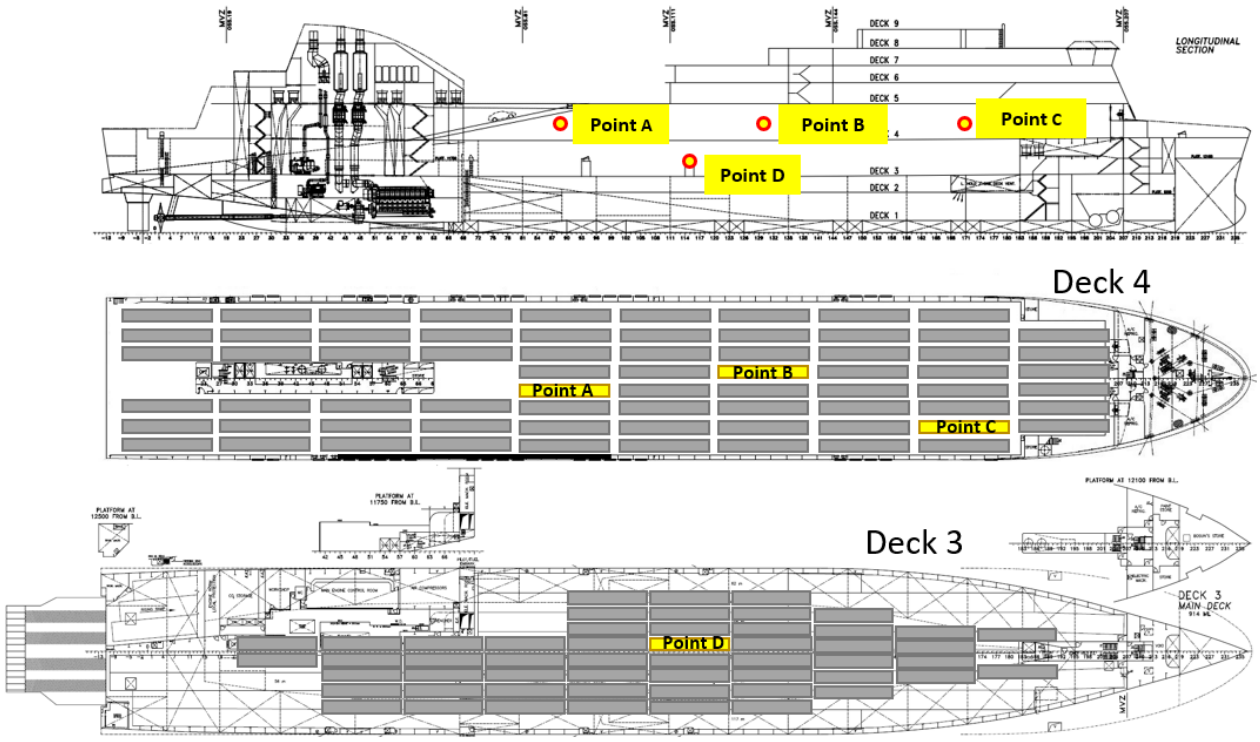

Figure 4: Fire starting points considered in the Stena Flavia simulations.

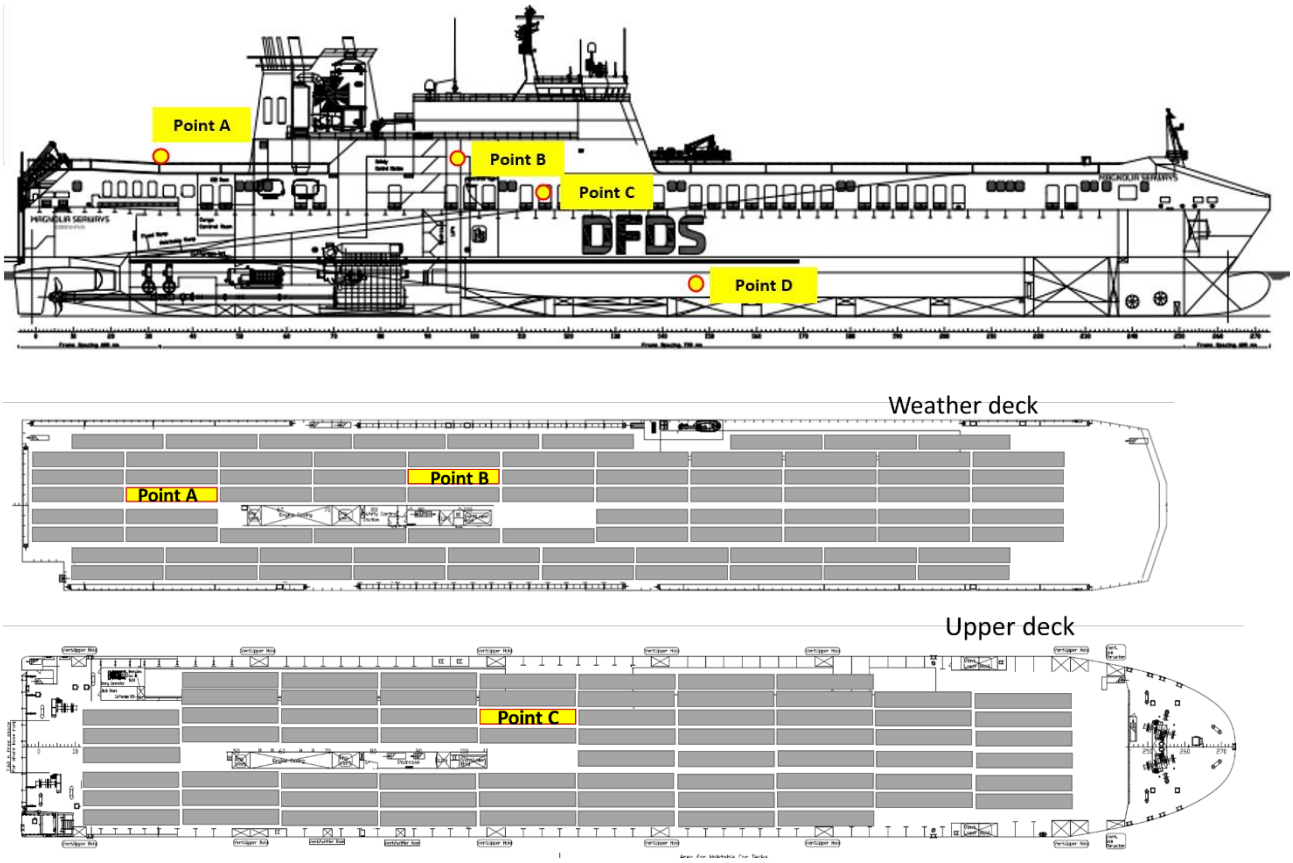

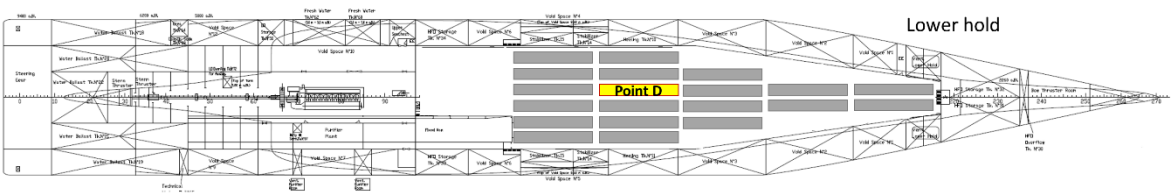

Figure 5: Fire starting points considered in the Magnolia Seaways simulations.

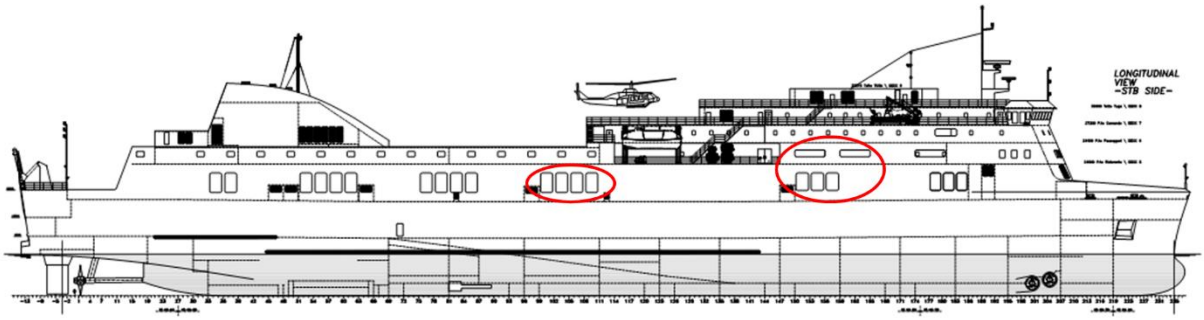

Figure 6: Area (red ellipses) where the openings around the LSA on both sides of the ship were closed for Scenario SF3.1.

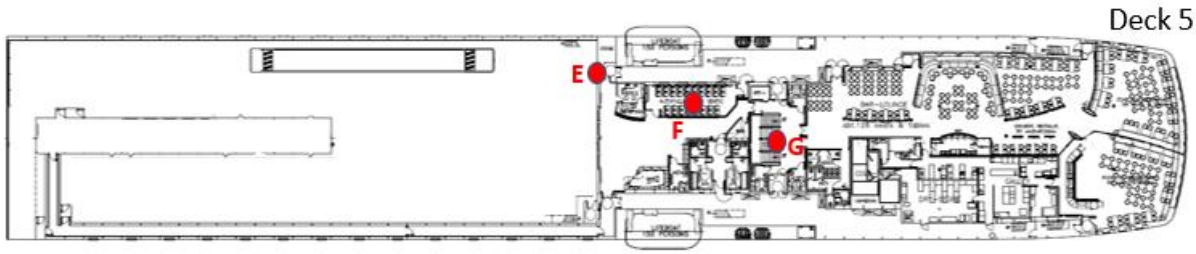

Figure 7: Locations of fire/smoke starting points in the accommodations of the Stena Flavia for scenarios SF3.2 (point E), SF3.3 (point F), and SF3.4 (point G).

For the simulations, the highest vehicle load capacity (100%) is considered, for which the most serious fire consequences are expected. The HGV truck dimensions used are 16 m (length) by 2.5 m (width) and 4 m (height), with a ground clearance (i.e., the distance between the support on which the vehicle rests and the lowest part of the chassis) of 1 m. They are placed very close to each other, generally with a spacing of about 50 cm in both horizontal directions (see Figure 4 and Figure 5).

As in the FIRESAFE studies [34], the average fuel molecule considered in the simulations is $C_{6.3}H_{7.1}O_{0.8}$, with soot and CO yields taken equal to 0.06 g/g and 0.1 g/g respectively. These relatively high values correspond to the combustion products of a mix of polymers (e.g., polystyrene or polyurethane) and cellulosic fuels, representative of the commodities carried by the goods vehicles [48].

5.4 Simulation data and parameters

To facilitate the analysis and exploitation of the results of the fire and smoke spread simulations, it was decided by the partners involved in Action 4-A and Action 11-B to assess the consequences of the fire in each drencher zone of each ro-ro space, as shown in Figure 8 and Figure 9. These figures also show the other areas of interest for the two generic ro-ro ships.

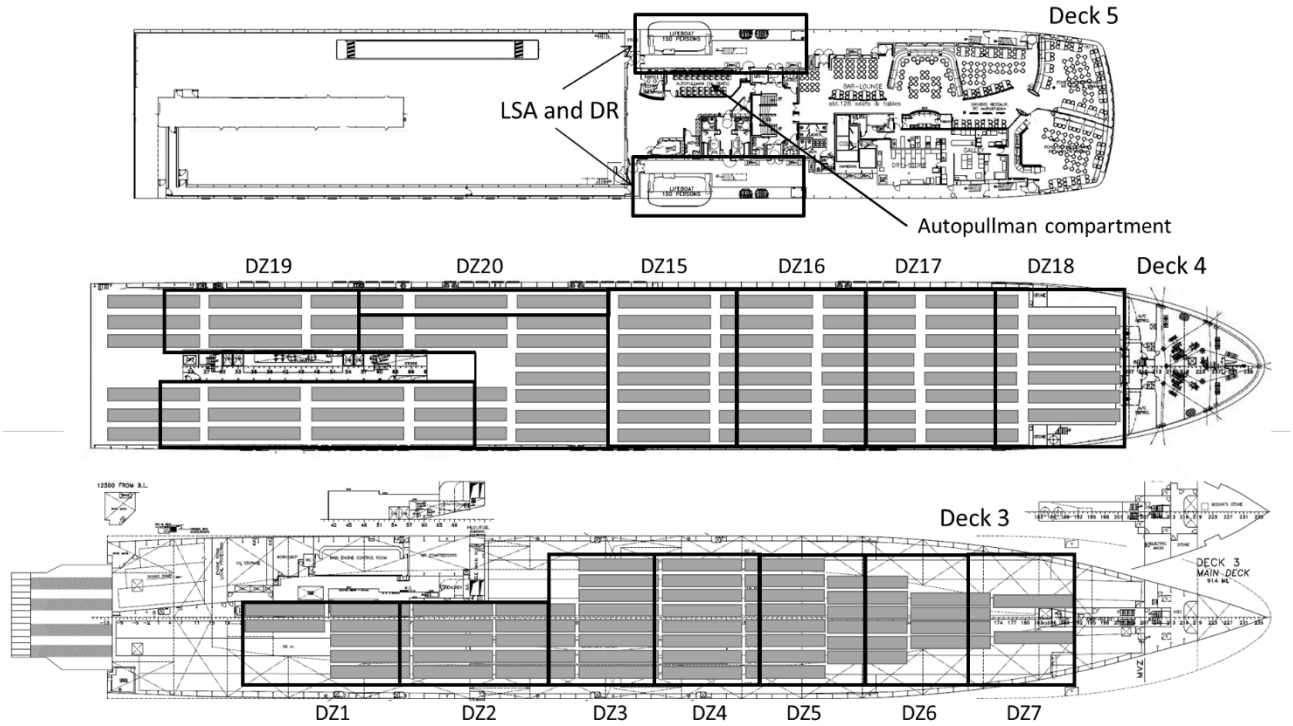

Figure 8: Zones of interest of the Stena Flavia: Drencher Zones (DZ), embarkation stations (LSA) and disembarkation routes (DR).

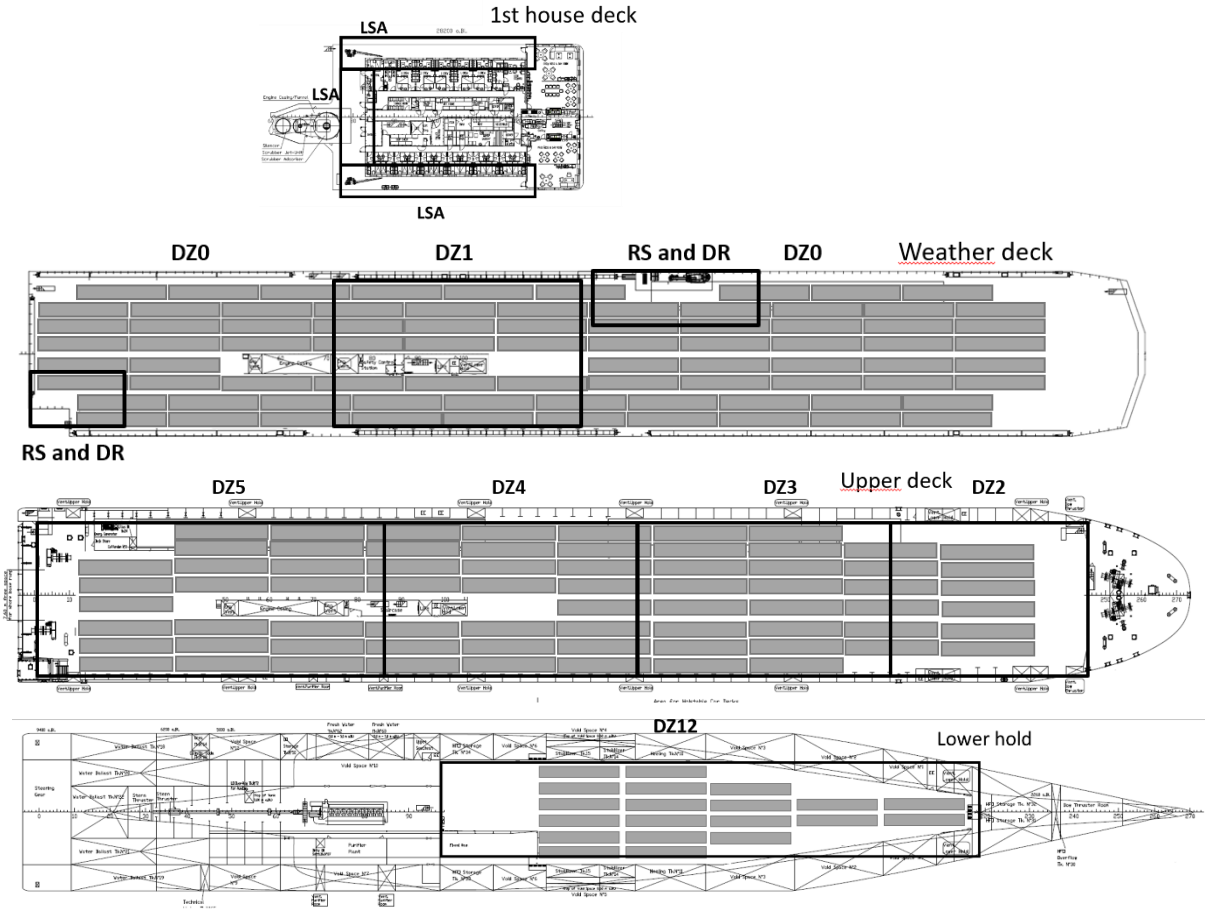

Figure 9: Zones of interest of the Magnolia Seaways: Drencher Zones (DZ), embarkation stations (LSA), rescue stations (RS) and disembarkation routes (DR).

5.4.1 Computational domain

The computational domain refers to an external volumetric region that surrounds the ship model. Aside from the bottom of the domain, the extents of the domain are free boundaries. These non-physical boundaries are placed away from the ship to avoid any significant influence on the results. In windless simulations, the computational domain is approximately $3L \times 3l \times 3h$, where L, l, and h are the dimensions of the ship. For headwind scenarios, it is extended upwind to twice the length of the ship. Non-uniform Cartesian meshes are used, with refinement in areas of interest or high gradient areas (e.g., near bulkheads and ceilings, and around trucks) and coarsening away from the ship. For example, for scenario SF2, the minimum cell dimensions are 12.5 cm×4.5 cm×10.5 cm, just above the trucks, while the maximum cell size is 50 cm×85 cm×90 cm, at the free boundaries.

5.4.2 Initial and boundary conditions

Standard boundary conditions are used, including outlet boundary conditions at free boundaries and wall (no-slip) boundary conditions at the bottom of the domain [49]. For headwind conditions, the incoming air flow is taken as that corresponding to the atmospheric surface layer with a uniform flat surface. Assuming neutral stratification of the atmosphere, air flow properties are calculated using Monin-Obukhov theory [50], with a reference (relative) wind speed at a given height (here, 10 m above the bottom of the domain). The initial conditions of the air are a relative humidity of 50% and a temperature of 20°C. The barometric formula gives the evolution of pressure as a function of altitude, with a reference pressure of 1 Atm at the bottom level.
Regarding conduction through the walls, all partitions are 1mm thick steel. One-dimensional heat conduction is calculated using the Fourier's law and steel properties from Eurocode 3 [51].

5.4.3 Design fires

5.4.3.1 Design fire of vehicle

The type and number of vehicles, as well as the type of goods carried by these vehicles, can vary considerably, resulting in different heat release rates (HRR). To determine the design fire, recommendations from various guidelines such as NFPA 502 [41], BD78/99 [42] and PIARC technical committee report [43] are often used as a basis. According to these recommendations, the peak HRR can vary from 20 to 30 MW [41,43] or 30 to 100 MW [42] for the heavy trucks (HGV) considered in the present simulations. An intermediate value of 40 MW has been retained for the HGV fire.
To characterize a design fire, one needs to know the different parameters of the heat release rate curve (i.e., fire growth phase, peak heat release rate, decay phase, time to reach peak heat release, total heat released and/or fuel load potential). Simplified characterization methods are proposed for the HRR curves of furniture items (e.g., [44-47]). These methods are the exponential and power law (i.e., a t-squared growth) representations of fire growth and decay, where parameters are calibrated from experiments. An alternative is to directly use the experimental curves giving the HRR versus time and scale to the given HRR peak value. This is the approach we have chosen by downscaling the experimental HRR curve of the 72 MW truck fire given in [48]. The resulting HRR curve is shown in Figure 10.

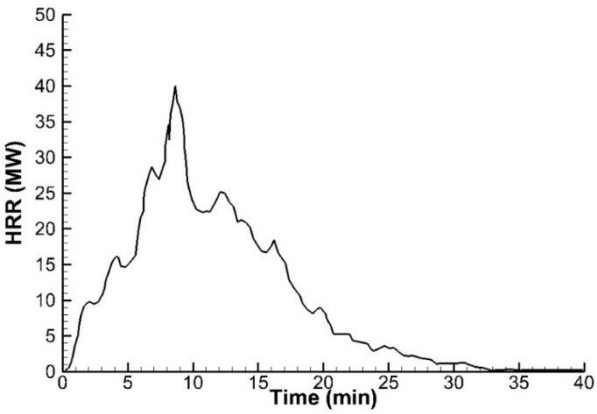

Figure 10: Heat release rate of a 40 MW HGV truck (deduced from [48]).

5.4.3.2 Design fire of accommodation compartments

As previously stated, the network model uses a compartment-scale zone model. Therefore, a design fire is required for each type of accommodation compartment (e.g., cabins, bar lounges, offices) based on the combustible elements and load contained therein. To achieve this, a specific procedure is used. This procedure assumes that the time evolution of the HRR follows three phases: a growth phase, followed by a phase where the HRR is constant, then a decay phase until extinction, so that:

$$HRR = \begin{cases} \alpha_c t^2 & if\ t < t_{fd} \\ HRR_{max} & if\ t_{fd} \leq t < t_{dec} \\ \alpha_{dec}(t_{end} - t)^2 & if\ t_{dec} \leq t \leq t_{end} \\ 0 & if\ t > t_{end} \end{cases}$$

where α_c is the growth coefficient, HRR_{max} the maximum HRR, α_{dec} the decay coefficient, t_{fd}, t_{dec} and t_{end} are the times when the fire reaches its maximum HRR, begins to decay and goes out.

The calculation of HRR requires knowledge of the initial fuel mass m_0, HRR_{max} and α_c, but also the percentage p of the initial fuel mass beyond which fire decay occurs. The other parameters are deduced from the following relationships:

$$t_{fd} = \left(\frac{HRR_{max}}{\alpha_c}\right)^{0.5} \qquad t_{dec} = t_{fd} + \frac{1}{HRR_{max}}\left(pm_0 hoc - \frac{1}{3}\alpha_c t_{fd}^3\right)$$

$$\alpha_{dec} = \frac{HRR_{max}^3}{[3m_0(1-p)hoc]^2} \qquad t_{end} = t_{dec} + \left(\frac{HRR_{max}}{\alpha_{dec}}\right)^{0.5}$$

Examples of design fires following this procedure and using the parameters given in Table 3, are plotted in Figure 11. They correspond to the Autopullman compartment and the adjacent hall on deck 5 of the Stena Flavia (Figure 8).

Table 3: Design fire parameters for the Autopullman compartment and the adjacent hall of the Stena Flavia deck 5.

	Combustible elements	Load (kg/m²)	m_0 (kg)	HRR_{max} (MW)	α_c (kW/s²)	p %
Autopullman	PU-foam	6.4	327	2.2	0.012	20
	Polymer (here, PMMA)	3.6	184	1.9		
Hall	Polymer (here, PMMA)	4.5	525	3.6		

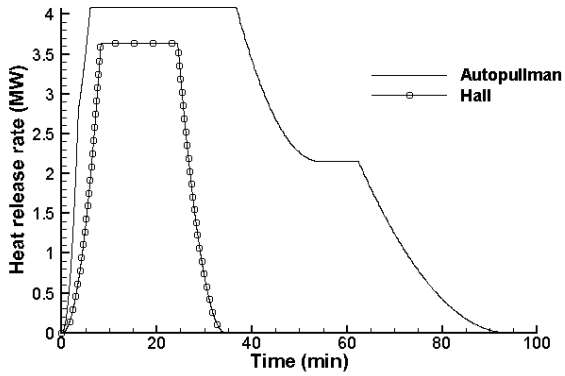

Figure 11: Design fires for the Autopullman compartment and the adjacent hall on deck 5 of the Stena Flavia.

5.4.4 Evacuation data and parameters

For the evacuation phase, the main input data comes from the general arrangement plan of each ship and includes the following items:

- The ship geometry: emergency exits, obstacles, doorways, stairs, …
- The initial people locations: for each evacuation simulation, the nominal people capacities of all the rooms are summed up to determine the total nominal number of people, which is then used to populate the evacuation zones;
- The thermal constraints imposed by a fire inside the ship (or tenability criteria), considering the fire propagation simulations performed previously:
    - The temperatures inside the accommodations;
    - The volume fraction of soot inside the ship.

The thermal constraints reduce the rate of evacuation either by decreasing the maximum value of free walking speed (proportional to the soot volume fraction ranging from 10^{-5} to 10^{-4} kg/m^3 according to a linear function) or by blocking the related paths inside the ship when the ambient temperature is too high (above 60°C).

The considered thermal constraints focus on temperature and soot concentration, as they are generally reached more quickly over time and are more restrictive for the overall evacuation than the levels of carbon monoxide (between 500-1200 ppm, according to IMO MSC.1/Circ. 1552) or the radiative fluxes (beyond 2.5 kw/m²), particularly near the accommodation areas.

5.4.4.1 Generic ship geometry

As the evacuation model AMERIGO is implemented in MATLAB, the ship geometry and all the input parameters (such as the initial locations of people) must be readable by MATLAB. Accordingly, the free software QGIS has been used to convert the map of each deck into raw data for MATLAB. This process has been done manually for each deck and for each ship (Stena Flavia and Magnolia Seaways) and has also been used to provide the necessary input files for the fire simulations performed using FDS (Fire Dynamics Simulator) as part of the fire spread study.

An example of the generic ship geometry generation is given in Figure 12. As can be seen, each wall/obstruction (represented in black), each doorway (in green), … must be manually redesigned from the general arrangement plan.

The main challenge for the task of geometry generation is the varied forms of source data which were available for the general arrangement plan of the ships, i.e., PDF files, CAD files, etc. Another challenge is accounting for the many features included in the general arrangement plan, which can be very different from one ship to another.

Figure 12: Generic ship geometry to be used by MATLAB.

5.4.4.2 Initial locations of people

People are assumed to be in cabins, offices, or workstations at the moment of the evacuation signal, as this is the worst-case scenario for the assembly phase of evacuation, so that no one is near the assembly station, and this is especially the case for a night scenario because many people are asleep. The location of these areas is available in the general arrangement plans provided by WP05.

Concerning the response time of people i.e., the time required for people to start their travel to the assembly station after they have heard the evacuation signal, the guidelines of MSC.1/Circ.1533 recommends 5 min for a day scenario and 10 min for a night scenario.

Although AMERIGO only determines the travel time of people, the abovementioned response time is important for the definition of compromised areas in which the travel of people to the assembly stations is hindered by thermal constraints (i.e., heat and/or smoke from the fire), such that the tenability criteria for temperature and/or soot concentrations become important in the design of the evacuation simulation.

6 Simulation results

Main authors of the chapter: Bernard Porterie and Yannick Pizzo, RS2N, and Anthony Collin, LUL.

6.1 Model outputs

6.1.1 Consequences of fire and smoke spread

As previously mentioned, the simulation results for selected fire scenarios (Table 2), are provided to project partners to feed the evacuation and risk models (as far as possible), in the form of directly usable summary files. These data files contain information about:

- Consequences to human: i.e., the times after which given thresholds (Section 4) are exceeded in each Drencher Zone (DZ) of each ro-ro space, around the LSA and rescue stations, and along disembarkation routes. For this purpose, smoke, temperature, O_2 and CO sensors are placed 1.80 m above the deck (orange circle symbols in Figure 13 and Figure 14).
- Swift detection: smoke, temperature, O_2 and CO sensors are placed at a height of 1.80 m within a 4 m radius of the first truck on fire, in order to estimate the available time for safe first response (ATSFR) [34] (black "X" symbols in Figure 13 and Figure 14).
- Heat and smoke detection: i.e., the times of smoke and heat detection in each DZ of each ro-ro space. The combined heat and smoke detectors are placed on the ceiling at the bottom level of the stiffeners (orange circle symbols in Figure 13 and Figure 14), with a maximum distance of 11 m between them, as recommended for unevenly distributed detectors [34].
- Structure damage: i.e., the times when the hull reaches a temperature of 500°C (start of deformation) in the hot zone of each DZ. Time evolution of ceiling temperature at selected locations are also recorded (blue "+" symbols in Figure 13 and Figure 14). This could be used to check whether fire propagation to the upper deck is possible.
- Cargo damage: i.e., the time evolution of the number of vehicles ignited per DZ and degradation level of trucks before ignition. Five levels are considered: 20, 40, 60, 80 and 100% of the FTP_{cr} of the trucks' rubber components. The time evolution of the total HRR is also provided. It is compared to the time evolution of the theoretical HRR (i.e., the total pyrolysis rate multiplied by the chemical heat of combustion[2]) to analyse the effects of under-oxygenation on combustion.
- Target damage: i.e., the ignition time of PVC targets on the ceiling of each DZ (orange circle symbols in Figure 13 and Figure 14). For this part, the total heat flux (THF) received by the target is recorded, which makes it possible to calculate the ignition time for another target material afterwards using the FTP method.

For human consequences and swift detection, the incident radiative heat flux at specific locations cannot be estimated from sensors due to the directional nature of radiation. It is then deduced from 2D fields obtained from SAFIR in the horizontal plane $y = 1.80$ m above the decks of interest.

[2] Chemical heat of combustion is defined as the calorific energy generated in chemical reactions leading to varying degrees of incomplete combustion per unit fuel mass consumed. It is the product of net heat of complete combustion and combustion efficiency.

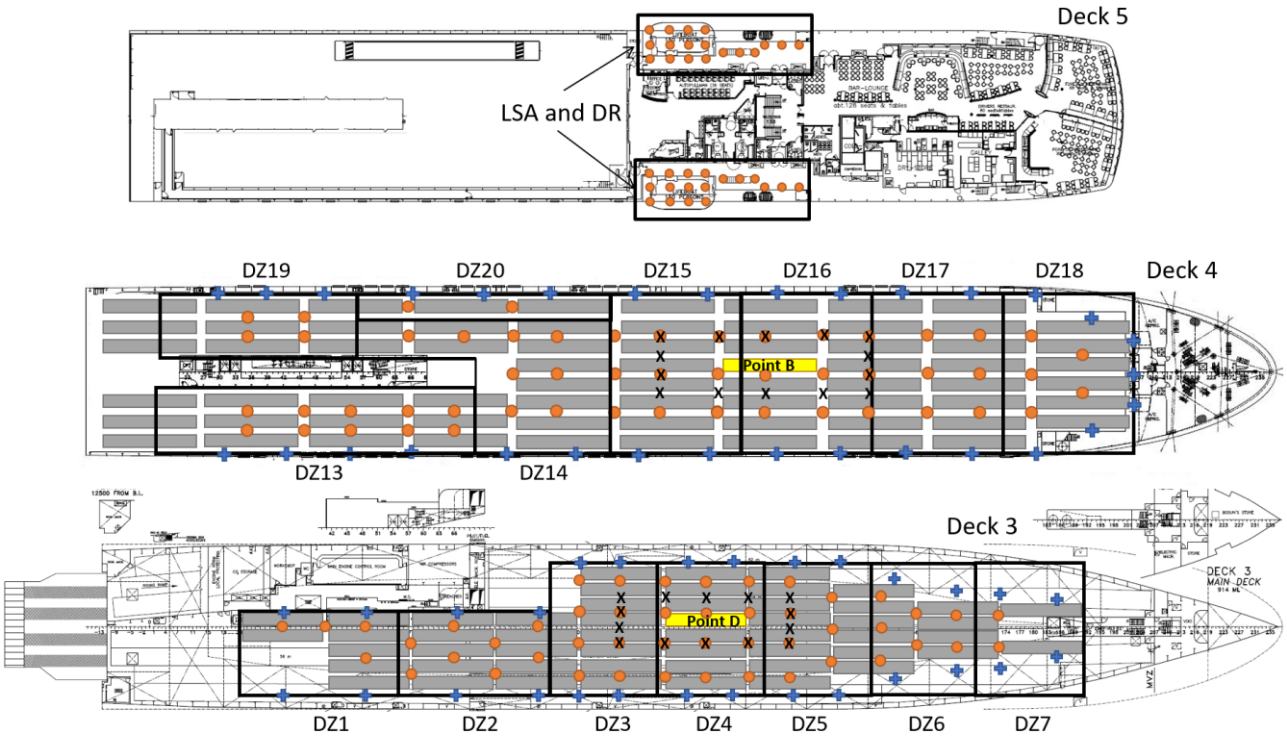

Figure 13: Location maps of detectors and sensors of the Stena Flavia. As examples, we placed Swift detectors around fire starting points B and D (black "X" symbols).

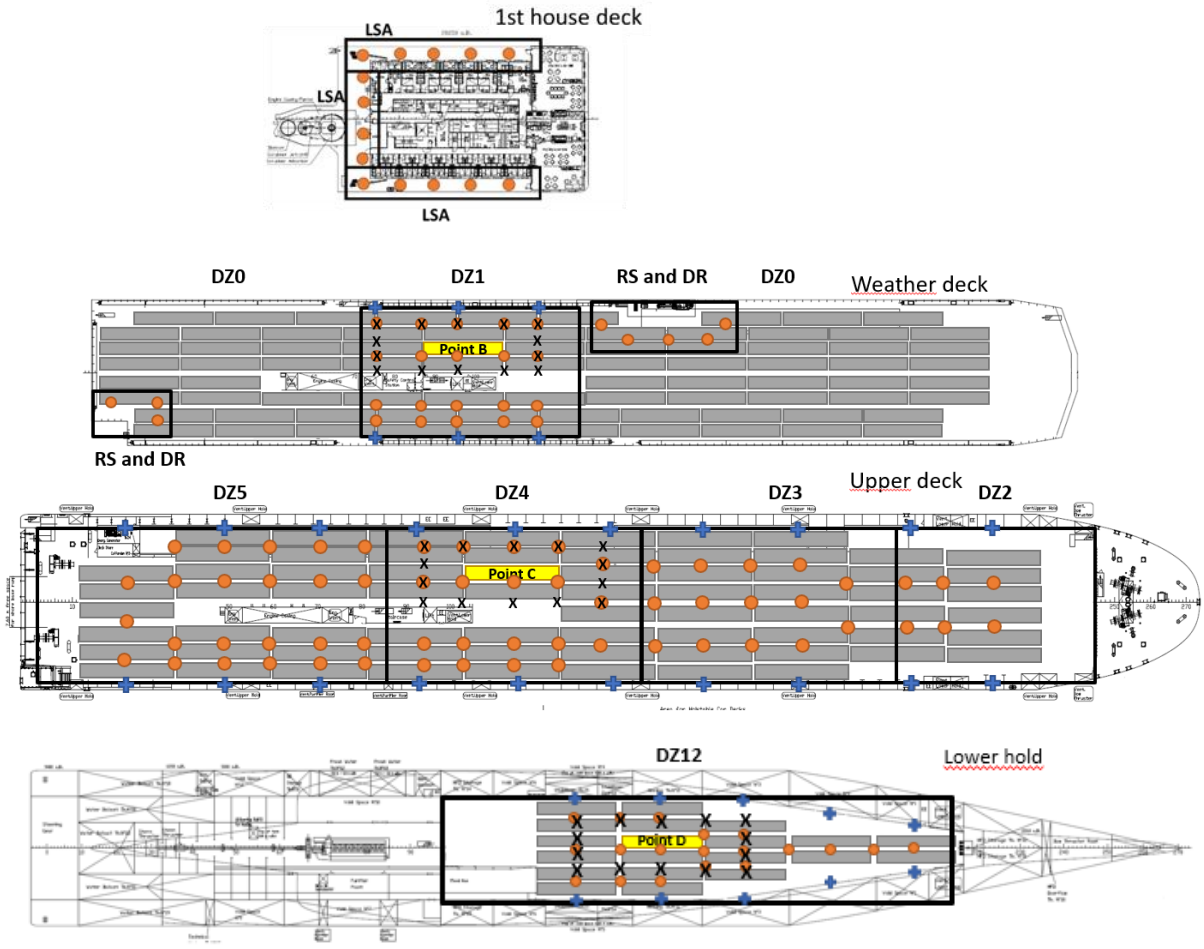

Figure 14: Location maps of detectors and sensors of the Magnolia Seaways. As examples, we placed Swift detectors around fire starting points B, C, and D (black "X" symbols).

Simulations from the network model in the accommodation spaces provides a mapping of fire and smoke every minute, indicating the compartments where ignition occurred, those where the flashover occurred, those where the fire was fully developed, and those that were destroyed by the fire, as well as the position of the smoke interface. These data are used to estimate consequences on people.
Concerning the evacuation model, several kinds of results can be performed by AMERIGO algorithm.

6.1.2 Evacuation maps

The evacuation maps generated by AMERIGO provide an overall view of the evacuation time required by a single person to reach the assembly station when travelling at the free walking speed. This provides a holistic view of the sensitive areas on the ship where the evacuation takes the longest, but the corresponding calculations are obtained assuming that there is no congestion formation and fire effects. This kind of evacuation maps is comparable to the Safety Plan (or Escape Plan) defined for each ship, which gives confidence in the results provided by AMERIGO.

6.1.3 Evacuation time distributions

By considering the congestion phenomenon at the doorways, AMERIGO provides the travel time distribution of people. When added by the response duration, this can provide the local RSET time for each location inside the ship.

Moreover, by analysing the transient results generated by AMERIGO, it is possible to identify the most sensitive doorways inside a ship. For the present project, we identified two classes of sensitive doorways:

- The doorways which are used a lot by the occupants and are thus useful for a quick escape; and
- The doorways causing congestion and long waiting times for people.

This kind of information is very important for the improvement and optimisation of the escape routes used by people to guarantee a quick evacuation process.

6.1.4 Estimation of fatalities for a scenario with fire effects

When a fire occurs, thermal constraints (or tenability criteria) can limit the escape of people. In certain areas, there may even be no escape routes available to people, so they are trapped or blocked by the fire. In the analysis of fatalities, a people trapped by the fire corresponds to one fatality.

For a given fire scenario, it is useful to estimate the number of fatalities and their locations relative to exits, as one can then identify critical locations requiring more fire protection investment, so that the availability and safety of escape routes in these areas can be guaranteed.

6.2 Example of simulation results

We detail below the results obtained for scenarios SF3.3 and SF6. All other results from the Stena Flavia and Magnolia Seaways simulations are summarized in Appendices 11.2 and 11.3 respectively.

6.2.1 Scenario SF3.3

Fire and smoke spread in ro-ro space

The results obtained by the SAFIR code show that the fire generated very high total heat flux (THF) on the deck 4 insulated ceiling. As shown in Figure 15, the ceiling insulation material was exposed to THF that exceeds 80 kW/m² for more than 3 min, around t =30 min, which can cause its destruction, resulting in the transmission of fire to the deck 5 accommodations and the ignition

of the Autopullman compartment located just above. In this scenario, we assumed that the fire spread from deck 4 to deck 5 after 29 min.
It is important to note that if the insulation material maintains its integrity, the temperature of the floor of deck 5 does not exceed 193°C. This temperature level is below the ignition temperature of vehicle tires (i.e., 300-350°C [52, 53]) or cellulosic items (i.e., about 300-350°C [54-57]), which does not allow the fire to spread from deck 4 to deck 5 through this mechanism.

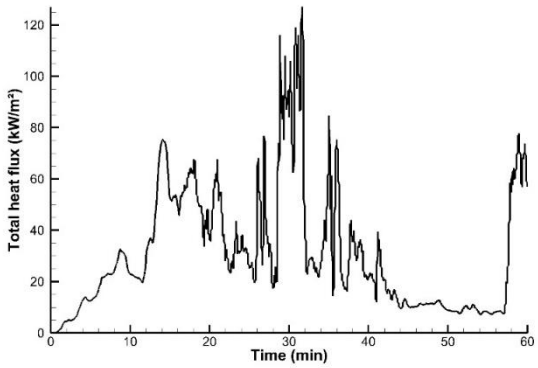

Figure 15 : Scenario SF3.3: time evolution of the total heat flux received by the deck 4 ceiling just below the Autopullman compartment.

Main results for scenario SF3.3 are given in Table 4, and from Figure 16 to Figure 18. They show that for this open ro-ro space:

- As expected, the conventional smoke detectors detect the fire the fastest, after 41 s in DZ16;
- Fire is “out of control” (see 6.3) in DZ15 after 15 min 35 s of fire;
- The comparison between the time evolutions of theoretical HRR (i.e., the total pyrolysis rate multiplied by the chemical heat of combustion) and effective HRR (Figure 16b), as well as the ratio of predicted to prescribed total heat contents (i.e., 1.42/1.64 TJ in Table 4), reveal that the combustion is relatively well oxygenated, which favours the spread of the fire to all the trucks on deck 4 in less than 43 min (last truck ignition in DZ18 in Table 4 and Figure 16a).
- Due to the severity of the fire, all drencher zones are impacted by the fire, as evidenced by the relatively short times when the structure begins to be damaged, and the ignition of PVC targets occurs.
- Exposure to excessive RHF around the first truck on fire (Swift detection) significantly limits the time available for a safe first response (ATSFR) at 7 min.
- Fire spreads to target cars on the aft part of upper deck 5 due to external flames.
- Depending on the area where they may be located, people may be exposed to excessive levels of temperature, incident RHF, or degraded visibility due to smoke. As shown in Table 4, smoke reduces visibility to less than 10 m (the ro-ro space area is greater than 100m²) in DZ17 and DZ18 after about 3 min of fire.
  Fire consequences to persons on board can be evaluated more precisely by analysing the time evolutions of maximum CO mole fraction, gas temperature, and soot volume fraction, and thus visibility, recorded by all the sensors located around the LSA and along the DR, as plotted in Figure 17, as well as the time evolution of the incident radiative heat flux at a height at 1.80 m above decks 4 and 5.
  It is found that the LSA and DR on both sides of the ship are safe during the first 10 min of fire (Figure 17). People in these areas could be exposed to a RHF exposure level greater than

2.5 kW/m² between 22 and 41 min on each side of the Stena Flavia (Figure 18b and c)[3]. Beyond 41 min of fire, the RHF in these areas no longer exceeds 2.5 kW/m². Figure 17 reveals that the most restrictive criterion is visibility since it makes LSA and DR impractical after 1 h of fire. People must wait in the AS for a long time, greater than 1 h. Longer simulations are needed to more accurately assess this period of time.

Table 4: Scenario SF3.3: simulation results. SWI means Swift detection, DR disembarkation route, SS starboard side, and PS port side. For consequences to human, the value in bold blue corresponds to the first tenability criterion that was exceeded in the areas of interest. Times are given in minutes and seconds (min's").

	DZ13	DZ14	DZ15	DZ16	DZ17	DZ18	DZ19	DZ20			
Heat detection at 54°C	4'46"	4'09"	2'39"	2'08"	3'35"	4'00"	5'27"	4'32"			
Heat detection at 78°C	5'48"	4'50"	3'30"	2'38"	4'49"	5'04"	7'01"	5'23"			
Smoke detection	2'26"	1'51"	1'15"	**0'41"**	1'26"	2'05"	2'59"	1'45"			
Structure damage	30'26"	28'16"	23'35"	31'51"	26'50"	43'53"	34'29"	30'54"			
Target ignition	20'58"	16'46"	12'42"	5'51"	23'15"	42'22"	22'06"	18'53"			
First truck ignition	19'23"	15'31"	0'00"	0'00"	11'54"	23'50"	20'50"	17'38"			
Last truck ignition	36'39"	20'53"	**15'35"**	19'48"	25'42"	42'45"	37'19"	21'19"			
no of trucks ignited	70/70										
Predicted/Prescribed total heat content (TJ)	1.42/1.64										
Consequences to human	DZ13	DZ14	DZ15	DZ16	DZ17	DZ18	DZ19	DZ20	LSA and DR - SS	LSA and DR - PS	SWI
RHF	**18'00"**	**14'00"**	**6'00"**	**6'00"**	21'00"	22'00"	**19'00"**	**18'00"**	22'00"	22'00"	**7'00"**
T60	29'54"	25'15"	21'32"	20'13"	20'40"	18'16"	33'16"	27'55"	19'08"	27'59"	21'32"
CO	32'53"	26'24"	22'28"	21'32"	20'44"	18'04"	33'44"	33'45"	34'32"	31'33"	22'14"
Visibility 5m	29'50"	25'43"	21'31"	12'41"	12'34"	3'01"	33'21"	25'43"	13'26"	12'12"	12'48"
Visibility 10m	28'18"	25'14"	21'31"	10'25"	**3'33"**	**2'57"**	33'09"	24'29"	**10'34"**	**9'39"**	10'16"

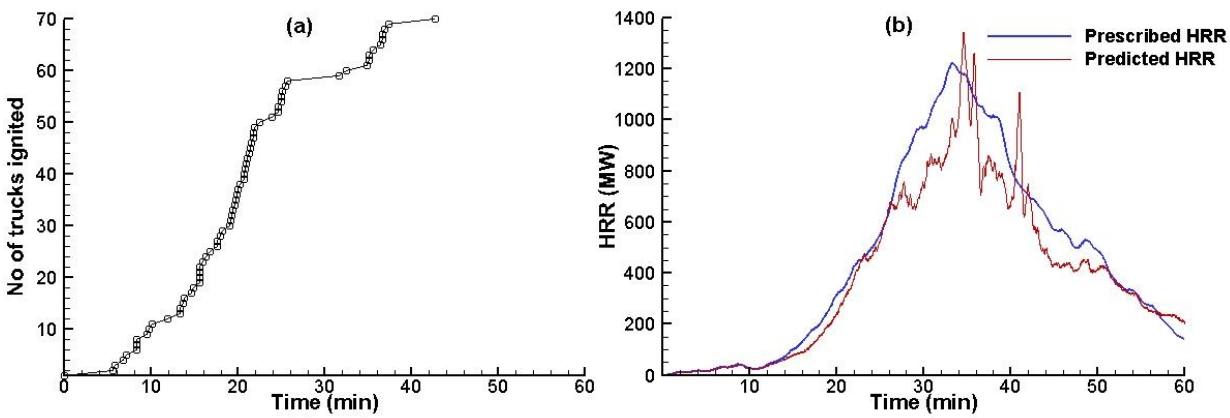

Figure 16: Scenario SF3.3: a) Number of truck ignited vs. time, and b) comparison between the time evolutions of the theoretical HRR (i.e., the total pyrolysis rate multiplied by the chemical heat of combustion) and effective HRR.

[3] Similar results were obtained for gas temperature and visibility, as well as for smoke, CO and O2 concentrations. This information could also be used 1) to verify whether access through the doors of the ro-ro space is safe or not, and 2) to check whether a first response is possible in the area close to the fire seat.

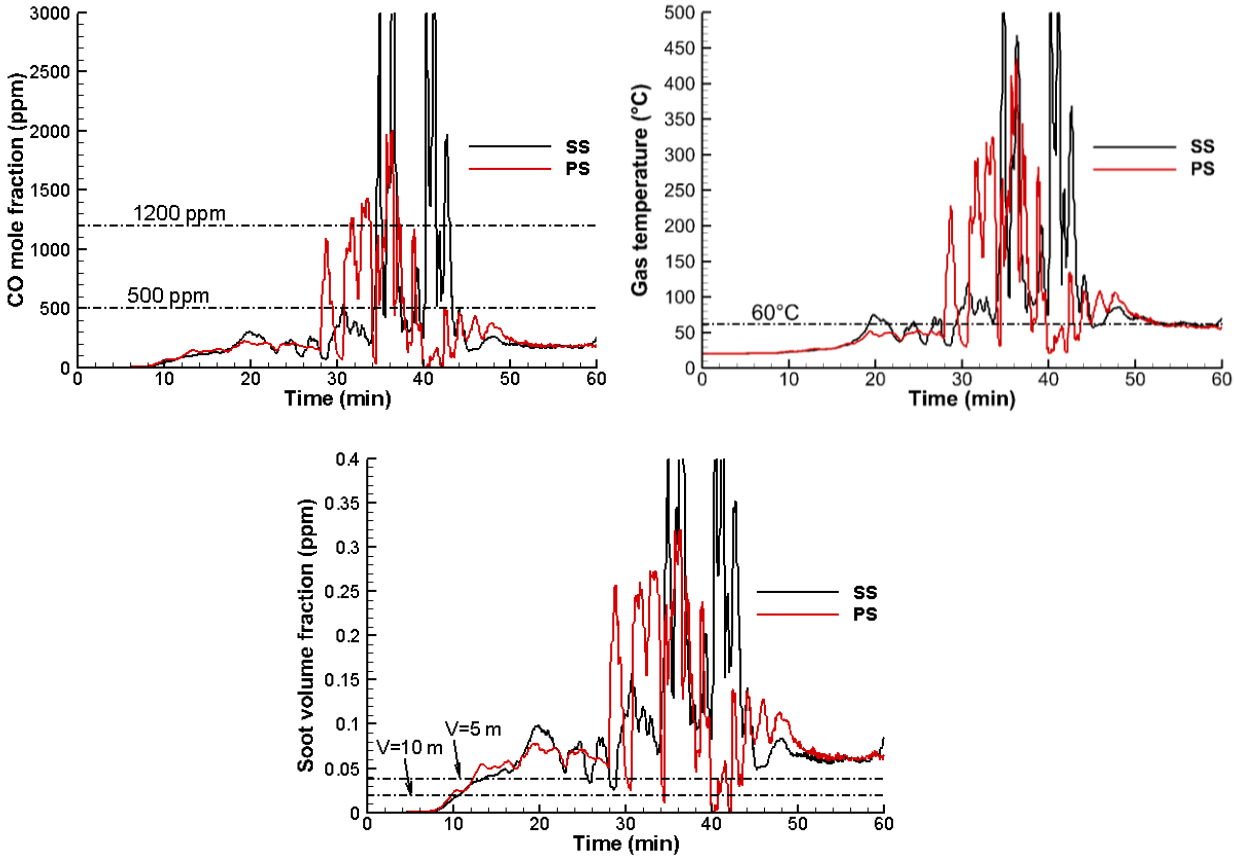

Figure 17: Scenario SF3.3: time evolutions of maximum CO mole fraction, gas temperature, and soot volume fraction at the monitored points in the LSA and DR on both sides of the Stena Flavia.

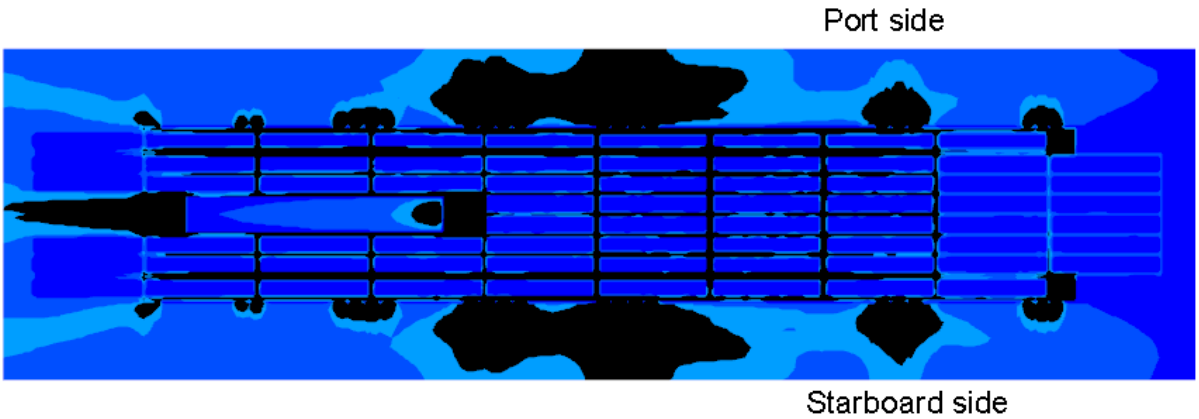

(a) Incident RHF above deck 4 after 22 min of fire.

(b) Incident RHF above deck 5 after 22 min of fire.

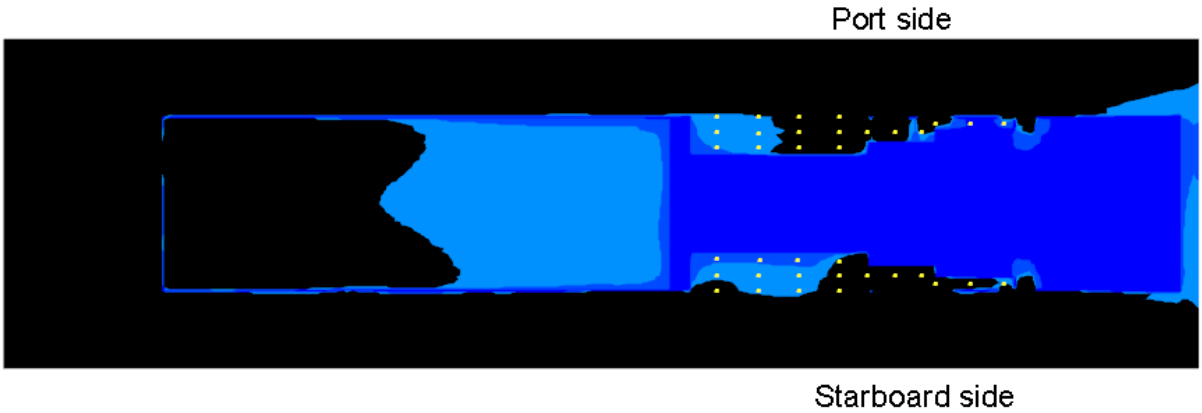

(c) Incident RHF above deck 5 after 41 min of fire.

Figure 18: Scenario SF3.3: 2D fields of the incident radiative heat flux at a height of 1.80 m above deck 4 after 22 min of fire (a), and above deck 5 after 22 min (b) and 41 min (c) of fire. Black areas correspond to areas where the radiative heat flux is greater than 2.5 kW/m².

Fire and smoke spread in accommodations

As predicted by the network model, the fire only spreads to the hall adjacent to the Autopullman compartment. Due to smoke propagation in the accommodations, the assembly station quickly become untenable. This is shown in Figure 19 and Figure 20, where the smoke interface falls below 1.80 m in height at $t \approx t_1 + 20$ min, i.e. at $t \approx 49$ min.

Figure 20 shows the chronology of the smoke filling the accommodations every 5 min. After t_1 + 5 min, the hall adjacent to the room where the fire originated is largely filled. The smoke reaches the upper decks in less than t_1 + 10 min. The entire open spaces of decks 5 to 7 are filled with smoke after t_1 + 25 min. The simulation results of Figure 20 could be used to reallocate safer areas or define alternative evacuation routes.

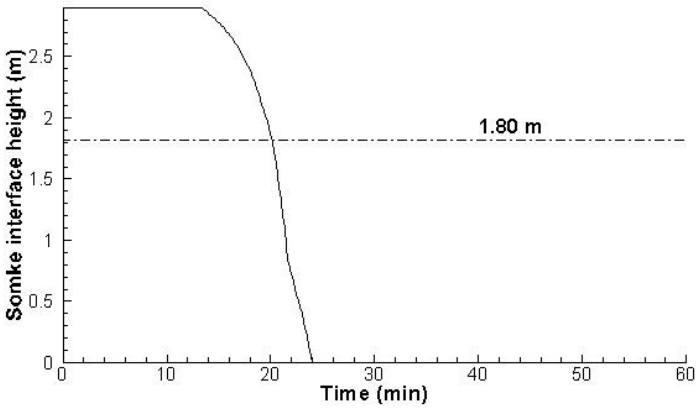

Figure 19: Scenario SF3.3: time evolution of the smoke interface height in the AS of the Stena Flavia, here the restaurant located on deck 5. The origin of time is the time t_1 at which fire and/or smoke reaches deck 5, here t_1 ≈29 min.

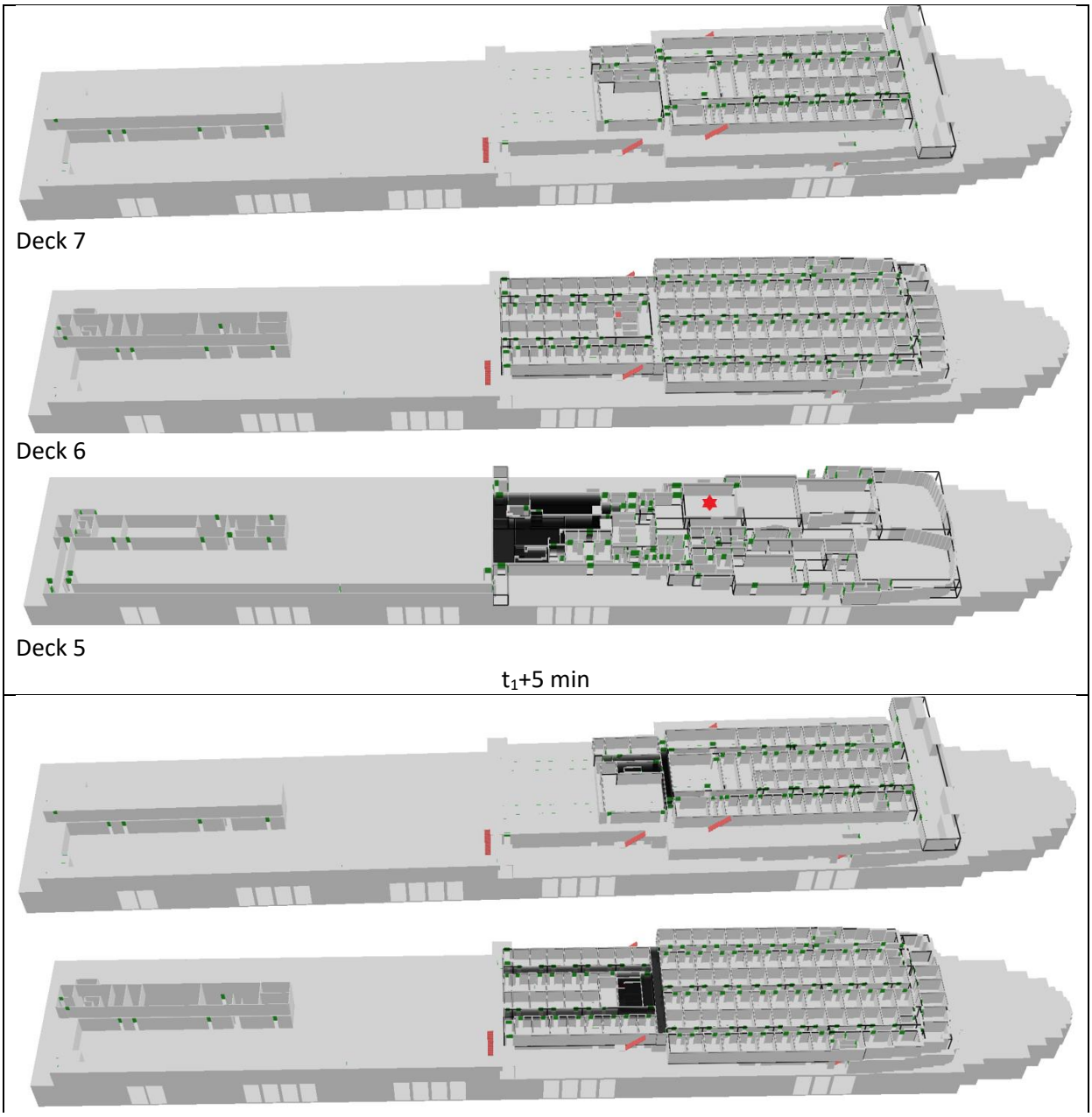

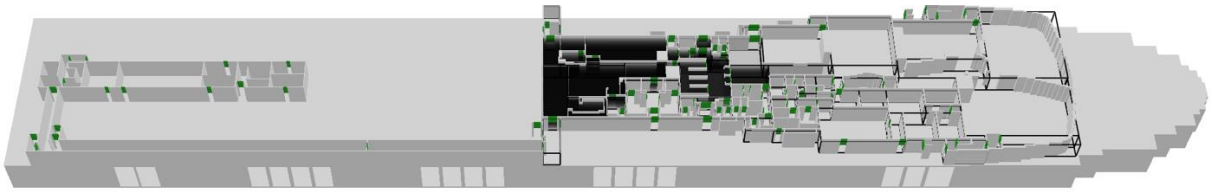

t_1+10 min

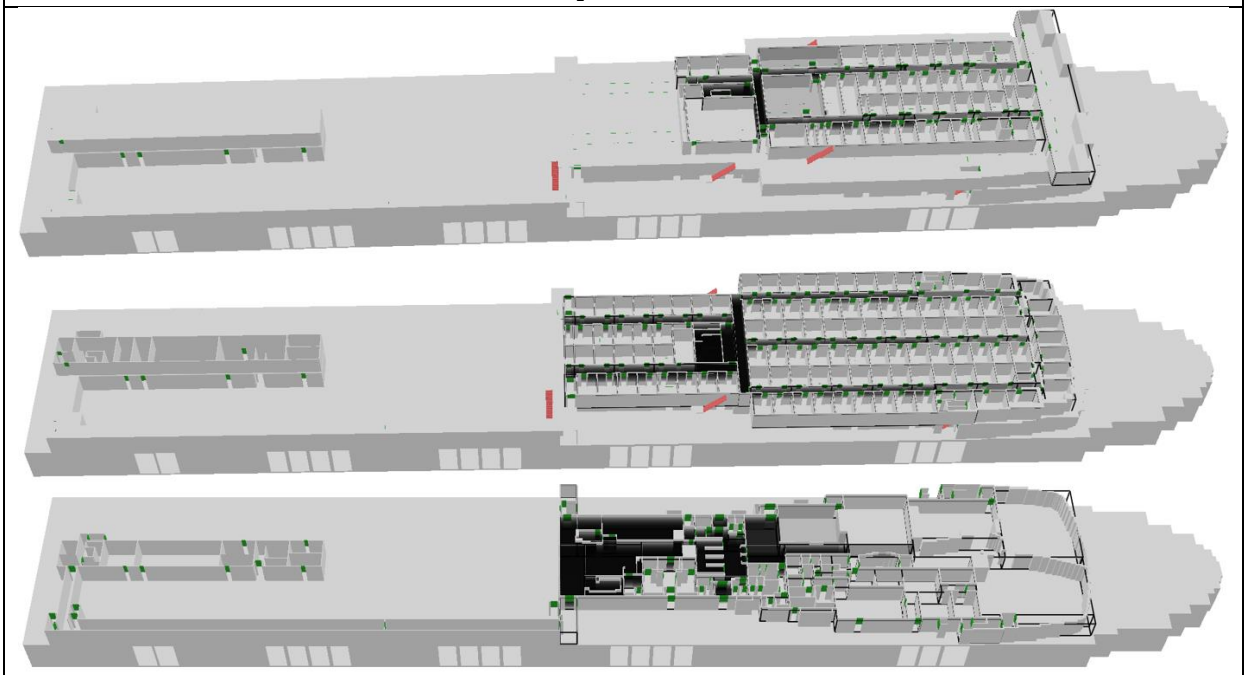

t_1+15 min

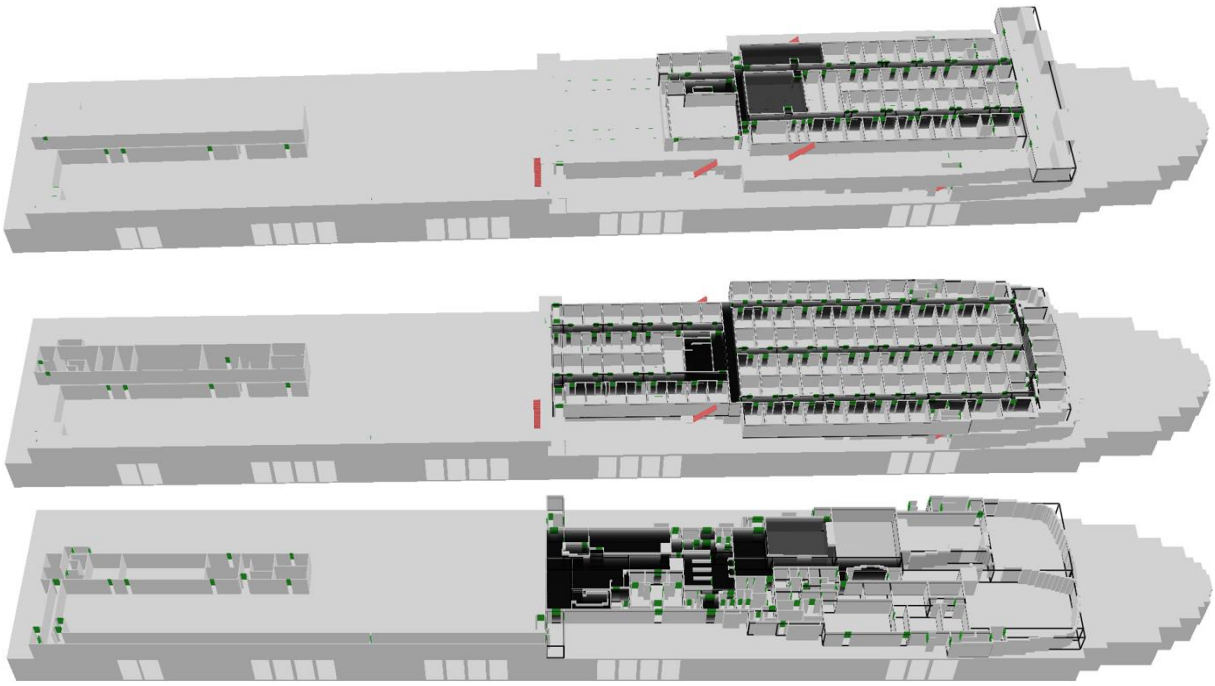

t_1+20 min

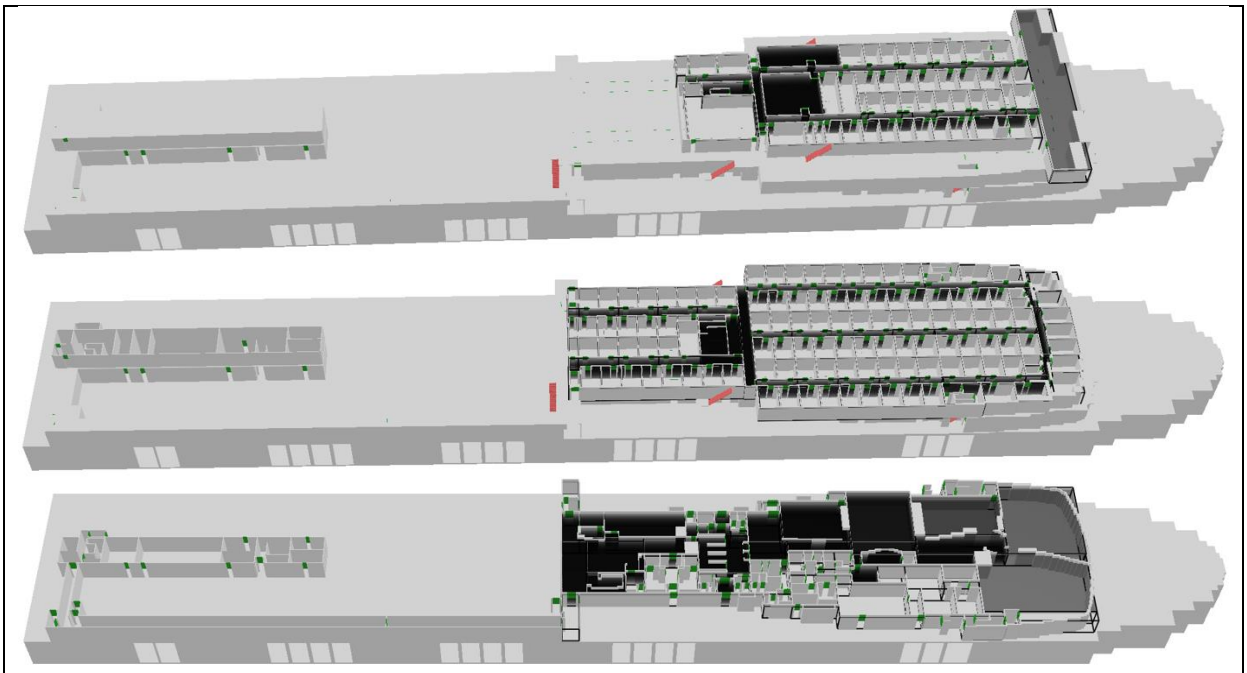

t_1+25 min

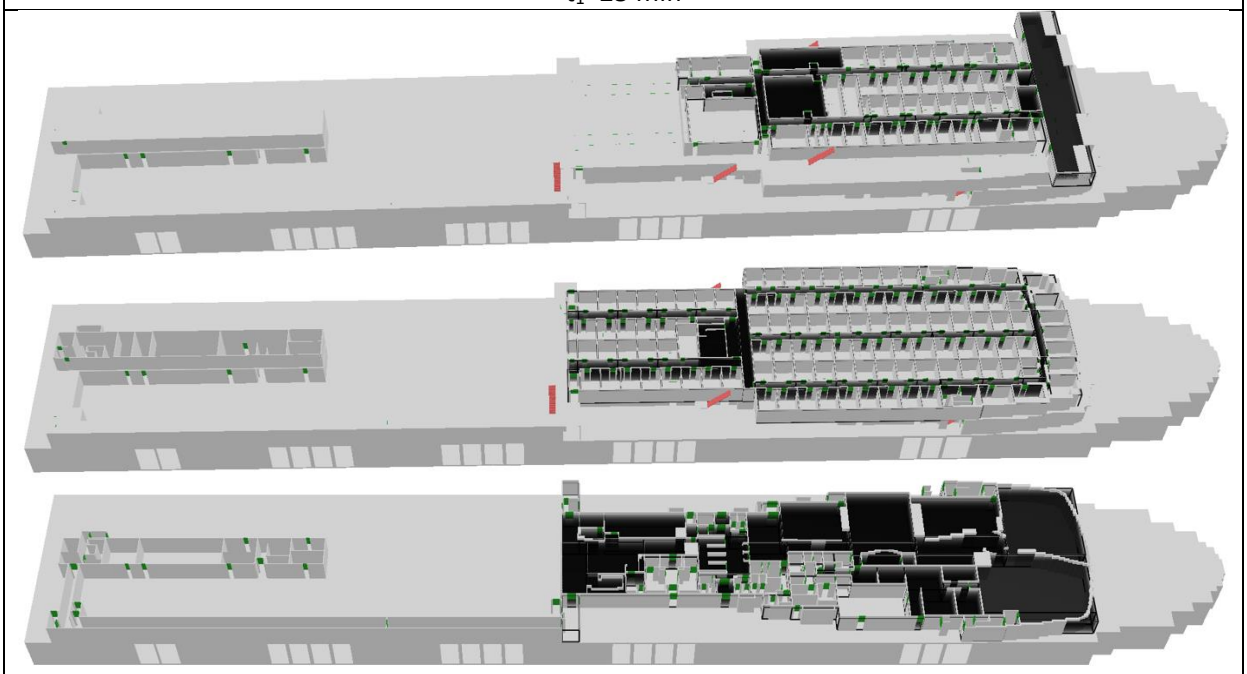

t_1+30 min

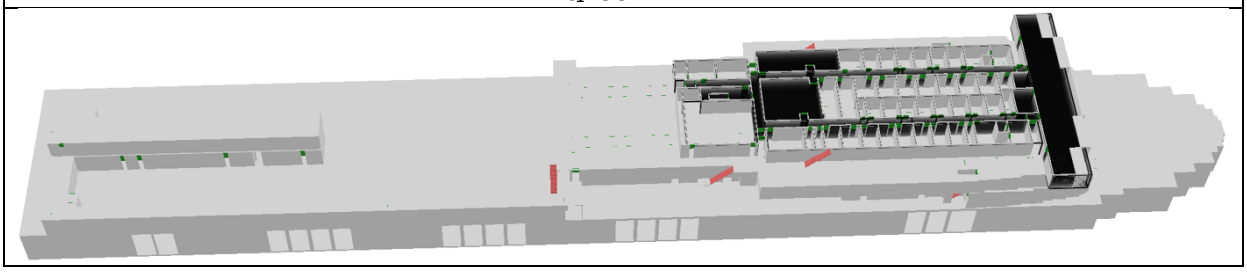

Figure 20: Scenario SF3.3: smoke spread in the accommodation part of the Stena Flavia (decks 5 to 7) at different times from time t_1, when the fire/smoke spreads to the accommodations, here t_1 ≈29 min. The "red star" symbol indicates the location of the AS (here, the restaurant) on deck 5.

Evacuation

The first step in the evacuation process is the assembly phase during which all passengers and crew must join one of the assembly stations when the evacuation order is given. The signal is given to people when the fire is detected (t_{dec}) and when the detection is confirmed by a clearing of doubt (t_{con} estimated at 3 min for these simulations). When the fire alarm sounds, it is necessary to take into account a response time of people (i.e., the time required for people to start their travel to the assembly station). According to the guidelines of MSC.1/Circ.1533 [49], these times are 5 min for a day scenario and 10 min for a night scenario.

According to the general arrangement plan of the Stena Flavia ship, 466 people are nominally considered to be on board the ship, initially located in their cabins (for passengers), workstations or offices (for crew members).

The model parameters are set to:

- 1.02 m/s for the free walking speed. This average value takes into account the different possible categories of people (Table 3.1 from MSC.1/Circ.1533, Appendices 1 and 3 [49]) and the walking speed on flat terrains (Table 3.4 from MSC.1/Circ.1533, Appendices 1 and 3 [49]);
- 1.10 pers./s/m for the maximal people flow density per meter at doorways (MSC.1/Circ.1533, Appendix 2 [49], as an average between 0.8 pers./s/m for stairs and 1.3 pers./s/m for doorways).
- 52% decreased free walking speed in stairs according to Table 3.5 from MSC.1/Circ.1533, Appendices 1 and 3 [49].

The restaurant located on deck 5 of the Stena Flavia is considered as the assembly station.

Figure 21 shows the total travel time of people predicted by AMERIGO for an evacuation drill concerning the ro-ro passenger ship Stena Flavia (i.e., without any fire induced effects): the evacuation paths for people are free and accessible. These results take into account the ship geometry, the number of people in the ship and the phenomenon of congestion formation during evacuation.

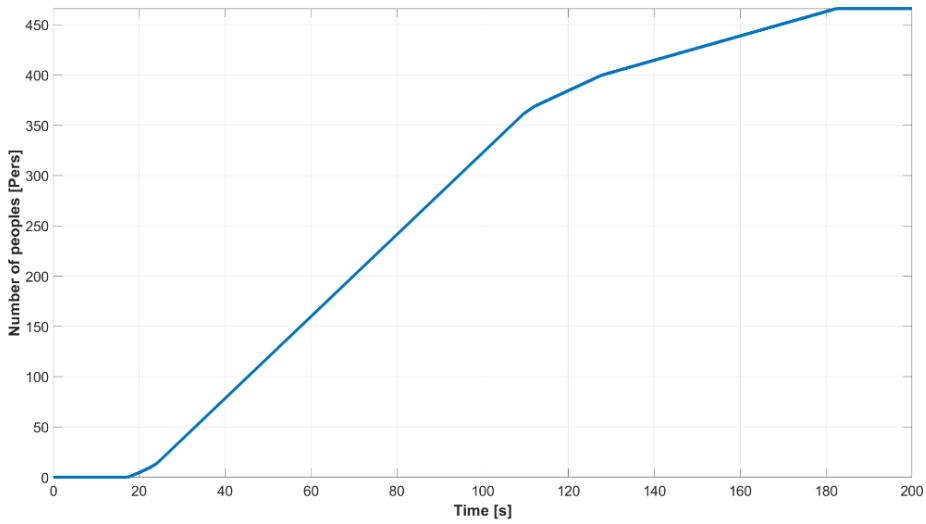

Figure 21: Total travel time of people predicted by AMERIGO for an evacuation drill of the Stena Flavia without fire induced effects. The restaurant is considered as the assembly station and is used as the target area for the assembly phase of evacuation.

The results shown in Figure 21 suggest that a total period of 183 s is needed for people to complete their travel to the assembly station. Considering the response time of 5 min for a day scenario and 10 min for a night scenario, as suggested by MSC.1/Circ.1533 [49], the total evacuation time is estimated at 483 s during the day and 783 s at night.

As a sensitivity analysis, several evacuation scenarios, with and without the presence of fire, have been simulated using the ship geometry and artificially penalizing/blocking such access openings inside the ship. Evacuation simulations show that the travel time of people does not change when considering that a fire has obstructed one of the central doorways connected to the cabins, because there are good alternative routes to the assembly station. This suggests that the geometry of the Stena Flavia is well designed for the fire scenarios considered, so that the people always have several possible paths available to them to safely reach an assembly station. Furthermore, it is observed that the time required for a safe evacuation to the assembly station is shorter than the propagation time of a major fire. Therefore, it is expected that evacuation calculations do not strongly require the

simultaneous modelling of fire development in conjunction with evacuation simulations. The results validate the procedure adopted for this work.

The second phase of evacuation is the abandonment of the ship. Here, we assume that abandonment takes place at sea, which is the case for 80% of ro-ro passenger ships (data available from WP04). The order to leave the ship is given by the Captain when the fire is out of control, for the purpose of the exercise, defined when a second drencher zone is impacted by the fire.

To abandon the Stena Flavia, people have several options: use the lifeboats (with a nominal capacity of 150 persons, see exits 1 and 3 in Figure 22) or the lifecrafts (by the embarkation ladder, see exits 2 and 4 in Figure 22). Moving forward, we set the people flux in using a given device to abandon the ship. This distribution is given in Figure 22.

It is assumed here that people are aware that the abandonment of the ship is imminent, prepared by the crew (reaction time is not taken into account) and that all evacuation devices are ready when the abandonment order is given. The people flux is set at the lifeboat embarkation at 0.166 pers./s/m and 0.104 pers./s/m for the lifecrafts.

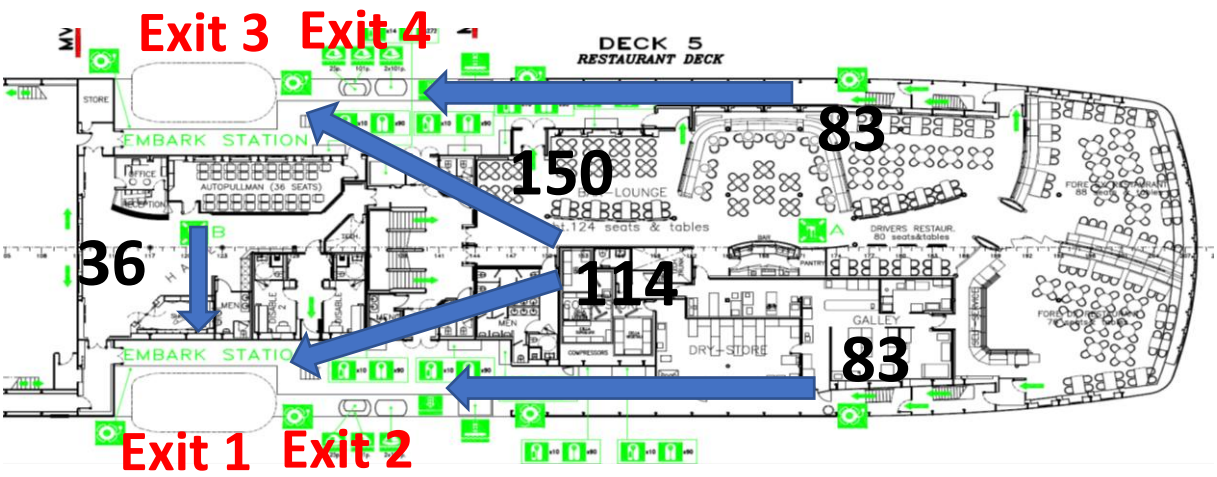

Figure 22: People flux distribution to leave the Stena Flavia.

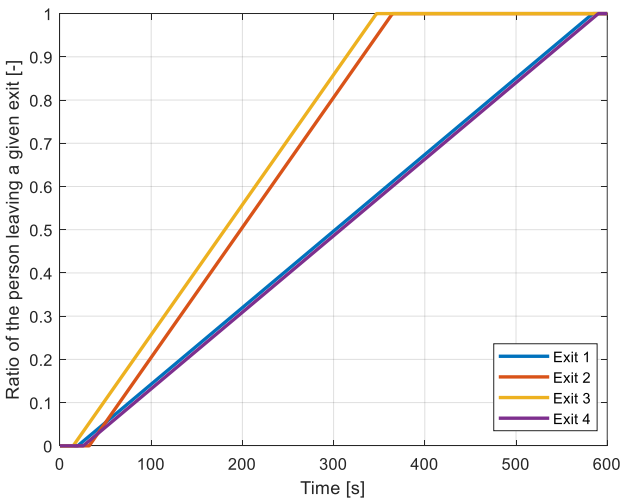

Figure 23: Ratio of the person leaving the ship for a given exit as a function of time. 1 means all the people have abandoned the ship.

Figure 23 represents the ratio of the person leaving the ship for a given exit as a function of time. In a nutshell, 584 s, 365 s, 347 s, and 590 s are necessary to fully evacuate the ship through exits 1, 2, 3 and 4, respectively. These distributions are important because they allow, when the fire reaches the LSA, to determine the total number of people trapped inside the ship by the fire.

As an example, the time lap of the fire scenario SF3.3 is developed below:

- $t = 0$ s fire ignition;
- $t = 41$ s fire detection;
- $t = 221$ s assembly order is given;
- $t = 704$ s people are all gathered in the assembly station;
- $t = 931$ s a second drencher zone is reached / abandonment order is given;
- $t = 1148$ s the thermal condition (temperature criteria) is reached at the LSA, and the safe abandonment is not possible anymore.

For this configuration, only 199 people can leave the ship either by lifeboats or lifecrafts. 267 people are still inside the assembly station and cannot safely leave the ship.

6.2.2 Scenario SF6

For scenario SF6, which corresponds to a fire started in a closed ro-ro space of the Stena Flavia, here deck 3, the same type of results was obtained. Note that we have assumed the presence of some leaks in the ceiling, which is quite realistic, in order to avoid a non-physical pressure rise in the ro-ro space. As shown in Table 5 and Figure 24, the lack of oxygen due to higher confinement makes combustion, and thus its consequences, much less severe than in scenario SF3:

- Smoke detection occurs at 24 s in DZ4;
- Exposure to degraded visibility around the first truck on fire (Swift detection) significantly limits the time available for a safe first response (ATSFR) at 6 min 21s.
- The effective total heat content is reduced to one-third of the theoretical content (i.e., 0.043/0.144 TJ in Table 5), which suggests under-ventilated fire conditions.
- Consequences to cargo, structure and targets are limited to DZ4. Only 6 trucks out of 53 caught fire.
- Regardless of the area of interest of deck 4, degraded visibility is the first tenability criterion that is exceeded.
- No transmission of fire to the upper decks is observed.
- The LSA and disembarkation routes remain safe over time. Persons on board can evacuate safely on both sides of the ship.

Table 5: Scenario SF6: simulation results. SWI means swift detection, DR disembarkation route, SS starboard side, and PS port side. For consequences to human, the value in bold blue blue corresponds to the first tenability criterion that was exceeded in the areas of interest. Times are given in minutes and seconds (min's").

	DZ1	DZ2	DZ3	DZ4	DZ5	DZ6	DZ7			
Heat detection at 54°C	7'13"	4'16"	3'36"	2'04"	3'59"	4'27"	6'24"			
Heat detection at 78°C	9'43"	5'11"	4'25"	2'39"	5'06"	6'08"	8'54"			
Smoke detection	2'56"	1'58"	1'22"	**0'24"**	1'22"	1'58"	2'42"			
Structure damage	-	-	-	12'14"	-	-	-			
Target ignition	-	-	-	6'43"	-	-	-			
First truck ignition	-	-	-	0'00"	-	-	-			
Last truck ignition	-	-	-	-	-	-	-			
no of trucks ignited	6/53									
Predicted/Prescribed total heat content (TJ)	0.043/0.144									
Consequences to human	DZ1	DZ2	DZ3	DZ4	DZ5	DZ6	DZ7	LSA and DR - SS	LSA and DR - PS	SWI
RHF				7'00"				-	-	15'00"
T60	15'18"	18'07"	21'05"	18'34"	20'56"	19'23"	16'20"	-	-	18'34"
CO	10'19"	11'04"	11'47"	11'47"	12'58"	11'54"	11'56"	-	-	
Visibility 5m	4'44"	5'13"	6'37"	6'46"	7'57"	5'42"	5'22"	-	-	6'37"
Visibility 10m	**4'11"**	**4'56"**	**6'12"**	**6'29"**	**7'31"**	**4'31"**	**4'27"**	-	-	**6'21"**

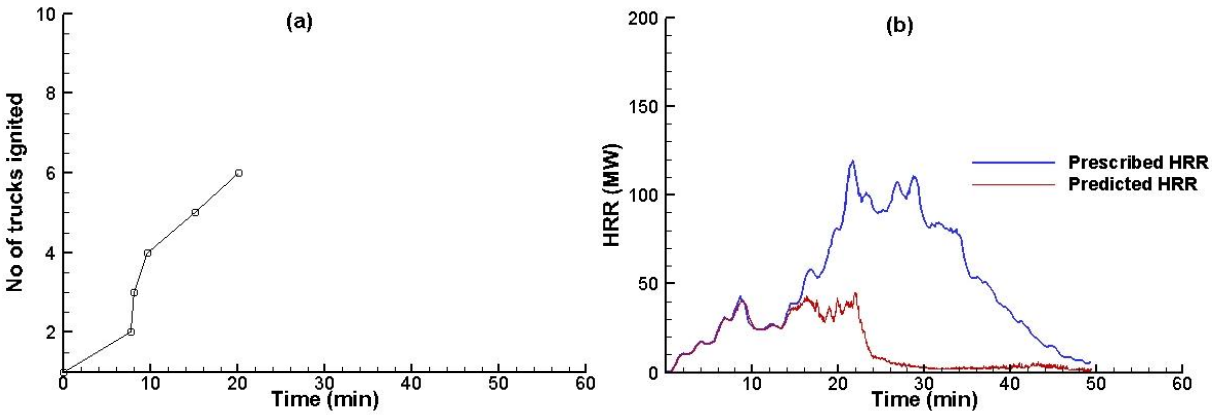

Figure 24: Scenario SF6: a) Number of truck ignited vs. time, and b) comparison between the time evolutions of the theoretical HRR (i.e., the total pyrolysis rate multiplied by the chemical heat of combustion) and effective HRR.

For the evacuation aspect, the SF6 scenario is not penalizing since the fire occurs on deck 3 and no second drencher zone is impacted by the fire. Therefore, it is assumed that no abandonment will be ordered. All people are safely gathered in the assembly station.

6.3 Qualitative comparison with reported ro-ro ship accident chronologies

To verify the severity of the simulation results, reported timelines of real ro-ro space accidents were considered (Table 6). However, firstly, past accidents cannot cover all possible outcomes and the level of detail of the consequences depends on what was reported by the investigators; secondly, the collected data that can be used turns out to be limited. For example, a few questions arise: what were the environmental conditions at the time of the fire? What was the origin of the fire, especially with respect to openings? What were the cargo load and layout? In addition, the data provided is open to interpretation: for example, what does "fire is on the entire deck" mean?

During the review, the reported time when firefighting (excepted boundary cooling or other firefighting to ensure safe evacuation) has been given up and ship abandonment has been ordered was subjectively categorized as “fire out of control”. For the comparison with the simulations, we assumed that the fire is out of control when a DZ is fully involved in the fire (all trucks in the DZ are on fire). For example, for scenario SF3.3, this occurred at 15 min 35 s when the last truck of DZ15 ignited (Table 4), while it does not occur for scenario SF6 (Table 5).
Nevertheless, and although the ship configurations are different, it is possible to compare the onset times of some events for comparable fire scenarios (e.g., no, or very late activation of fixed water-based fire extinguishing system; type of ro-ro ship), as shown in Table 6.

For fires originating from ro-ro spaces, the qualitative comparison shows that numerical results are consistent with the observations reported by the investigators, whereas the predicted consequences of a fire started in a closed ro-ro space were underestimated. On this last point, the total absence of ventilation and the high level of confinement considered in the numerical simulations may explain the differences observed.

Table 6: Timelines of some ro-ro space accidents.

Ship name	Ship type	Fire origin (ro-ro space)	Fixed fire-extinguishing system released?	Timeline of past accidents	Present simulations
Lisco Gloria	Ro-pax	Open (garage)	No	t_0 +9 min: Smoke in cabins	Not observed for Magnolia Seaways, scenario 8 (MS8): insulation integrity and ro-ro containment are preserved in this fire simulation
				t_0 +11 min - $t0$ +15 min: Fire in the whole garage t_0 +46 min: Fire on the entire deck	MS8: Fire is out of control at t_0 +38 min. The fire ignited the 29 vehicles located in the covered part of the deck, but it did not propagate to the entire deck
Norman Atlantic	Ro-pax	Open	No	t_0 +15 min: Flames out from side openings	t_0 +21 min for SF1 and SF3: Flames emerged from side openings
				t_0 +23 min: Fire out of control	Fire is out of control at: t_0 +16 min - t_0 + 22 min for SF1 to SF5 (For the ro-ro cargo Magnolia Seaways: t_0 +43 min for MS9 and t_0 +58 min for MS10)
Republica Di Roma	Ro-ro cargo	Closed	Yes (but very late)	t_0 +40 min: Fire spreads rapidly and significant ship damages. t_0 +145 min: Fire out of control, smoke spreads to the entire ship	Not observed for closed ro-ro spaces of the Magnolia Seaways (MS11) (nor for the ro-pax Stena Flavia, SF6)
Und Adriyatik	Ro-ro cargo	Closed	No	t_0 +7 min: Several trucks burning	MS11: 2 trucks burning at t_0 +8 min (for SF6 on the ro-pax Stena Flavia: 3 trucks burning at t_0 +8 min)
				t_0 +15 min - t_0 +20 min: Fire on the entire deck	Not observed for closed ro-ro spaces of the Magnolia Seaways (MS11) (nor for the ro-pax Stena Flavia, SF6)
				t_0 +23 min: Smoke in accommodations	At t_0 +20 min for SF6 and at t_0 +14 min for MS11, the hot smoke filled the deck and could spread through unexpected openings (not modelled)
				t_0 +23 min - t_0 +27 min: Fire spreads to deck above	t_0 +10 min for MS11: Fire spreads to deck above
				t_0 +27 min - t_0 +30 min: Smoke in muster station t_0 +35 min - t_0 +42 min: Fire blocks escape routes to the LSA t_0 +45 min – t_0 +72 min: Fire spreads to accommodation and bridge	Not observed for MS11: insulation integrity and ro-ro containment are preserved (idem for the ro-pax Stena Flavia, SF6)

t_0: Detection time.

7 Identification of critical fire scenarios

Main authors of the chapter: Bernard Porterie and Yannick Pizzo, RS2N, and Anthony Collin, LUL.

Fire simulation and evacuation modelling can be used to identify critical fire scenarios. This can be done by analysing the consequences to people, cargo, and ship structure for a wide range of fire scenarios, varying, for example, the location of fire, the vehicle load, environmental conditions, or ventilation conditions. Unfortunately, the number of scenarios for simulating fires in ro-ro spaces is severely limited by the computational time needed (i.e., about one week for an hour of fire simulation). Within this context, the partners involved in Action 4-A selected fire scenarios that were expected to have severe consequences, to which were added some accidental scenarios (see Table 2 and [39]). Table 7 summarizes the fire consequences to people, cargo, and ship for the selected fire scenarios.

Except for fire scenarios SF6, MS7, and MS11, the selected fire scenarios can be considered as critical depending on the target considered:

- Persons on board:
  If people can stay in the assembly station long enough, waiting the fire to decay, a safe and orderly evacuation can be ensured for most of the fire scenarios studied. The path to reach the LSA may depend on the fire source location and wind conditions.
  Fire scenarios SF3.2 to SF3.4 can be considered as very critical because accommodations were involved in fire and/or smoke, which could lead to serious consequences to persons on board, especially when they are gathered in the assembly station. A reassignment of the assembly station is therefore necessary.
- Ship:
  Fires originating from open ro-ro space (scenarios SF1 to SF5, MS9 and MS10) led to severe consequences to ship and targets. All or most of the DZ and targets in the ro-ro space were damaged. For MS8, the fire that started in the open (garage) ro-ro space ignited the 29 vehicles located in the covered part of the deck, but it did not propagate to the entire deck.
- Cargo:
  When the fire originated from an open ro-ro space, all or most of the cargo was damaged. This occurred for scenarios SF1 to SF5, MS9 and MS10.
  For scenarios SF6 and MS11, where the fire originated from a closed ro-ro space, the combustion was strongly under-oxygenated, which limits the consequences of fire to cargo. When the fire started on a partially covered deck, the cargo damage was dependent on the location of the fire-starting point. When the fire ignition point was in the covered part of the weather deck (i.e., garage), all the trucks located herein ignited (scenario MS8); otherwise, damage was strongly limited (scenario MS7).

The criticality of the selected fire scenarios must be nuanced for two main reasons: first, no means of firefighting the fire has been engaged, and secondly, the load capacity of vehicles in the ro-ro spaces was 100%. However, the results obtained for the selected serious fire scenarios could be used to evaluate, or even challenge, the solutions related to fire containment and evacuation that might be proposed.

Table 7: Summary of fire consequences to people, ship, and cargo for the selected scenarios. SF stands for Stena Flavia, MS for Magnolia Seaways, SS for starboard side, PS for port side. Times are given in minutes and seconds (min's").

Fire scenario	Fire "out of control"	Cargo damage*	Ship damage**		Fire integrity	
			Structure	Targets	AS	LSA and DR, and RS if applicable
SF1	17'13"	All	All	All	Safe	SS: safe for $t \lesssim 11'$ PS: safe for $t \lesssim 11'$ and $t > 57'$
SF2	21'40"	All	6/8	All	Safe	SS and PS: safe for $t < 19'$ and $t > 27'$
SF3	15'35"	All	All	All	Safe	Safe for $t \lesssim 10'$. The most restrictive criterion is visibility since it makes LSA and DR impractical after 1 h of fire***
SF3.1	15'36"	All	All	All	Safe	SS: safe for $t \lesssim 25'$ and $t > 44'$ PS: safe for $t \lesssim 25'$ and $t > 43'$ After 44' of fire, evacuation can be done safely, with a visibility of 5 m or more on the portside, and no restriction on the starboard side.
SF3.2	15'35"	All	All	All	Unsafe for $t \gtrsim 1h05'$	Safe for $t \lesssim 10'$ The most restrictive criterion is visibility since it makes LSA and DR impractical after 1 h of fire***
SF3.3	15'35"	All	All	All	Unsafe for $t \gtrsim 49'$	
SF3.4	15'35"	All	All	All	Unsafe for $t \gtrsim 18'$	
SF4	17'51"	All	All	All	Safe	Due to the short duration and low levels of exposure to heat and smoke, evacuation can be done safely on both sides of the ship
SF5	19'29"	All	7/8	All	Safe	SS: safe for $t \lesssim 14'$ and $t > 51'$ PS: safe for $t \lesssim 14'$ and $t > 53'$
SF6	-	6/53	1/7	1/7	Safe	Safe at all times
MS7	-	-	-	-	Safe	Safe at all times
MS8	38'29"	29/80	-	All	Safe	RS and DR on the PS of the weather deck: safe for $t \lesssim 21'$ and $t > 56'$ RS on the SS of the weather deck: always safe, but the path to get there could be exposed to an excessive RHF LSA on the 1st house deck: safe for $t \lesssim 20'$***
MS9	43'05"	61/70	All	All	Safe	RS and DR on the PS of the weather deck: safe for $t \lesssim 19'$ RS on the SS of the weather deck: safe for $t \lesssim 48'$ LSA on the 1st house deck: safe for $t \lesssim 7'$***
MS10	57'43"	61/70	2/4	3/4	Safe	RS and DR on the PS of the weather deck: safe for $t \lesssim 19'$ RS on the SS of the weather deck: always safe, but the path to get there could be exposed to an excessive RHF LSA on the 1st house deck: safe for $t \lesssim 6'32"$***
MS11		3/20	-	All	Safe	Safe at all times

*Number of trucks ignited in the ro-ro space where the fire originated.
**Number of drencher zones in the fire origin ro-ro space where the structure was damaged, or targets ignited.
***Need for longer simulations to cover 3 hours of fire for the orderly evacuation and abandonment of the ship.

8 Conclusion

Main authors of the chapter: Bernard Porterie, RS2N.

A simulation tool was developed to evaluate the consequences of fire to people, cargo, and ship's structure, for selected scenarios. Simulations of fire propagation in closed and open ro-ro spaces, as well as on the weather decks, of two generic ro-ro ships, namely the Stena Flavia and the Magnolia Seaways, have been conducted varying the location of the first ignition truck and wind conditions.

Fire consequences in ro-ro spaces, accommodations, embarkation stations and disembarkation routes, were evaluated in terms of delays after which given thresholds, related to the safety of persons on board and the integrity of the ship's structure, cargo, and potential targets, are exceeded. For the selected fire scenarios, the simulation results were provided to project partners to feed the risk model (as far as possible), in the form of directly usable summary files (refer to LASH FIRE deliverable D04.5 "Development of holistic risk model report"). For example, the fire and smoke spread results were used to quantify the cargo and ship loss associated to scenario B ("medium fire") described in D04.5. Critical scenarios were identified that could be used to evaluate, or even challenge, the solutions related to fire containment and evacuation that might be proposed.

It was found that the evacuation process is strongly dependent on the geometry of the ship, its cargo, and the total number of people on board.

For the Stena Flavia, several worst credible fire scenarios had a huge impact on consequences for passengers and crew. In particular, for cases SF3.2 to SF3.4, more than half of the total people can be trapped by the fire and are unable to safely leave the ship. Nevertheless, the consequences of such fires can be minimized by using emergency response procedures already implemented by ship operators (such as firefigthing, boundary cooling, etc.) or by external intervention (fire rescue team, tug boat, or helicopter), which cannot be taken into account in a numerical simulation.

On the contrary, for the fire scenarios proposed on the Magnolia Seaway, there were no consequences on the total number of fatalities because the fire did not reach the accommodations and the total number of people aboard this ship is very low.

9 References

1. McGrattan, K., Hostikka, S., McDermott, R., Floyd, J., Weinschenk, C., & Overholt, K. (2020). Fire Dynamics Simulator, Technical Reference Guide, Volume 1: Mathematical Model, NIST Special Publication 1018-1, National Institute of Standards and Technology, Gaithersburg, Maryland.
2. McGrattan, K., Hostikka, S., Floyd, J., McDermott, R., & Vanella, M. (2020). Fire Dynamics Simulator, Technical Reference Guide, Volume 3: Validation, NIST Special Publication 1018-3. National Institute of Standards and Technology, Gaithersburg, Maryland.
3. Mense, M., Pizzo, Y., Prétrel, H., Lallemand, C., & Porterie, B. (2019). Experimental and numerical study on low-frequency oscillating behaviour of liquid pool fires in a small-scale mechanically-ventilated compartment. *Fire Safety Journal, 108*, 102824. doi.org/10.1016/j.firesaf.2019.102824
4. Trouve, A., & Wang, Y. (2010). Large eddy simulation of compartment fires. *International Journal of Computational Fluid Dynamics, 24*, 449-466. doi.org/10.1080/10618562.2010.541393
5. Suard, S., Lapuerta, C., Kaiss, A., & Porterie, B. (2013). Sensitivity analysis of a fire field model in the case of a large-scale compartment fire scenario. *Numerical Heat Transfer, 63*(12), 879-905. 10.1080/10407782.2012.725010
6. Jones, W. W., Peacock, R. D., Forney, G. P., & Reneke, P. A. (2004). CFAST – Consolidated Model of Fire Growth and Smoke Transport (version 5) – Technical reference guide, NIST Special Publication 1030.
7. Cheng, H., & Hadjisophocleous, G. V. (2011). Dynamic modeling of fire spread in building. *Fire Safety Journal, 46*(4), 211-224. 10.1016/j.firesaf.2011.02.003
8. Floyd, J., Hunt, S., Williams, F., & Tatem, P. (2005). A Network Fire Model for the Simulation of Fire Growth and Smoke Spread in Multiple Compartments with Complex Ventilation. *Journal of Fire Protection Engineering, 15*, 199-228. 10.1177/1042391505051358
9. Ramachanandran, G. (2002). Stochastic models of fire growth, Section 3, Chapter 15, The SFPE Handbook of Fire Protection Engineering (3rd ed.), NFPA, Quincy, MA.
10. Helbing, D. (1991). A mathematical model for the behavior of pedestrians. *Behavioral science, 36(4)*, 298-310. 10.1002/bs.3830360405
11. Hughes, L. (2002). A continuum theory for the flow of pedestrians. *Transportation Research Part B: Methodological, 36*, 6507-535. 10.1016/S0191-2615(01)00015-7
12. Kuligowski, E. D., Peacock, R., & Hoskins, B. L. A Review of Building Evacuation Models Technical Note (NIST-TN) - 1680, 2010.
13. Meng Shi, Eric Wai Ming Lee, Yi Ma, Wei Xie, & Cao, R. (2021). The density-speed correlated mesoscopic model for the study of pedestrian flow. *Safety Science, 133*, 105019. 10.1016/j.ssci.2020.105019
14. K. Togawa. Study on fire escapes based on the observation of multitude currents Building Research Institute, Ministry of Construction, 1955.
15. MSC/Circ.1002 (2001). Guidelines on Alternative Design and Arrangements for Fire Safety. International Maritime Organization, London.

16. MSC.1/Circ.1552 (2006). Amendments to the Guidelines on Alternative Design and Arrangements for Fire Safety (MSC/Circ. 1002). International Maritime Organization, London.
17. Spearpoint, M. J. (2008) Fire engineering design guide (3rd ed), Christchurch, N.Z.: New Zealand Centre For Advanced Engineering, Chapter 4, 217-234.
18. Purser, D. A. (2008). Assessment of Hazards to Occupants from Smoke, Toxic Gases, and Heat, in The SFPE Handbook of Fire Protection Engineering (4th ed), National Fire Protection Association; Society of Fire Protection Engineers: Quincy, Mass. Bethesda, Md., Section 2, Chapter 6, pp. 2-96.
19. Kirby, B. R. (1986). Recent developments and applications in structural fire engineering design – A review. *Fire Safety Journal, 11(3)*, 141-179.
20. Rackauskaite, E., Kotsovinos, P., & Rein, G. Computational analysis of failure criteria of a multi-storey steel frame exposed to fires: thermal vs. Structural, Imperial College London, 2017.
structuresinfireforum.com/sites/structuresinfireforum.com/files/attachments/freestyle-page/20170630/ERackauskaite_2017_TFM.pdf
21. Consalvi, J-L., Porterie, B., & Loraud, J-C. (2003). Method for computing the interaction of fire environment and internal solid regions. *Numerical Heat Transfer-Part A 43*(8), 777-805.
doi.org/10.1080/713838149.
22. Consalvi, J-L., Porterie, B., & Loraud, J-C. (2005). A Blocked-Off Region Strategy to Compute Fire Spread Scenarios Involving Internal Flammable Targets. *Numerical Heat Transfer-Part B 47*, 419-441.
doi.org/10.1080/10407790590919234.
23. Smith, E. E., & Satija, S. (1983). Release Rate Model for Developing Fires. *Journal of Heat Transfer 105*(2), 281-287.
dx.doi.org/10.1115/1.3245575
24. Smith, E. E., & Green, T. J. (1988). *Release rates for a mathematical model*. American Society for Testing and Materials, Philadelphia.
25. Toal, B. R., Silcock, G. W. H., & Shields, T. J. (1989). An examination of piloted ignition characteristics of cellulosic materials using the ISO ignitability test. *Fire and Materials 14*(3), 97-106.
dx.doi.org/10.1002/fam.810140304
26. Shields, T. J., Silcock, G. W. H., & Murray, J. J. (1993). The effects of geometry and ignition mode on ignition times obtained using a cone calorimeter and ISO ignitability apparatus. *Fire and Materials 17*(1), 25-32.
dx.doi.org/10.1002/fam.810170105
27. Shields, T. J., Silcock, G. W. H., & Murray, J. J. (1994). Evaluating ignition data using the flux time product. *Fire and Materials 18*(4), 243-254.
dx.doi.org/10.1002/fam.810180407
28. Silcock, G. W. H., & Shields, T. J. (1995). A protocol for analysis of time-to-ignition data from bench scale tests. *Fire Safety Journal 24*(1), 75-95.
dx.doi.org/10.1016/0379-7112(95)00003-C
29. Tohir, M. (2015). PhD thesis, University of Canterbury, NZ.
30. SFPE Engineering Guide (2002). Piloted ignition of solid materials under radiant exposure.
31. Jin, T. (1978). Visibility through fire smoke. *Journal of Fire and Flammability, 9*, 135-155.
32. Mulholland, G. W., & Croarkin, C. (2000). Specific Extinction Coefficient of Flame Generated Smoke. *Fire and Materials 24*, 227–230.

10.1002/1099-1018(200009/10)24:53.0.CO;2-9

33. Evans, D. D., & Stroup, D. W. (1985). Methods to Calculate the Response Time of Heat and Smoke Detectors Installed Below Large Unobstructed Ceilings, NBSIR 85-3167, National Bureau of Standards.
34. FIRESAFE II – Detection and Decision. (2018). Final Report, Version 1.1.
35. Huang, Y., Chen, X., & Zhang, C. (2019). Numerical simulation of the variation of obscuration ratio at the fire early phase with various soot yield rate. *Case Studies in Thermal Engineering 18*, 100572. 10.1016/j.csite.2019.100572
36. MSC.1/Circ.1035 (2002). Guidelines for the use and installation of detectors equivalent to smoke. International Maritime Organization, London.
37. "Revised guidelines on the evacuation analysis for new and existing passenger ships", MSC.1/Circ.1533, International Maritime Organization, 2016.
38. Kacem, A., Lallemand, C., Giraud, N., Mense, M., De Gennaro, M., Pizzo, Y., Loraud, J-C., Boulet, P., & Porterie, B. (2017). A Small-World Network Model for the Simulation of Fire Spread Onboard Naval Vessels. IAFSS 2017, Lund, Sweden.
39. Scenarios' identification workshop, LASHFIRE Project, November 6, 2021.
40. Bailey, J. L., Forney, G. P., & Tatem, P. A., Jones, W. W. (2002). Development and Validation of Corridor Flow Submodel for CFAST. *Journal of Fire Protection Engineering 12*, 139-161. 10.1177/10423910260620473
41. NFPA 502 (2004). *Standards for road tunnels, bridges and other limited access highways*. National Fire Protection Association.
42. BD 78/99 (1999). *Design manual for roads and bridges*. The Highways Agency.
43. PIARC (1999). *Fire and smoke control in road tunnel*. Permanent International Association of Road Congress.
44. Babrauskas, V., & Walton, W. D. (1986). A simplified characterization of upholstered furniture heat release rates. *Fire Safety Journal 11*(3), 181-192. dx.doi.org/10.1016/0379-7112(86)90061-5271
45. Mowrer, F. W., & Williamson, R. B. (1990). Methods to characterize heat release rate data. *Fire Safety Journal 16*(5), 367-387. dx.doi.org/10.1016/0379-7112(90)90009-4
46. Numajiri, F., & Furukawa, K. (1998). Mathematical expression of Heat Release Rate Curve and proposal of Burning Index. *Fire and Materials 22*(1), 39-42. dx.doi.org/10.1002/(SICI)1099-1018(199801/02)22:1<39::AID-FAM629>3.0.CO;2-H
47. Ingason, H. (2009). Design fire curves for tunnels. *Fire Safety Journal 44*(2), 259-265. dx.doi.org/10.1016/j.firesaf.2008.06.009
48. Cheong, M. K., Spearpoint, M. J., & Fleischmann, C. M. (2008). Design fires for vehicles in road tunnels. Proc. 7th International Conference on Performance-Based Codes and Fire Safety Design Methods, Auckland, New Zealand, pp.229-240. www.sfpe.org/upload/conference_program_updated_012408.pdf
49. Versteeg, H. K., & Malalasekera, W. (1995). *An Introduction to Computational Fluid Dynamics: The Finite Volume Method*. Longman Scientific & Technical.
50. Panofsky, H., & Dutton, J. (1984). *Atmospheric Turbulence*. Wiley.
51. European Committee for Standardization. (2005). Eurocode 3: Design of steel structures. Part 1-2: General rules. Structural fire design. (EN Standard EN 1993-1-2:2005).
52. Hansen, P. A. (1995) Heat release rate and response of vehicles. SYNTEF Report STF25 A95039.

53. Juma, N., Korenova, Z., Markos, J., Jelemensky, L., & Bafrnec, M. (2006). Experimental study of pyrolysis and combustion of scrap tire. *Polymers for Advanced Technologies 18*(2), 144-148. 10.1002/pat.811
54. Babrauskas, V. (2003). Ignition Handbook, Fire Science Publishers, Issaquah, WA.
55. Graf, S.H. (1949). Ignition temperatures of various papers, woods, and fabrics, Bulletin n° 26, Engineering Experiment Station, Oregon State College, Corvallis.
56. ASTM Standard D777. (1997, Reapproved 2002). Standard Test Methods for Flammability of Treated Paper and Paperboard, ASTM International, 100 Barr Harbor Drive, PO Box C700, West Conshohocken, PA 19428-2959, United States.
57. White, K.A. (1996). Ignition of Cellulosic Paper at Low Radiant Fluxes, NASA Technical Memorandum 107311, Lewis Research Center, Cleveland, Ohio.

10 Indexes

10.1 Index of tables

10.2 Index of figures

11 Appendices

11.1 Test cases and model validation for evacuation.

This section is dedicated to the qualitative and quantitative verification and validation of the evacuation model AMERIGO according to the guidelines of MSC.1/Circ.1533 from IMO [37]. Several configurations are considered for this purpose, including test cases from MSC.1/Circ.1533 as well as real evacuation experiments, demonstrating the capabilities of AMERIGO.

11.1.1 Test cases of IMO

In this part, the evacuation model is evaluated based on test cases proposed by IMO in MSC.1/Circ.1533 [37]. There are 12 test cases proposed by MSC.1/Circ.1533 but some of them are out of the scope of a mesoscopic model like AMERIGO, since such models do not aim to track the movement of each individual passenger, so those tests cases are not considered here. The other test cases evaluate the evacuation model holistically such that they are more appropriate for the evaluation of mesoscopic models like AMERIGO. Accordingly, we consider three such test cases, namely cases 8, 9 and 10 in MSC.1/Circ.1533 [37].

Test Case #8. The geometry considers two connected rooms. The two rooms are 10 m wide and 10 m long, connected via a corridor that is 10 m long and 2 m wide and links to the centre of one side of each room. As depicted in Figure 25, one hundred persons are initially located at the back of room 1, and then they start to move to room 2. When the last person enters room 2, this marks the time of evacuation completion.

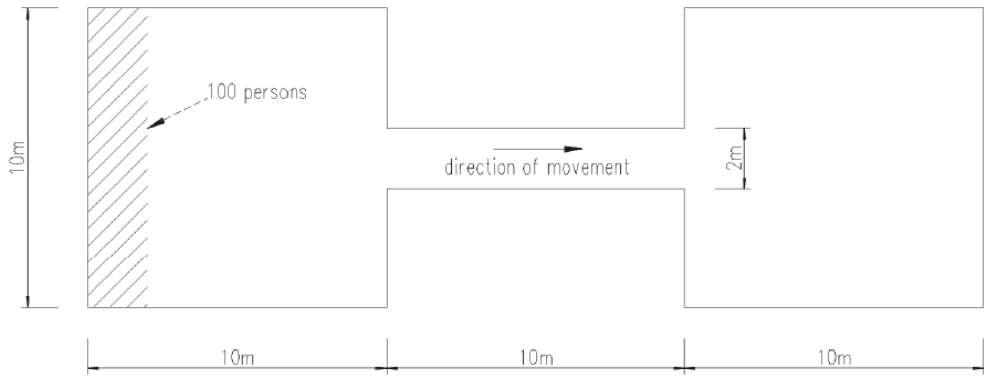

Figure 25: Test case #8 from IMO – Two rooms connected via a corridor.

The free walking speed in the numerical simulations is set at 1.3 m/s according to MSC.1/Circ.1533, appendix 1, Table 3.4 [37], considering that the evacuees are male and 30-50 years old. Moreover, the flux of people at the doorway is limited to 1.1 pers./s/m according to MSC.1/Circ.1533, appendix 2. The model of test case 8 in the corresponding AMERIGO simulation is shown in Figure 26.

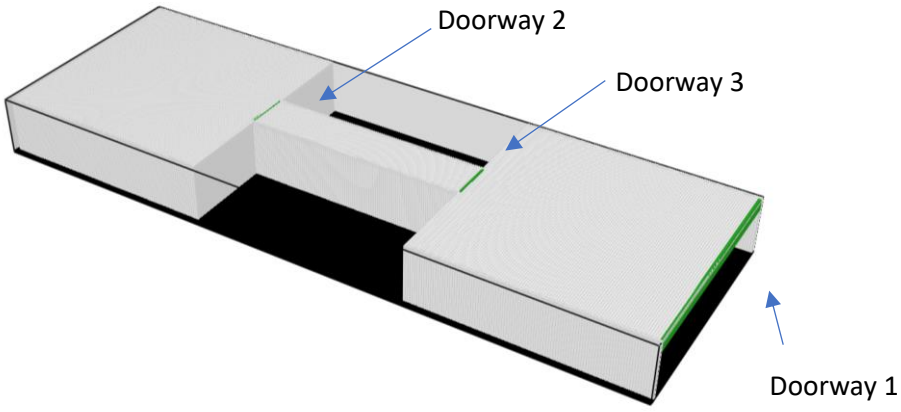

Figure 26: Model of test case 8 in the AMERIGO simulation. The evacuees travel from the left side to the right side and then complete their evacuation by going through doorway 1.

The evolution of the total number of people waiting behind the doorways is shown in Figure 27. The results suggest that a congestion is quickly generated at the first doorway found by the evacuees (i.e., doorway 2 shown in Figure 26). The waiting line counts up to 83 persons. Beyond this "bottleneck" formed at the beginning of the corridor, there is no congestion further along the rest of the escape route. This can be seen in Figure 27 in terms of the zero number of people waiting behind doorway 3.

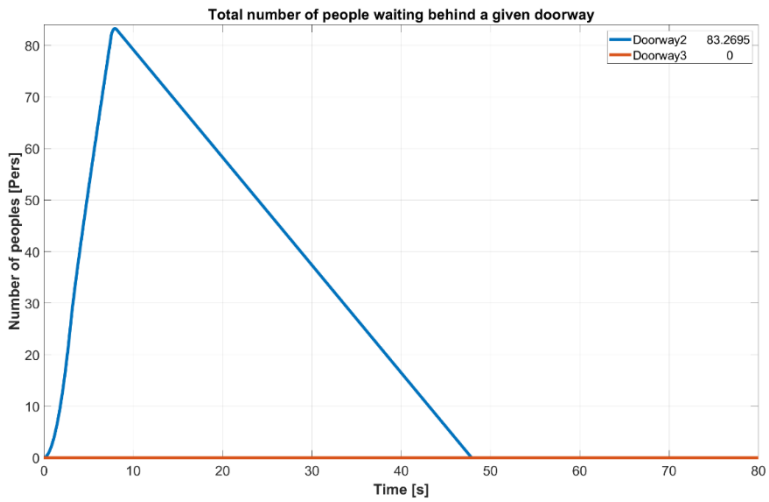

Figure 27: Evolution of the total number of people waiting behind the doorways against time. Doorway 2 is the exit of the first room and doorway 3 is the corridor's exit which connects to the next room (as shown in Figure 26).

Figure 28 gives the evolution of the total number of people leaving the different doorways. One may find it surprising that the number of evacuees leaving the room starts increasing very quickly at the beginning of the evacuation while all the people are initially located at the back of room 1. This is due to an assumption made by the mesoscopic model: the people are uniformly distributed over the defined room area once the evacuation starts to make it possible to determine the influx of people feeding the congestion behind the doorway (i.e., parameter φ_i^{in}). For this test case, a period of 55 s is necessary for the last evacuee to leave the corridor and enter room 2, as Figure 28 indicates. Subsequently, the time of complete evacuation through doorway 1 is predicted to be 63 s. The numerical results show that the maximal flux of people at doorway 2 and 3 is limited to

2.09 pers/s, corresponding approximatively to a people flux of 1.1 pers./s/m given that the corridor is 2 m wide.

These results demonstrate that AMERIGO is capable of reasonably reproducing the evacuation scenario of test case 8 (step 1), with the model being able to predict the reduction of people flux in the corridor connecting the two rooms. The step 2 of test case 8 involves observing the effect of counterflow in the evacuation through the corridor, but this is not considered in the present work because the model of AMERIGO can only consider the travel of people toward the *nearest* target area, such that even if there are multiple target areas, the evacuation proceeds toward only one direction at each given location, and this prevents the creation of counterflow.

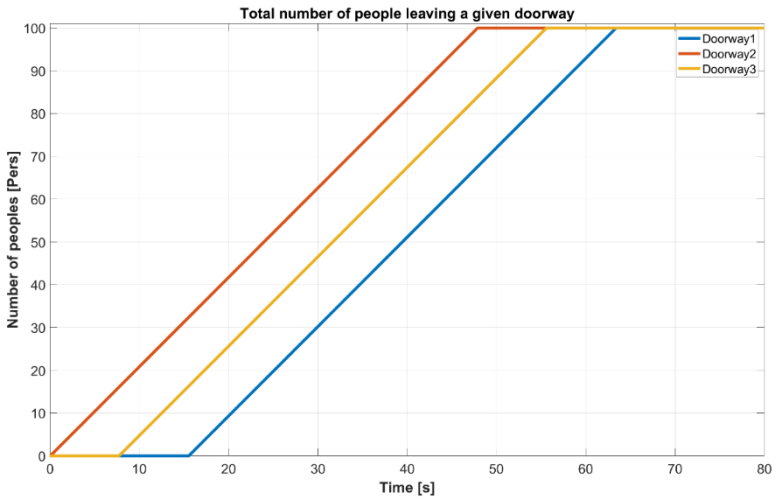

Figure 28: Variation of the total number of persons leaving a given doorway. Doorway 1 is the final exit, doorway 2 is the exit of the first room and doorway 3 is the corridor's exit (as shown in Figure 26).

Test Case #9. The geometry consists of a public room containing 4 exits and 1000 persons uniformly distributed in the room, as presented in Figure 29. In this configuration, persons should leave the room via the nearest exits. Here again, the free walking speed is 1.3 m/s according to MSC.1/Circ.1533, appendix 1, Table 3.4 [37], considering that the evacuees are male and 30-50 years old. Moreover, the flux of people at doorways is limited to 1.1 pers./s/m according to MSC.1/Circ.1533, annex 2. The model of test case 8 in the corresponding AMERIGO simulation is shown in Figure 30.

In the first step, the simulation considers that all the exits are available for the evacuation. Therefore, the total number of people leaving the room by each doorway must be the same, since the people are uniformly distributed within the room at the beginning.

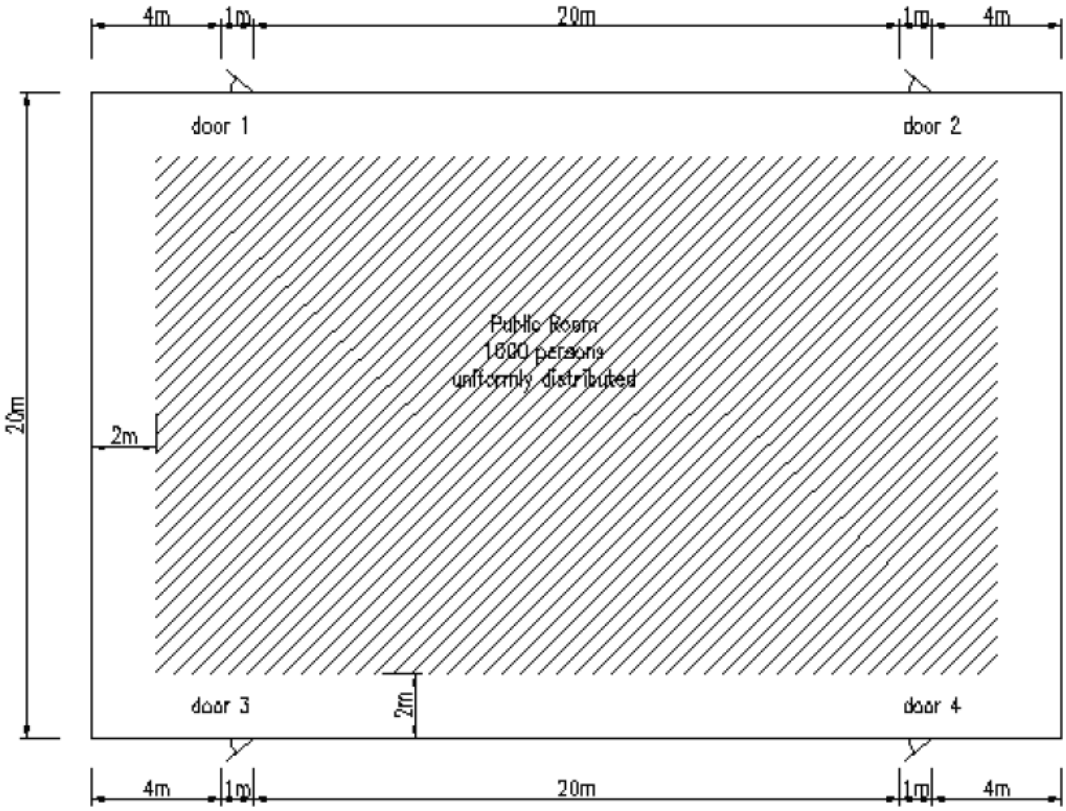

Figure 29: Configuration used for test case 9, looking at the flux of people leaving a large public room.

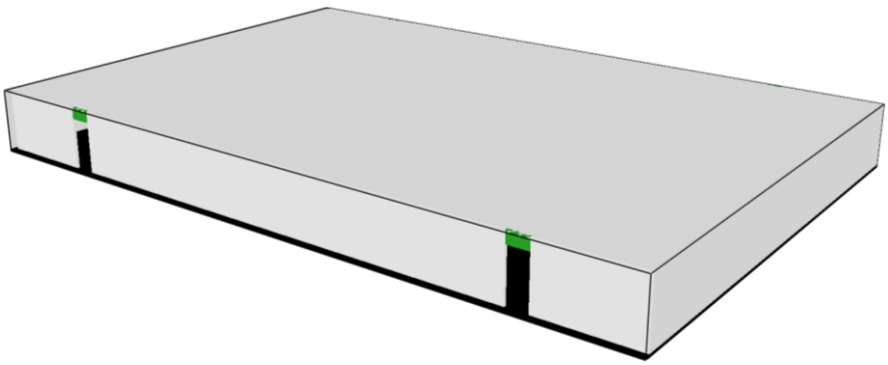

Figure 30: Model of test case 9 in the AMERIGO simulation.

The results of AMERIGO for the free evacuation time of a single person in the geometry of test case 9 are presented in Figure 31 as a function of the person's initial position. Most importantly, Figure 31 shows that all the four exits are used similarly, featuring symmetric contours of evacuation time for the exits. Moreover, it is evident in Figure 31 that for the location farthest away from all the exits, i.e., the centre of the room, a period of 11 s is required to exit the room if there is no congestion.

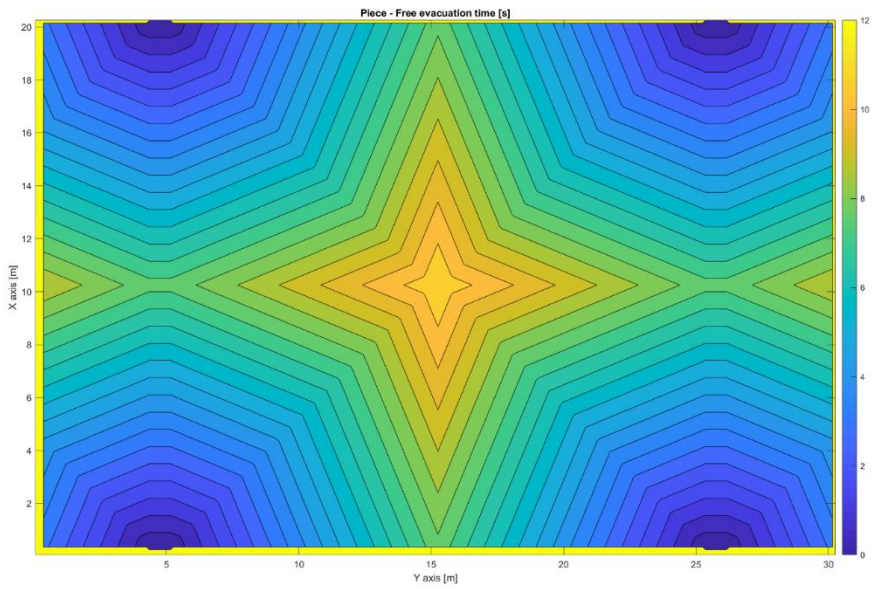

Figure 31: Contour plot of free evacuation time for a single person (no congestion) in test case 9.

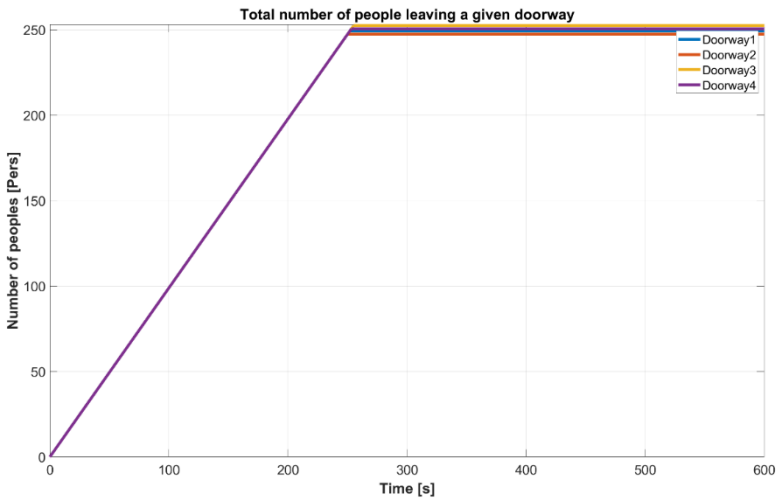

Figure 32: Evolution of the total number of people who have left the four exits of the public room in test case 9 over time.

Figure 32 shows the evolution of the total number of people who have left the public room in test case 9 over time. Given that 1000 people are considered in total and that the geometry is symmetric, it is reasonable that 250 people leave through each exit (after a period of 252 s). This demonstrates that the predictions made by AMERIGO match with the expected results, such that the model is able to simulate the first step of test case 9 successfully.

In the second step of test case 9, two of the four exits are closed, such that the evacuation time is expected to be twice as long as that in the first step. As Table 8 indicates, the predicted evacuation time in the second step is indeed twice as that predicted in the first step, confirming that AMERIGO is capable of reasonably reproducing the evacuation scenario of test case 9.

Table 8: Predictions of evacuation time for the first and second steps of test case 9 (refer to text for the step definitions).

Step	Evacuation time [s]
1	252
2	502

Test Case #10. This case concerns the use of exit routes. As depicted in Figure 33, test case 10 considers a geometry with 12 cabins, a common corridor section and two exits. The initial location of the evacuees is also given in this figure. The two exits are named in Figure 33 as "main exit" (i.e., exit 2) and "secondary exit" (i.e., exit 1). Just as in the previous test cases, the free walking speed is 1.3 m/s according to MSC.1/Circ.1533, appendix 1, Table 3.4 [4], considering that the evacuees are male and 30-50 years old. Moreover, the flux of people at doorways is limited to 1.1 pers./s/m according to MSC.1/Circ.1533, annex 2. The identification number of each cabin door is also shown in Figure 33 in green, while that of the exit doors is shown in red. The expected result is that people proceed to their appropriate exit, i.e., the exit closest to them.

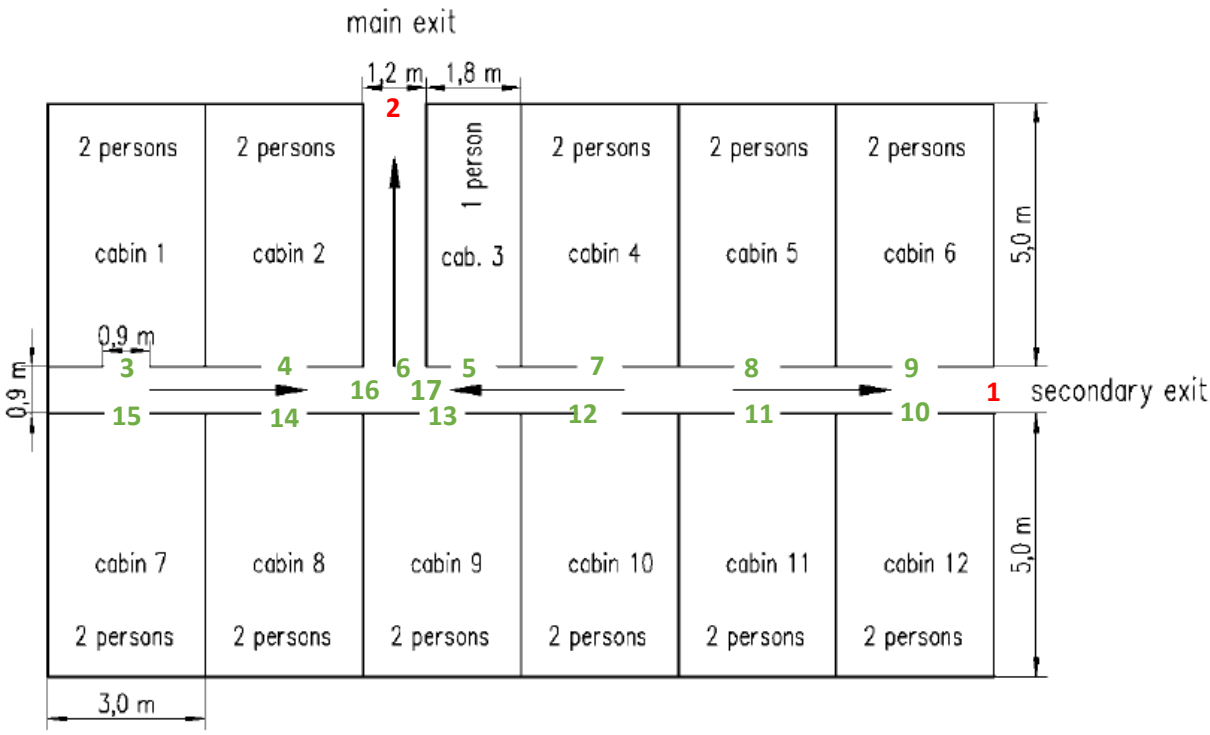

Figure 33: The geometry of the cabin area evacuation in test case 10. The green numbers indicate the identification number of the doors while the red numbers indicate that of the exits.

When no formation of congestion is considered, the AMERIGO simulation predicts that a delay of 12 s is necessary for a single person to evacuate his cabin when it is located at the farthest point from the exit. When congestion is taken into account, the evacuation of the 23 people inside the cabins takes 17.5 s. Consequently, the phenomenon of congestion has only a small effect on the evacuation time in this particular configuration.

The selection of exits 1 or 2 by people in the AMERIGO simulation is shown in Figure 34. The results are very similar to those expected by IMO in MSC/Circ. 1533, although with one minor difference: people in the central cabins 4 and 10 (see cabin numbers in Figure 33) are normally expected to evacuate using the main exit (i.e. doorway 2), although it is not the shortest escape route. However, AMERIGO relies on the shortest escape route and therefore predicts that these

cabins should be evacuated using the secondary exit (i.e., doorway 1), although the resulting difference in the overall evacuation time is insignificant.

For this configuration, it is useful to specify that the congestion phenomenon occurs mainly at doorways 16 and 6 (see doorway numbers in Figure 33), their queue reaching up to 4 people.

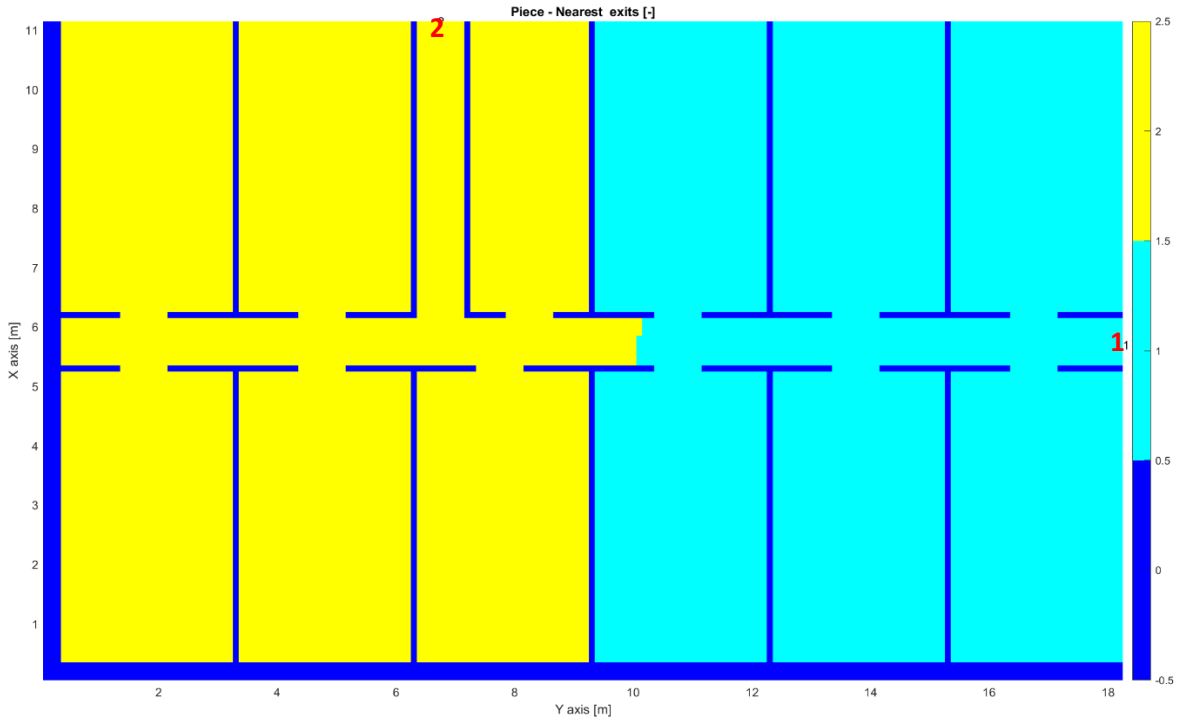

Figure 34: The nearest-exit map as a function of location: the yellow-coloured area is nearest to exit 2, while the cyan-coloured area is nearest to exit 1.

11.1.2 Model validation based on evacuation experiments

The second validation step of AMERIGO is performed on the basis of experimental data, namely those of 140 experiments conducted at the University of Lorraine for the study of congestion formation during the evacuation process of a single room. As shown in Figure 35, the room considered in the experimental study is rectangular in shape and measures 10 m² (4 m long and 2.5 m wide), with a single exit with a width of 0.85 m. Experiments consist of either ten people evacuating the room (performed 20 times), five people evacuating (performed 20 times), or one person evacuating (performed 100 times).

For each experiment, the location and the orientation of each person are randomly sorted. Accordingly, the initial location of each person in the room is recorded using a total of 40 floor grid cells, each measuring 0.5 m x 0.5 m. Moreover, the initial orientation of each person is taken into account by referencing the wall the person is facing. In addition, each individual's exit time is recorded using a visual camera installed above the doorway while the overall evacuation overview is recorded via a second camera installed in a suitable corner. The age of the participants ranges from 20 to 47, and they know the location of the exit, evacuating the room without panic or scrambling. All participants were valid.

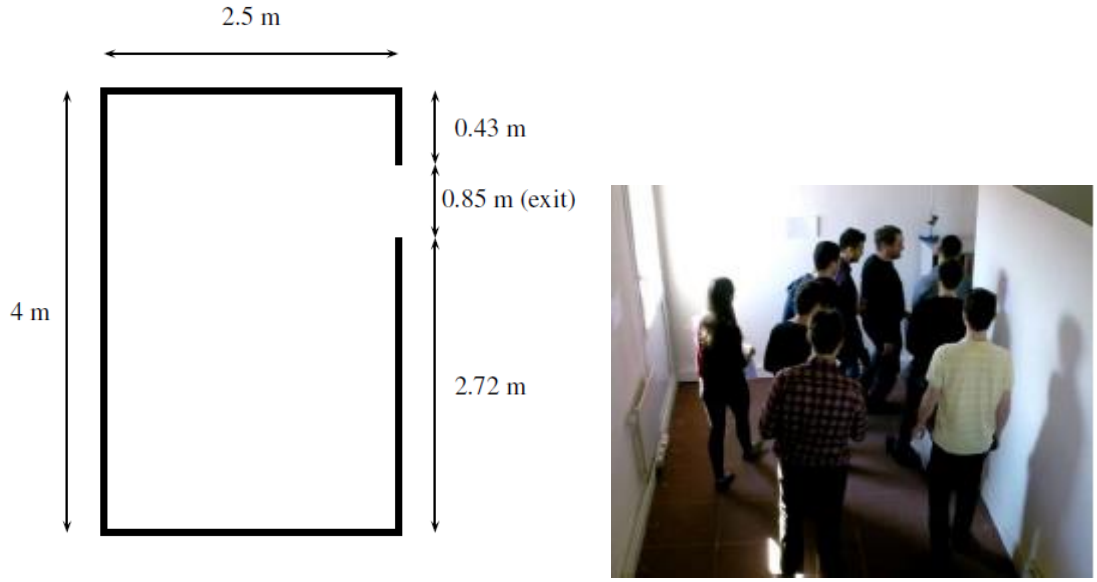

Figure 35: Geometrical details of the room used for the evacuation experiments.

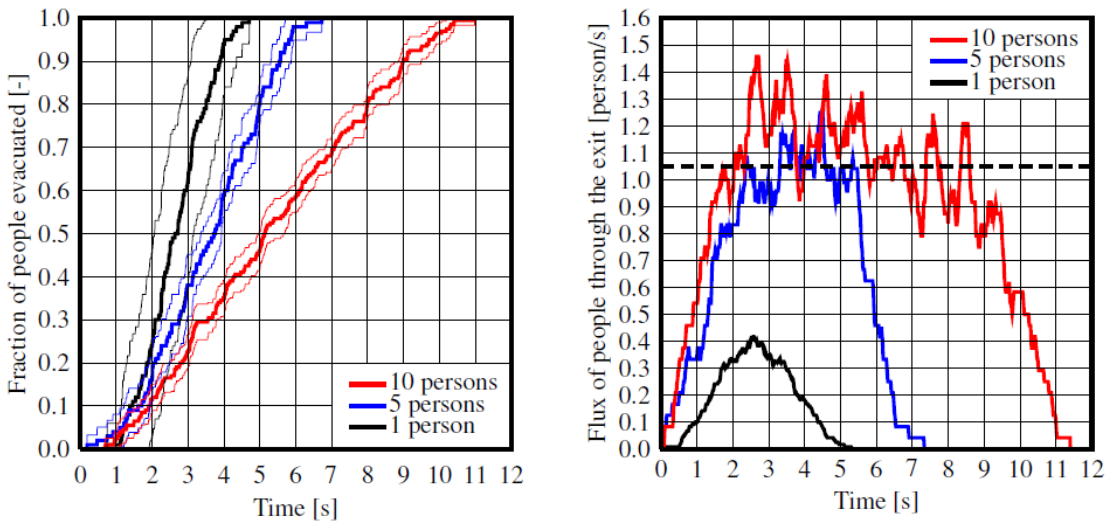

(a) Fraction of people evacuated *(b) Flux of people through the exit*

Figure 36: Experimental data of evacuation for the cases of one, five or ten individuals in the room.

Figure 36(a) shows the fraction of people evacuated as a function of time for one, five and ten people in the room. For each configuration, the average of the collected data is shown with 95% confidence intervals. As indicated in Figure 36(a), congestion formation increases each person's evacuation time by about 2 s when five people are present and by about 6 s when ten people are present. In this regard, it should be noted that the evacuation time with congestion formation is composed of two different steps: the first one concerns the time needed to reach the doorway (similar to the case of a single person evacuation), and the second one is related to the time required to evacuate all the people who were waiting behind the doorway in the congestion.

Figure 36(b) shows the flux of people through the exit in experiments. These results are in line with the main assumption of the AMERIGO model: the flux reaches a maximum value close to

1.05 person per second on average in the case of evacuation of five or ten people, and this threshold value corresponds to $\varphi_{i\,max}^{\text{out}}$ discussed in section 4.1.2.

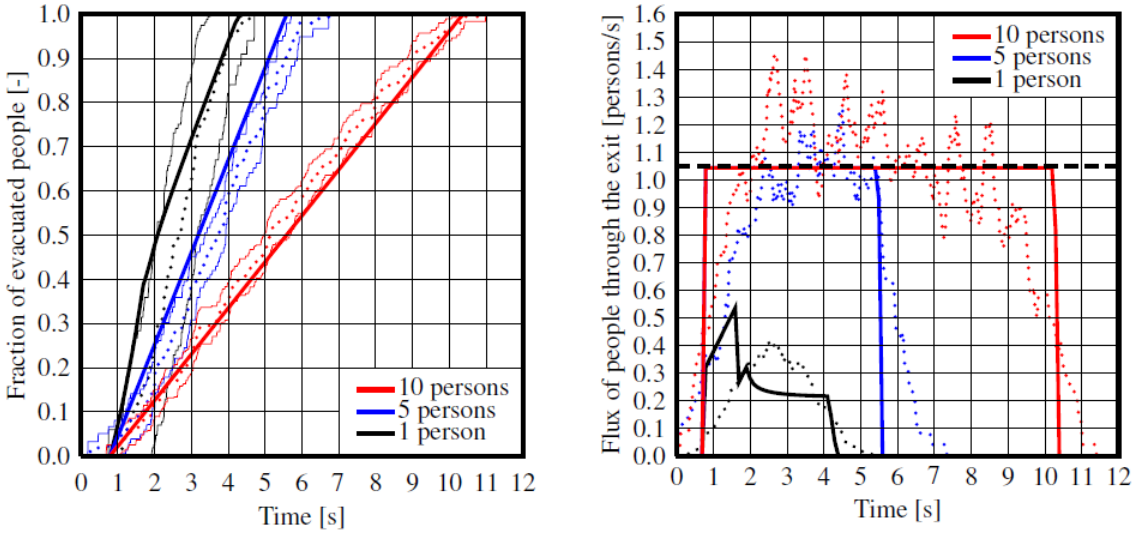

(a) Fraction of people evacuated *(b) Flux of people through the exit*

Figure 37: Fraction of evacuated people and the flux of people through the exit in the experiments with one, five or ten evacuees (dotted lines) and the corresponding numerical solution (thick solid lines). The thin solid lines indicate the 95% confidence interval.

In accordance with the theory discussed in section 4.1.2, in order to be able to reproduce the evacuation times observed in the experiments, the parameters of the AMERIGO model parameters must be calibrated. In particular, the free walking speed and the response time need to be known. The search space considered for the estimation of V_{fw} covers the range from 0.6 to 1.3 m/s and that of t_{reac} covers the range from 0.5 to 2 s. These two parameters are important to determine the incoming people flux, φ_i^{in}. Correlatively, the optimal value of V_{fw}, found with a PSO optimization algorithm, is estimated at 0.91 m/s while that of t_{reac} is estimated at 0.69 s. The estimated free walking speed is lower than the average literature value of 1.3 m/s but remains within the possible range of 0.8 to 1.6 m/s reported for adults. In this case, the response time is not very long because all the participants are fully aware of the evacuation drill.

Figure 37 presents the results of this model for the configurations with one, five and ten evacuees in comparison with the data of the experiments. The results are in good agreement for the fraction of people evacuated over time and the flux of people through the exit, with differences not exceeding 10% for the evacuation time.

11.2 Stena Flavia: summary of simulation results.

SCENARIO SF1

Observations

As shown in Table 9, and from Figure 38 to Figure 40:

- Smoke detection occurs at 43 s in DZ14.
- Fire is out of control at 17 min 13 s in DZ14.
- All the cargo in the ro-ro space (deck 4) where the fire broke out is ignited in just over 43 min, as well as targets in about 41 min. The structure is damaged in all DZ of deck 4.
- ATSFR: 5 min due to excessive incident RHF (>2.5 kW/m²).
- Fire spreads to target cars on the aft part of upper deck 5 due to external flames.
- No fire transmission through the deck 4 insulated ceiling. The maximum temperature of the deck 5 floor is 271°C, lower than the ignition temperature of vehicle tires.
- LSA and DR are safe for approximately the first 11 min of fire on both sides of the ship. After this time, one or more tenability criteria are exceeded.
  On the starboard side, after 1 h of fire, the CO concentration has already decreased to acceptable levels (due to a decrease in HRR, as shown in IR04.21), but visibility and temperature tenability criteria remain too high for safe evacuation. Moreover, people could be exposed to an incident RHF greater than 2.5 kW/m² between 22 and 49 min on the starboard side (Figure 40a). On the portside, the levels of exposure to CO, gas temperature, and smoke are lower, but people could be exposed to an incident RHF greater than 2.5 kW/m² between 22 and 57 min of fire (Figure 40b). This suggests that evacuation could be done safely on the port side after nearly an hour of waiting in the AS (!).

Table 9: Scenario SF1: simulation results. SWI means Swift detection, DR disembarkation route, SS starboard side, and PS port side. For consequences to human, the value in bold blue corresponds to the first tenability criterion that was exceeded in the areas of interest. Times are given in minutes and seconds (min's").

	DZ13	DZ14	DZ15	DZ16	DZ17	DZ18	DZ19	DZ20			
Heat detection at 54°C	3'28"	2'08"	2'59"	4'15"	5'30"	5'37"	4'28"	2'04"			
Heat detection at 78°C	4'20"	2'34"	3'51"	5'46"	7'31"	7'56"	5'48"	2'31"			
Smoke detection	1'24"	**0'43"**	1'16"	1'47"	2'26"	3'02"	2'03"	0'51"			
Structure damage	25'40"	21'05"	22'30"	47'03"	37'38"	43'58"	34'09"	27'02"			
Target ignition	15'38"	6'05"	15'17"	23'51"	33'47"	40'54"	20'16"	14'40"			
First truck ignition	7'58"	0'00"	9'44"	22'41"	26'58"	32'54"	16'21"	15'04"			
Last truck ignition	32'08"	**17'13"**	23'58"	29'24"	35'57"	43'10"	32'21"	18'38"			
no of trucks ignited	70/70										
Predicted/Prescribed total heat content (TJ)	1.41/1.60										
Consequences to human	DZ13	DZ14	DZ15	DZ16	DZ17	DZ18	DZ19	DZ20	LSA and DR - SS	LSA and DR - PS	SWI
RHF	**14'00"**	**4'00"**	**7'00"**	23'00"	25'00"	25'00"	**16'00"**	**9'00"**	22'00"	22'00"	**5'00"**
T60	30'40"	21'47"	20'19"	20'21"	20'11"	19'59"	42'43"	28'36"	28'35"	28'12"	21'01"
CO	37'56"	37'51"	14'59"	18'35"	18'31"	17'52"	-	-	31'19"	28'42"	26'00"
Visibility 5m	30'41"	25'36"	10'11"	12'04"	4'33"	3'56"	42'22"	26'45"	13'38"	14'28"	10'29"
Visibility 10m	26'01"	21'43"	9'34"	**4'51"**	**4'15"**	**3'50"**	39'43"	22'16"	**10'36"**	**11'18"**	8'40"

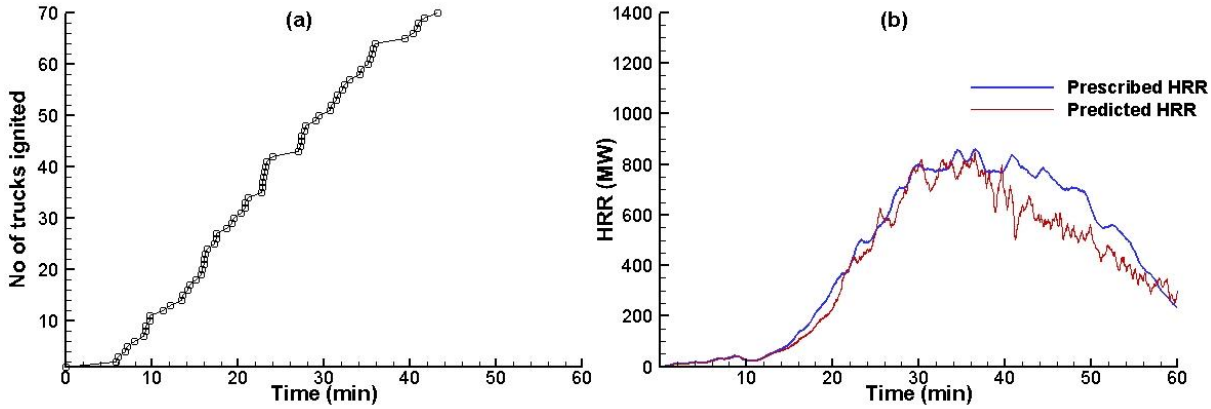

Figure 38: Scenario SF1: a) Number of truck ignited vs. time, and b) comparison between the time evolutions of the theoretical HRR (i.e., the total pyrolysis rate multiplied by the chemical heat of combustion) and effective HRR.

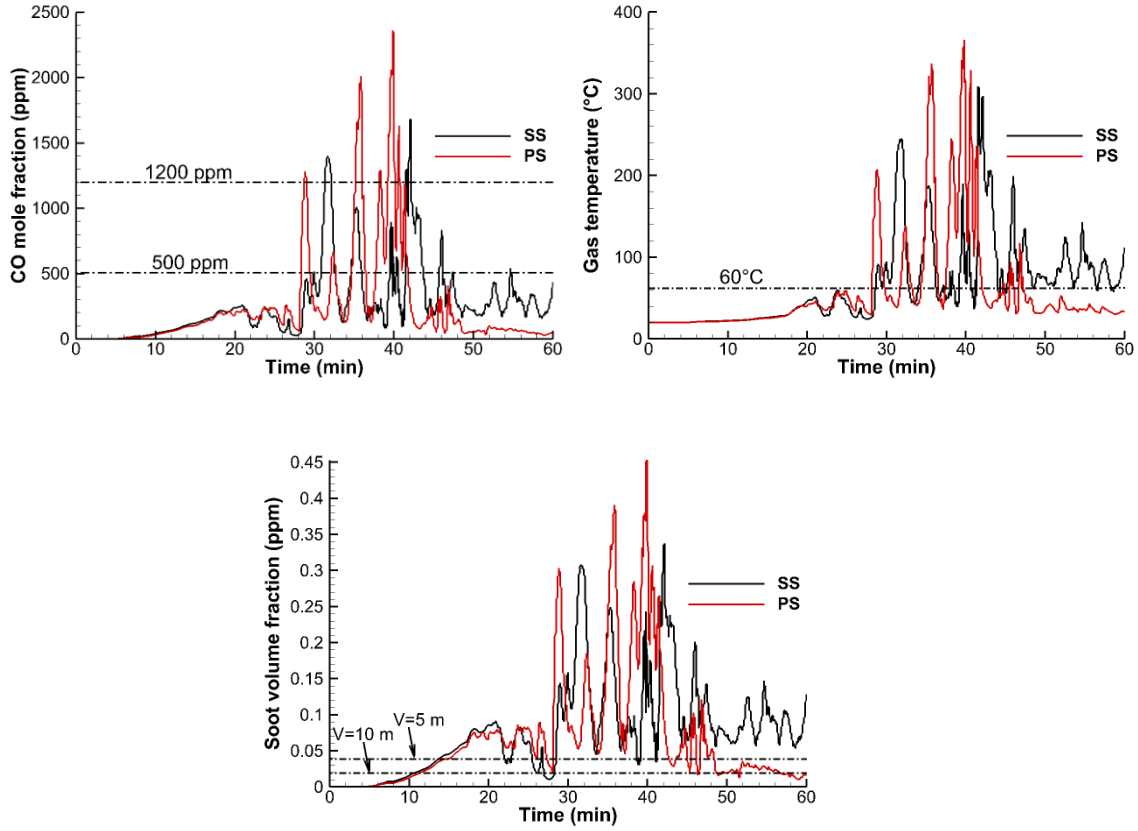

Figure 39: Scenario SF1: time evolutions of maximum CO mole fraction, gas temperature, and soot volume fraction at the monitored points in the LSA and DR on both sides of the Stena Flavia.

(a) Incident RHF after 49 min of fire.

(b) Incident RHF after 57 min of fire.

Figure 40: Scenario SF1: 2D field of the incident radiative heat flux obtained at a height of 1.80 m above deck 5 after 49 and 57 min of fire. Black areas correspond to areas where the radiative heat flux is greater than 2.5 kW/m².

SCENARIO SF2

Observations

As shown in Table 10*Table 9*, and from Figure 41 to Figure 43:

- Smoke detection occurs at 24 s in DZ14.
- Fire is out of control at 21 min 40 s in DZ15.
- ATSFR: 3 min 2 s due to degraded visibility.
- All the cargo in the ro-ro space (deck 4) where the fire broke out is ignited in less than 43 min, as well as targets in 38 min. The structure is damaged in all drencher zones of deck 4, except in DZ15 and DZ17.
- No fire spread to upper deck either by the external flames or through the deck 4 ceiling.
- The 18-knot headwind pushes the smoke aft, making the LSA and DR on both sides of the Stena Flavia safe for most of the fire (Figure 42). The visibility and gas temperature criteria are only exceeded for a short period of time, between approximately 19 and 27 min. The incident RHF never exceeds 2 kW/m² in the LSA and DR, as shown in Figure 43 when the exposure to the RHF in the LSA and DR is maximum, at t =41 min.
  Evacuation can be done safely on both sides of the ship from 27 min of fire.

Table 10: Scenario SF2: simulation results. SWI means Swift detection, DR disembarkation route, SS starboard side, and PS port side. For consequences to human, the value in bold blue corresponds to the first tenability criterion that was exceeded in the areas of interest. Times are given in minutes and seconds (min's").

	DZ13	DZ14	DZ15	DZ16	DZ17	DZ18	DZ19	DZ20			
Heat detection at 54°C	3'13"	2'13"	2'42"	4'18"	6'12"	6'31"	4'38"	2'07"			
Heat detection at 78°C	4'32"	2'50"	3'45"	6'17"	7'53"	8'41"	6'18"	2'33"			
Smoke detection	1'26"	**0'24"**	1'05"	1'37"	2'07"	2'46"	1'48"	0'47"			
Structure damage	27'53"	25'26"	-	32'10"	-	46'24"	32'50"	30'55"			
Target ignition	16'59"	5'36"	12'46"	15'48"	33'26"	38'00"	24'23"	17'22"			
First truck ignition	9'11"	0'00"	7'04"	14'30"	18'03"	25'32"	21'32"	17'01"			
Last truck ignition	30'19"	21'47"	**21'40"**	25'17"	32'48"	42'56"	31'03"	21'35"			
no of trucks ignited	70/70										
Predicted/Prescribed total heat content (TJ)	1.41/1.60										
Observations	Fire spread to target cars on upper deck 5										
Consequences to human	DZ13	DZ14	DZ15	DZ16	DZ17	DZ18	DZ19	DZ20	LSA and DR - SS	LSA and DR - PS	SWI
RHF	20'00"	5'00"	7'00"	16'00"	19'00"	33'00"	21'00"	16'00"	-	-	6'00"
T60	16'42"	15'28"	15'08"	10'08"	14'02"	13'17"	19'06"	17'22"	20'08"	20'11"	15'24"
CO	19'21"	17'55"	15'55"	14'52"	14'45"	14'20"	24'05"	18'59"	-	-	17'38"
Visibility 5m	8'25"	5'11"	3'45"	4'36"	5'46"	4'01"	8'42"	14'23"	19'05"	19'02"	3'57"
Visibility 10m	**3'16"**	**3'26"**	**3'02"**	**4'12"**	**4'42"**	**3'50"**	**6'55"**	**4'13"**	**18'48"**	**18'46"**	**3'02"**

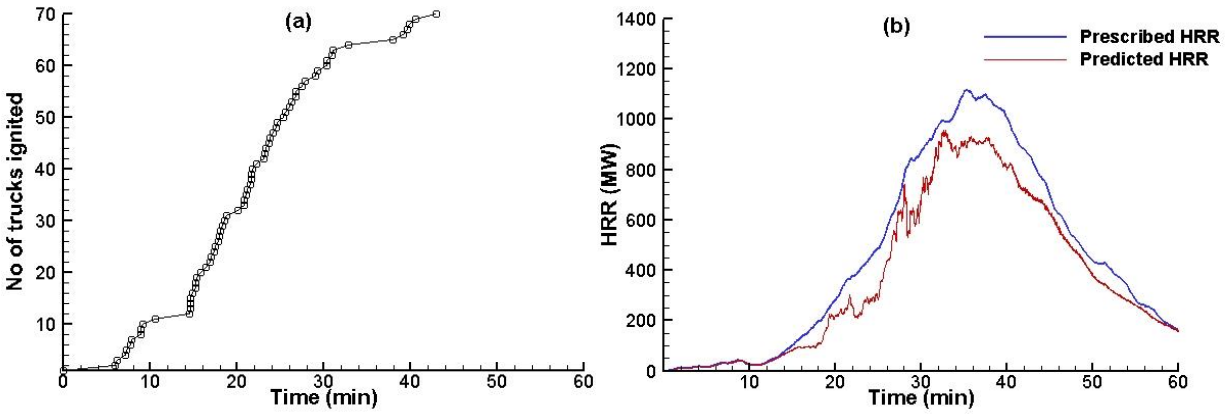

Figure 41: Scenario SF2: a) Number of truck ignited vs. time, and b) comparison between the time evolutions of the theoretical HRR (i.e., the total pyrolysis rate multiplied by the chemical heat of combustion) and effective HRR.

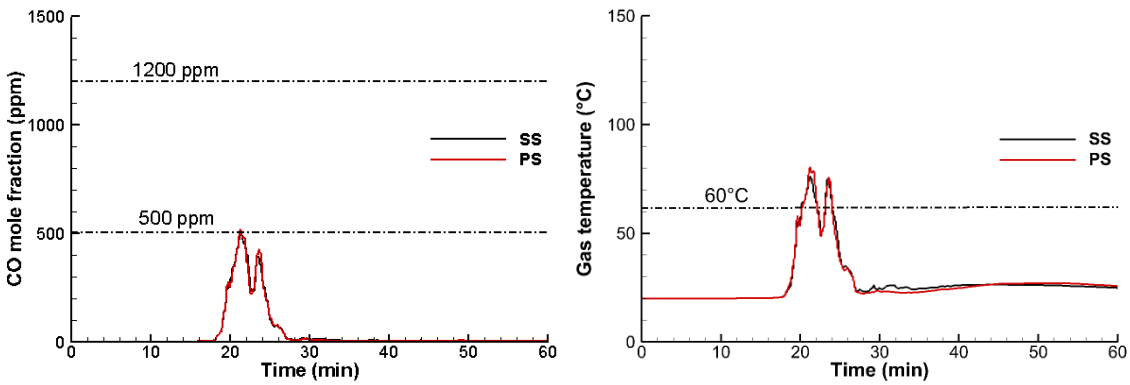

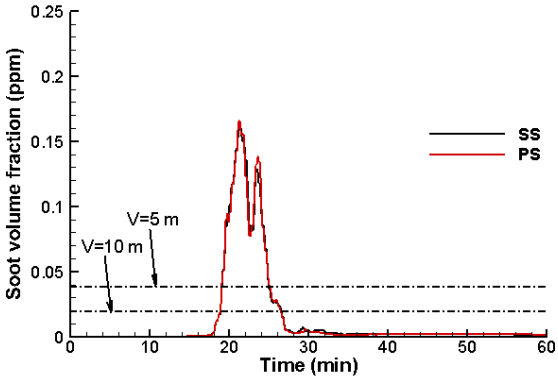

Figure 42: Scenario SF2: time evolutions of maximum CO mole fraction, gas temperature, and soot volume fraction at the monitored points in the LSA and DR on both sides of the Stena Flavia.

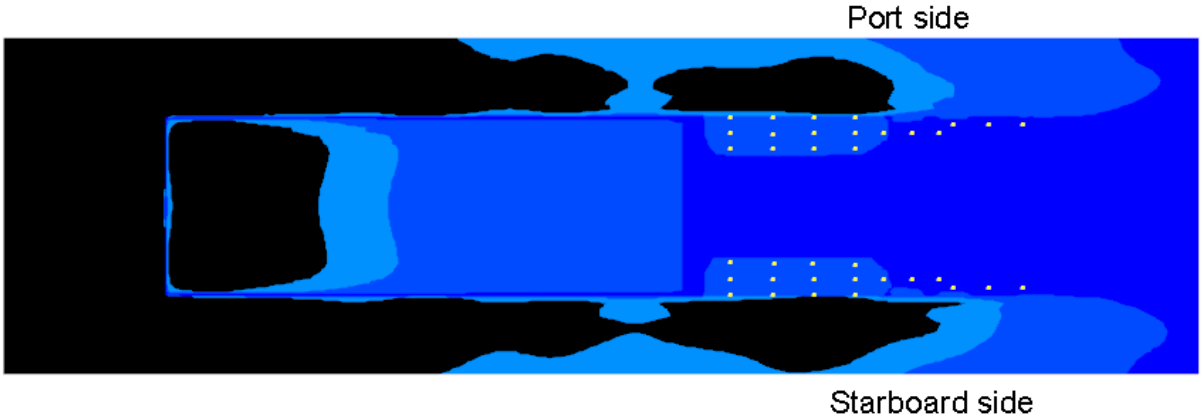

Figure 43: Scenario SF2: 2D field of the incident radiative heat flux obtained at a height of 1.80 m above deck 5 after 41 min of fire, when the radiative exposure is maximum. Black areas correspond to areas where the radiative heat flux is greater than 2.5 kW/m².

SCENARIO SF3

Fire consequences in the LSA and DR for scenario SF3 are similar to those obtained for scenario SF3.3. However, this is not the case in the accommodations where the preserved integrity of the insulation system and ro-ro space containment prevent fire and smoke from spreading into the accommodations (see scenarios SF3.2 to SF3.4).

SCENARIO SF3.1

Observations

As shown in Table 11, and from Figure 44 to Figure 46:

- Smoke detection occurs at 20 s in DZ16.
- Fire is out of control at 15 min 36 s in DZ15.
- ATSFR: 7 min due to excessive RHF.

- All the cargo in the ro-ro space (deck 4) where the fire broke out is ignited in less than 40 min, as well as targets in about 43 min. The structure is damaged in all drencher zones of deck 4.
- No fire spread to upper deck either by the external flames or through the deck (NB: the maximum temperature of the deck 5 floor is 231°C, lower than the ignition temperature of vehicle tires).
- Closing the openings around the LSA on both sides of the ship significantly reduces the impact of fire and smoke in the LSA and DR. This can be observed by comparing fire consequences for the present scenario (see below) with those obtained for scenario SF3.3 (see Table 4, and Figure 16-Figure 18). As shown in Figure 45, it clearly appears that LSA and DR are much safer.
  The RHF exceeds 2.5 kW/m² from 25 min to 43 min on the port side and to 44 min on the starboard side.
  Short-lived peaks in gas temperature and soot volume fraction appear when the HRR is maximum, at approximately 36 min.
  After about a quarter of an hour of fire, evacuation can be done safely, with a visibility of 5 m, or more, on the portside and no restriction on the starboard side.

Table 11: Scenario SF3.1: simulation results. SWI means Swift detection, DR disembarkation route, SS starboard side, and PS port side. For consequences to human, the value in bold blue corresponds to the first tenability criterion that was exceeded in the areas of interest. Times are given in minutes and seconds (min's").

	DZ13	DZ14	DZ15	DZ16	DZ17	DZ18	DZ19	DZ20			
Heat detection at 54°C	3'18"	2'04"	1'20"	1'10"	1'54"	2'34"	4'14"	2'57"			
Heat detection at 78°C	4'23"	3'30"	2'02"	1'17"	2'46"	3'07"	5'14"	3'56"			
Smoke detection	2'24"	1'48"	1'12"	**0'20"**	1'23"	2'02"	2'58"	1'42"			
Structure damage	30'23"	28'22"	23'53"	39'54"	27'24"	43'47"	35'33"	30'42"			
Target ignition	21'03"	16'46"	12'42"	5'51"	23'28"	42'57"	21'56"	18'55"			
First truck ignition	19'18"	15'31"	0'00"	0'00"	11'54"	24'40"	20'43"	17'37"			
Last truck ignition	39'25"	20'48"	**15'36"**	20'11"	25'56"	39'19"	39'02"	21'30"			
no of trucks ignited	70/70										
Predicted/Prescribed total heat content (TJ)	1.48/1.64										
Consequences to human	DZ13	DZ14	DZ15	DZ16	DZ17	DZ18	DZ19	DZ20	LSA and DR-SS	LSA and DR-PS	SWI
RHF	**18'00"**	**16'00"**	**6'00"**	**6'00"**	21'00"	22'00"	**20'00"**	**18'00"**	**25'00"**	**25'00"**	**7'00"**
T60	30'23"	24'48"	21'47"	20'50"	19'53"	18'26"	30'39"	26'42"	35'46"	35'47"	20'43"
CO	33'11"	26'20"	24'48"	24'00"	20'55"	17'52"	34'49"	34'31"	-	-	22'02"
Visibility 5m	30'21"	25'15"	21'53"	12'41"	12'33"	3'01"	30'36"	26'01"	33'"47"	34'24"	12'48"
Visibility 10m	26'41"	24'47""	21'44"	10'25"	**3'33"**	**2'57"**	30'29"	25'58"	33'37"	34'00"	10'16"

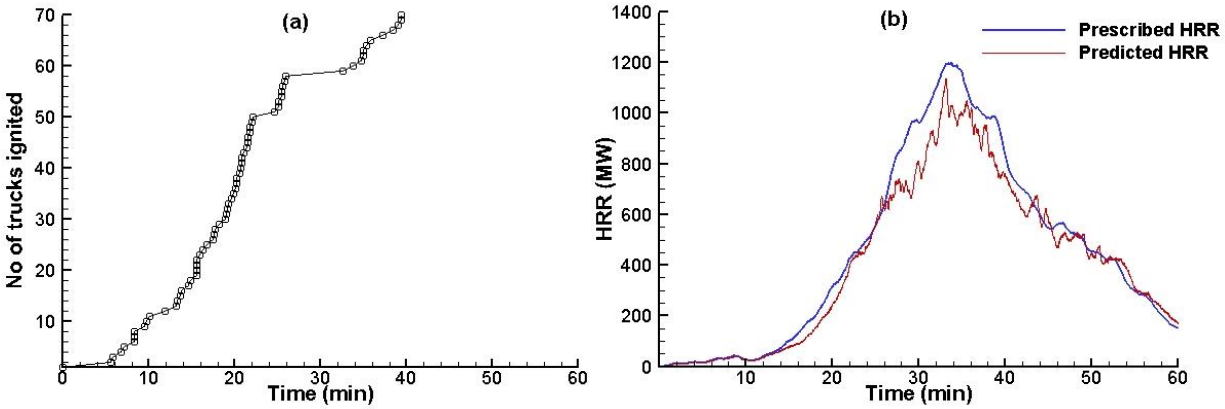

Figure 44 : Scenario SF3.1: a) Number of truck ignited vs. time, and b) comparison between the time evolutions of the theoretical HRR (i.e., the total pyrolysis rate multiplied by the chemical heat of combustion) and effective HRR.

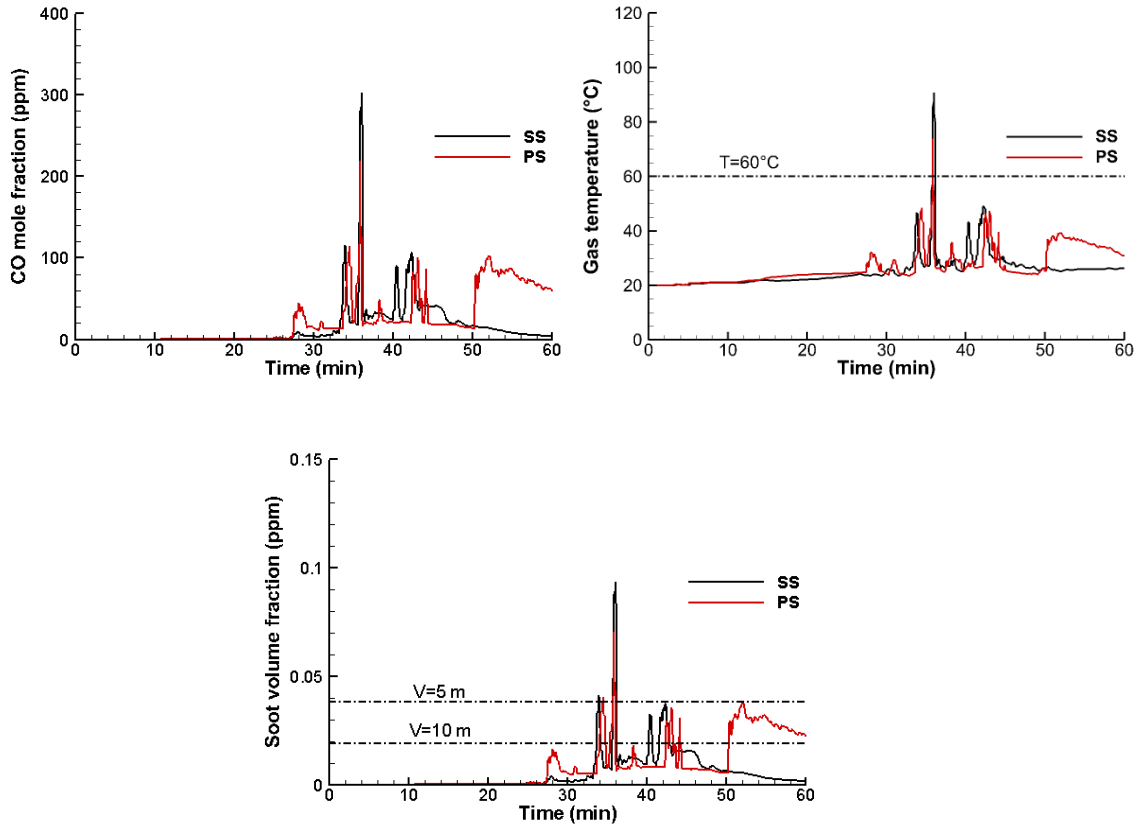

Figure 45: Scenario SF3.1: time evolutions of maximum CO mole fraction, gas temperature, and soot volume fraction at the monitored points in the LSA and DR on both sides of the Stena Flavia.

Figure 46: Scenario SF3.1: 2D field of the incident radiative heat flux obtained at a height of 1.80 m above Deck 5 after 43 min of fire. Black areas correspond to areas where the radiative heat flux is greater than 2.5 kW/m².

SCENARIO SF3.2

Observations

- Fire consequences in the LSA and DR for scenario 3.2 are the same as those obtained for scenario SF3.3. However, they differ in the accommodations. For this accidental scenario due to a loss of ro-ro space containment (opening defect), AS quickly become untenable. This is shown in Figure 47 and Figure 48, where the smoke interface falls below 1.80 m in height at $t \approx t_1 + 35$ min. Here, t_1 was estimated from CFD results to be about 30 min. The simulation results of Figure 48 could be used to reallocate safer areas or define alternative evacuation routes.

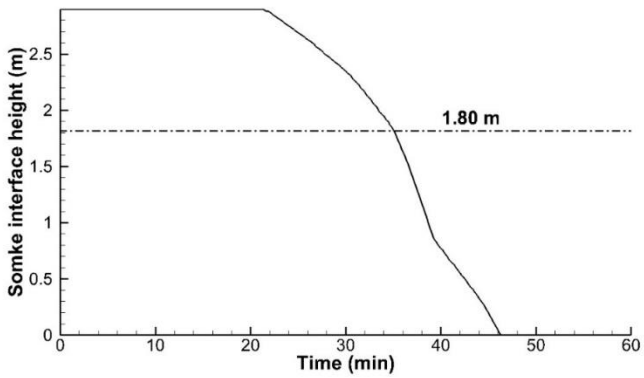

Figure 47: Scenario SF3.2: time evolution of the smoke interface height in the AS of the Stena Flavia, here the restaurant located on deck 5. The origin of time is the time at which fire and/or smoke reaches deck 5, here $t_1 \approx 30$ min.

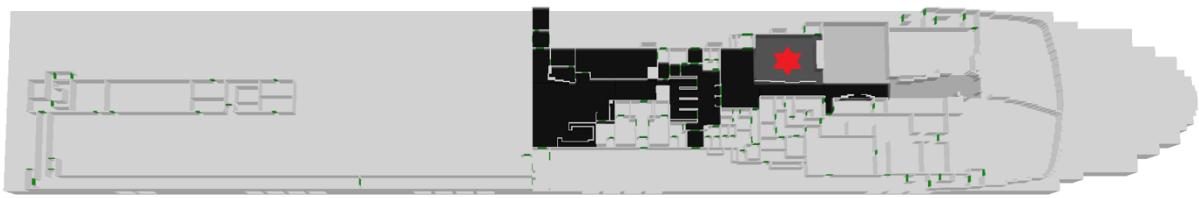

Figure 48: Scenario SF3.2: smoke spread throughout deck 5 just as the smoke reaches the AS (here, the restaurant, at the position indicated by the "red star" symbol).

SCENARIO SF3.3

See Section 6.2.

SCENARIO SF3.4

Observations

- Fire consequences in the LSA and DR for scenario SF3.4 are the same as those obtained for scenario SF3.3. However, they differ in the accommodations. The CFD results show that the fire on deck 4 generates a very high total heat flux (THF) on the ceiling (Figure 49) which can lead to the destruction of the ceiling insulation, resulting in the transmission of fire to the accommodations near the stairwell. As shown in Figure 49, the ceiling insulation material is exposed to THF that quickly exceeds 80 kW/m², which can cause its destruction from $t_1 \approx 6$ min.
- Due to the loss of insulation system integrity, AS quickly become untenable. This is shown in Figure 50 and Figure 51, where the smoke interface falls below 1.80 m in height at $t \approx t_1 +$ 12 min ≈ 18 min.

The simulation results of Figure 51 could be used to reallocate safer areas or define alternative evacuation routes.

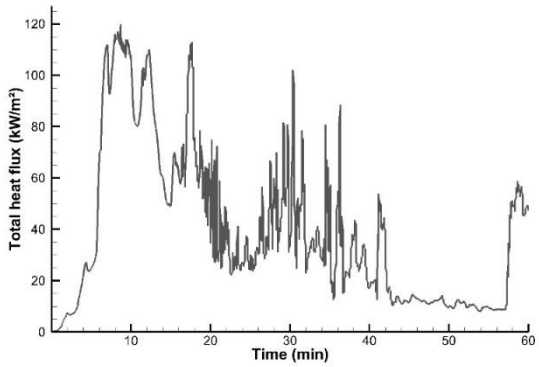

Figure 49 : Scenario SF3.4: time evolution of the total heat flux received by the deck 4 ceiling below the stairwell.

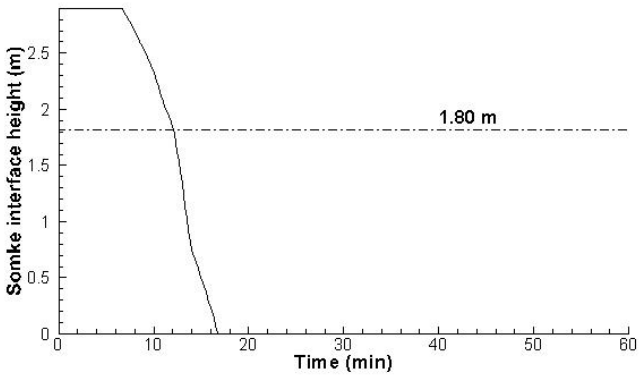

Figure 50: Scenario SF3.4: time evolution of the smoke interface height in the AS of the Stena Flavia, here the restaurant located on deck 5. The origin of time is the time at which fire and/or smoke reaches deck 5, here $t_1 \approx 6$ min.

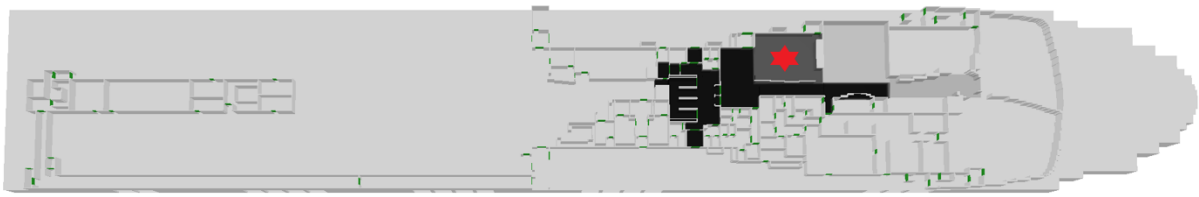

Figure 51: Scenario SF3.4 : smoke spread throughout deck 5 just as the smoke reaches the AS (here, the restaurant, at the position indicated by the "red star" symbol).

SCENARIO SF4

Observations

As shown in Table 12, Figure 52 and Figure 53:

- Smoke detection occurs at 22 s in DZ16.
- Fire is out of control at 17 min 51 s in DZ16.
- ATSFR: 3 min 11 s due to degraded visibility.
- All the cargo in the ro-ro space (deck 4) where the fire broke out is ignited in less than 41 min, as well as targets in less than 41 min. The structure is damaged in all drencher zones of deck 4.
- No fire spread to upper deck either by external flames or through the deck 4 ceiling.
- The 18-knot headwind pushes the smoke aft, making the LSA and DR safe for most of the fire, except for short-lived peaks in the time evolutions of gas temperature and soot volume fraction (Figure 53). The radiative heat flux never exceeds 2.5 kW/m². Due to the short duration and low levels of exposure to heat and smoke, evacuation can be done safely on both sides of the ship.

Table 12: Scenario SF4: simulation results. SWI means Swift detection, DR disembarkation route, SS starboard side, and PS port side. For consequences to human, the value in bold blue corresponds to the first tenability criterion that was exceeded in the areas of interest. Times are given in minutes and seconds (min's").

	DZ13	DZ14	DZ15	DZ16	DZ17	DZ18	DZ19	DZ20			
Heat detection at 54°C	4'33"	4'01"	2'34"	2'10"	4'17"	4'59"	5'30"	3'44"			
Heat detection at 78°C	7'35"	5'34"	3'04"	2'38"	5'05"	6'10"	8'52"	6'02"			
Smoke detection	2'09"	1'56"	1'37"	**0'22"**	1'04"	1'50"	2'22"	1'55"			
Structure damage	29'33"	28'41"	28'46"	26'39"	27'45"	42'49"	36'42"	28'00"			
Target ignition	25'43"	23'45"	15'17"	5'50"	14'31"	40'30"	25'27"	23'26"			
First truck ignition	23'25"	19'33"	0'00"	0'00"	7'55"	15'02"	23'54"	20'21"			
Last truck ignition	35'21"	24'34"	18'40"	**17'51"**	23'13"	40'39"	33'27"	23'54"			
no of trucks ignited	70/70										
Predicted/Prescribed total heat content (TJ)	1.30/1.65										
Consequences to human	DZ13	DZ14	DZ15	DZ16	DZ17	DZ18	DZ19	DZ20	LSA and DR-SS	LSA and DR-PS	SWI
RHF	19'00"	19'00"	5'00"	6'00"	15'00"	18'00"	23'00"	22'00"	-	-	7'00"
T60	16'27"	13'24"	12'34"	8'12"	12'57"	13'05"	19'07"	17'55"	36'39"	36'32"	7'42"
CO	19'05"	18'34"	17'51"	14'15"	14'17"	13'25"	22'27"	21'16"	-	-	14'42"
Visibility 5m	4'43"	4'17"	3'51"	4'11"	6'32"	6'46"	8'59"	12'55"	18'07"	18'00"	3'40"
Visibility 10m	**3'49"**	**3'06"**	**3'13"**	**3'05"**	**4'16"**	**2'48"**	**4'44"**	**8'10"**	**17'43"**	**17'35"**	**3'11"**

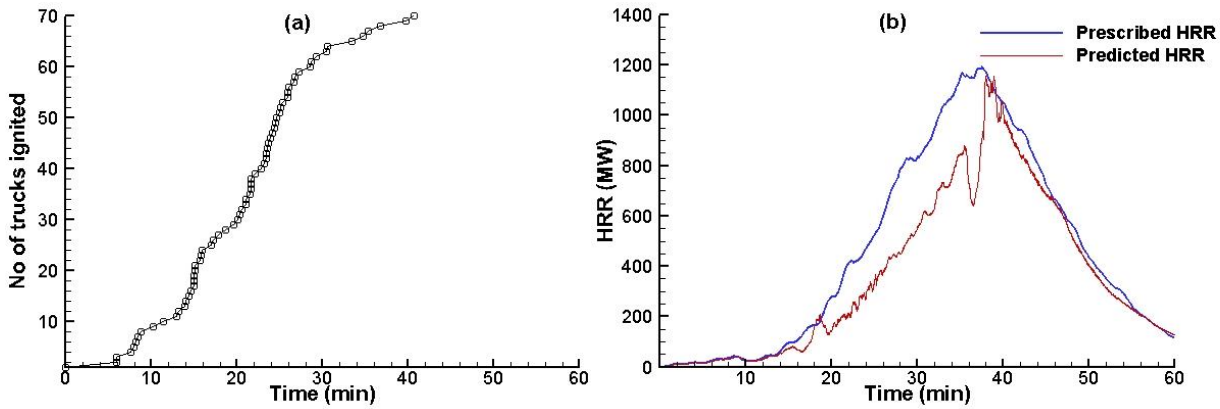

Figure 52: Scenario SF4: a) Number of truck ignited vs. time, and b) comparison between the time evolutions of the theoretical HRR (i.e., the total pyrolysis rate multiplied by the chemical heat of combustion) and effective HRR.

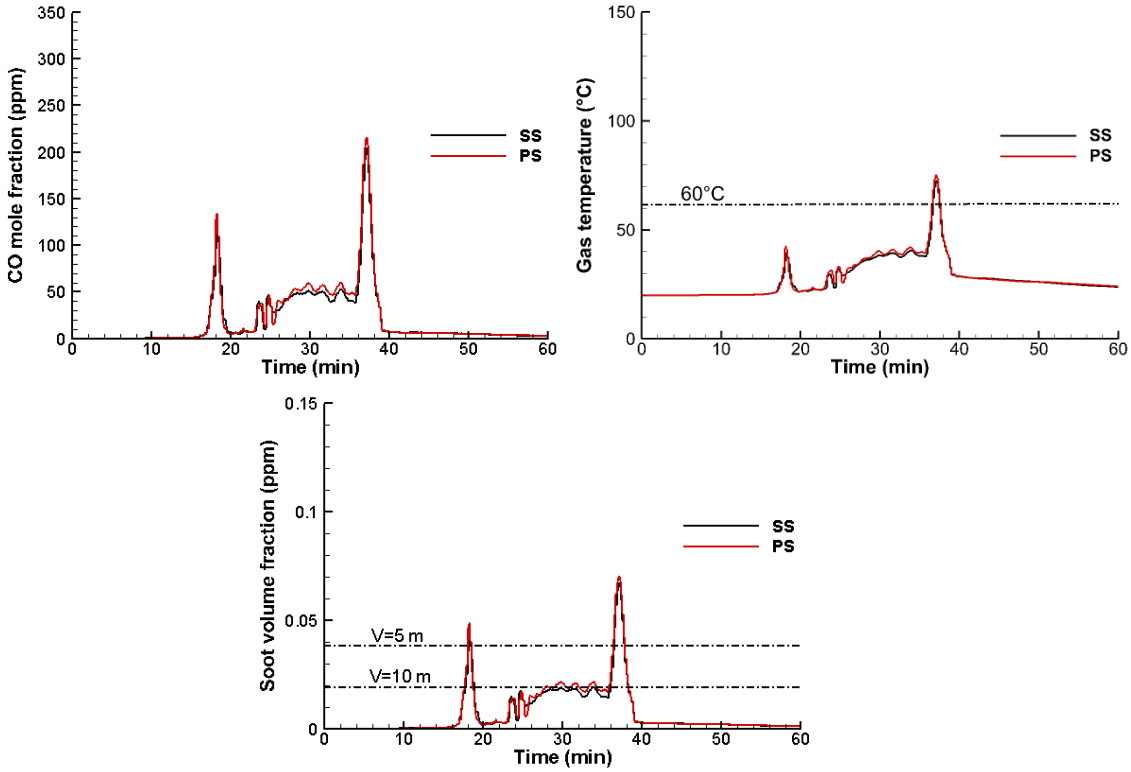

Figure 53: Scenario SF4: time evolutions of maximum CO mole fraction, gas temperature, and soot volume fraction at the monitored points in the LSA and DR on both sides of the Stena Flavia.

SCENARIO SF5

Observations

As shown in Table 13, and from Figure 54 to Figure 56:

- Smoke detection occurs at 20 s in both DZ17 and DZ18.
- Fire is out of control at about the same time, in less than 20 min, in both DZ17 and DZ18.
- ATSFR: 2 min 7 s due to degraded visibility.

- All the cargo in the ro-ro space (deck 4) where the fire broke out is ignited in less than 39 min, as well as targets in just over 26 min. The structure is damaged in all drencher zones of deck 4, except in DZ16.
- Fire spread to target cars on upper deck 5 due to external flames.
- No fire spread through the deck 4 ceiling. The maximum temperature of the deck 5 floor is 262°C, lower than the ignition temperature of vehicle tires.
- As shown in Figure 55, LSA and DR are safe during the first 14 min of fire. This is followed by a long period where tenability criteria are mostly exceeded. The RHF no longer exceeds 2.5 kW/m² after 44 min of fire (Figure 56). Conditions in the LSA and DR become tenable again after 54 min of fire on the PS and after 51 min on the SS, when the exposure levels to CO, gas temperature and smoke return below the critical thresholds (Figure 55).

Table 13: Scenario SF5: simulation results. SWI means Swift detection, DR disembarkation route, SS starboard side, and PS port side. For consequences to human, the value in bold blue corresponds to the first tenability criterion that was exceeded in the areas of interest. Times are given in minutes and seconds (min's").

	DZ13	DZ14	DZ15	DZ16	DZ17	DZ18	DZ19	DZ20			
Heat detection at 54°C	5'15"	4'43"	3'59"	2'50"	1'26"	2'01"	5'44"	4'53"			
Heat detection at 78°C	6'54"	5'51"	4'55"	3'30"	1'35"	2'29"	7'35"	6'15"			
Smoke detection	3'14"	2'41"	2'06"	1'23"	**0'20"**	**0'20"**	3'41"	2'38"			
Structure damage	34'23"	32'51"	27'46"	-	20'28"	18'07"	36'58"	34'40"			
Target ignition	23'32"	23'13"	18'18"	14'10"	4'07"	7'25"	22'28"	25'29"			
First truck ignition	21'12"	20'17"	14'43"	7'25"	0'00"	0'00"	22'08"	22'47"			
Last truck ignition	38'58"	23'53"	21'23"	20'00"	**19'29"**	19'38"	38'29"	24'49"			
no of trucks ignited	70/70										
Predicted/Prescribed total heat content (TJ)	1.40/1.65										
Consequences to human	DZ13	DZ14	DZ15	DZ16	DZ17	DZ18	DZ19	DZ20	LSA and DR-SS	LSA and DR-PS	SWI
RHF	**20'00"**	20'00"	**15'00"**	**13'00"**	**6'00"**	6'00"	**21'00"**	**22'00"**	20'00"	20'00"	4'00"
T60	32'59"	26'46"	24'21"	20'59"	20'14"	20'38"	29'54"	34'45"	16'57"	18'13"	6'02"
CO	34'31"	30'21"	25'54"	25'09"	22'32"	21'34"	34'41"	35'02"	31'14"	31'50"	21'53"
Visibility 5m	33'51"	27'28"	16'00"	14'11"	20'13"	20'40"	29'47"	30'15"	14'28"	14'22"	2'13"
Visibility 10m	30'31"	**3'43"**	15'20"	13'19"	15'01"	**2'10"**	29'05"	28'32"	**14'03"**	**13'41"**	**2'07"**

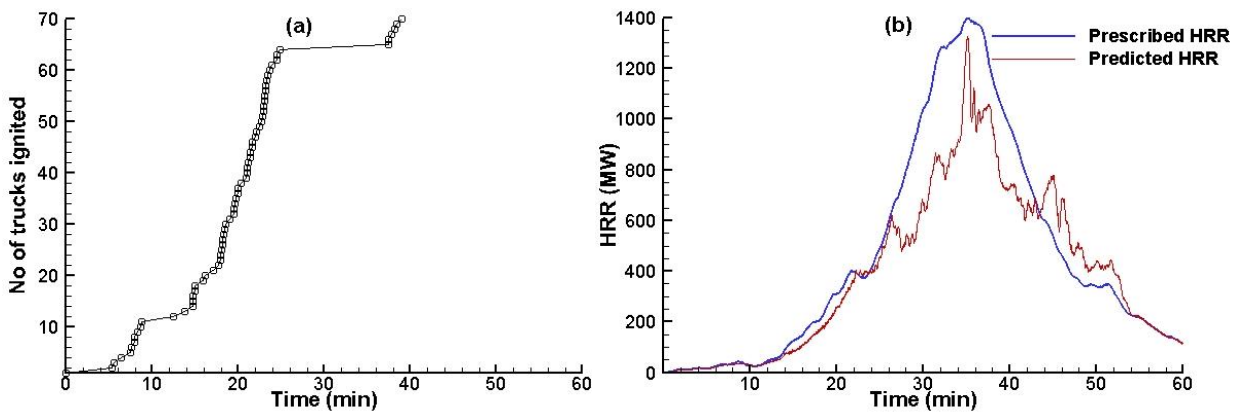

Figure 54: Scenario SF5: a) Number of truck ignited vs. time, and b) comparison between the time evolutions of the theoretical HRR (i.e., the total pyrolysis rate multiplied by the chemical heat of combustion) and effective HRR.

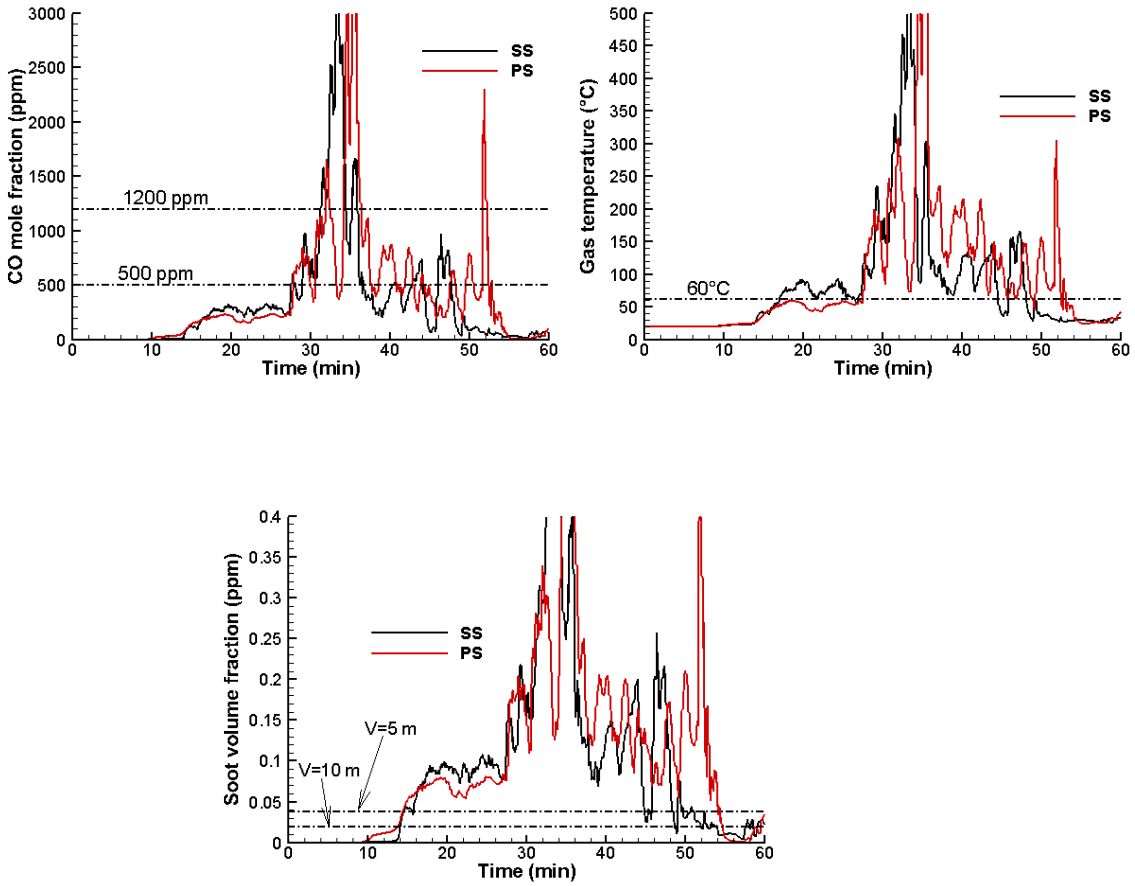

Figure 55: Scenario SF5: time evolutions of maximum CO mole fraction, gas temperature, and soot volume fraction at the monitored points in the LSA and DR on both sides of the Stena Flavia.

Figure 56: Scenario SF5: 2D field of the incident radiative heat flux obtained at a height of 1.80 m above Deck 5 after 44 min of fire. Black areas correspond to areas where the radiative heat flux is greater than 2.5 kW/m².

SCENARIO SF6

See Section 6.2

11.3 Magnolia Seaways: summary of simulation results

SCENARIO MS7

Observations

- Heat and smoke detection: not applicable.
- No fire propagation. Only the truck at the origin of fire is burning (Figure 57).
- No human and target damage.
- Predicted/Prescribed total heat content (TJ): 0.0249/0.0262.

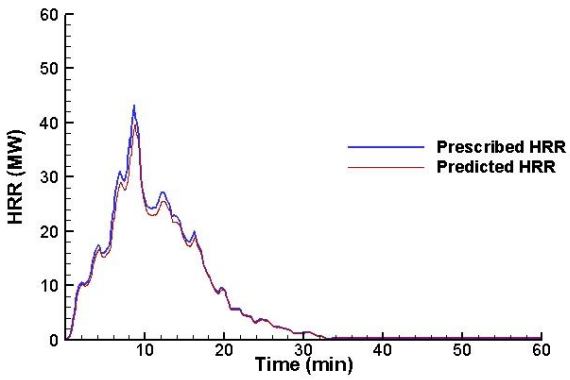

Figure 57: Scenario MS7: Comparison between the time evolutions of the theoretical HRR (i.e., the total pyrolysis rate multiplied by the chemical heat of combustion) and effective HRR.

SCENARIO MS8

Observations

As shown in Table 14, and from Figure 58 to Figure 60:

- Smoke detection occurs at 50 s in DZ1.
- Fire is out of control at 38 min 29 s in DZ1. The fire ignites the 29 vehicles located in the covered part of the deck, but it does not propagate to the entire deck.
- ATSFR: 7 min due to excessive RHF.
- RS and DR on the PS of the weather deck remain safe for most of the fire, except for short-lived and low-level peaks in the time evolutions of gas temperature and soot volume fractions. Moreover, people could be exposed to an incident RHF greater than 2.5 kW/m² from 21 min of fire and up to 56 min.
  RS on the starboard side is always safe, but the path to get there could be exposed to an excessive RHF.
  The LSA located on the 1st house deck begin to be touched by a fire induced RHF greater than 2.5 kW/m² from 20 min. Figure 60 shows the field of RHF in the LSA after 1 h of fire.

Table 14: Scenario MS8: simulation results. SWI means Swift detection, LSA embarkation stations, DR disembarkation route, RS rescue station, SS starboard side, and PS port side. For consequences to human, the value in bold blue corresponds to the first tenability criterion that was exceeded in the areas of interest. Times are given in minutes and seconds (min's").

	DZ0	DZ1
Heat detection at 54°C	na	1'43"
Heat detection at 78°C	na	2'00"
Smoke detection	na	**0'50"**
Structure damage	na	-
Target ignition	na	3'52"
First truck ignition	23'36"	0'00"
Last truck ignition	32'54"	**38'29"**
no of trucks ignited	29/80	
Predicted/Prescribed total heat content (TJ)	0.651/0.681	

Consequences to human	DZ0	DZ1	RS-SS	RS and DR-PS	LSA	SWI
RHF	**19'00"**	**6'00"**	-	**21'00"**	**20'00"**	**7'00"**
T60	37'33"	38'39"	-	38'52"	44'37"	39'35"
CO	-	-	-	-	-	-
Visibility 5m	38'28"	38'37"	-	38'46"	44'35"	41'03"
Visibility 10m	38'17"	28'11"	-	38'39"	41'11"	41'00"

na: not applicable

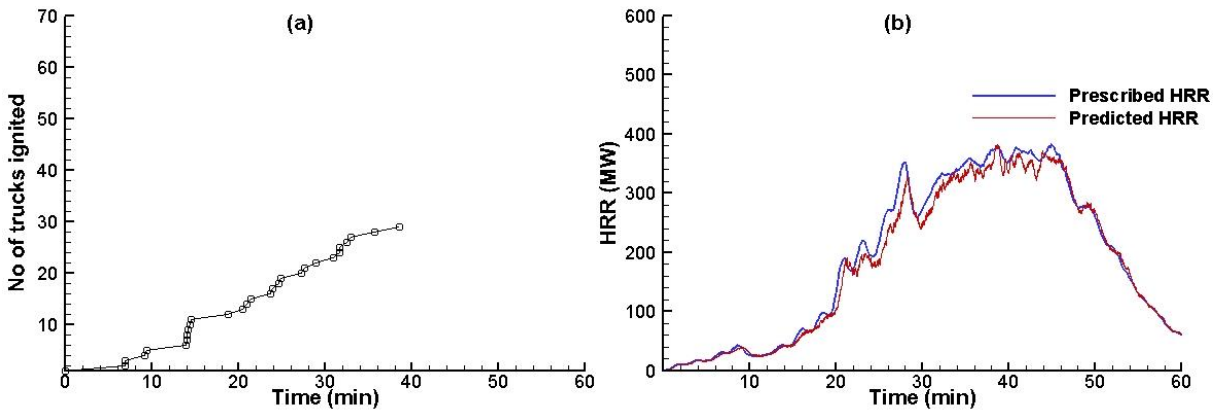

Figure 58: Scenario MS8: a) Number of truck ignited vs. time, and b) comparison between the time evolutions of the theoretical HRR (i.e., the total pyrolysis rate multiplied by the chemical heat of combustion) and effective HRR.

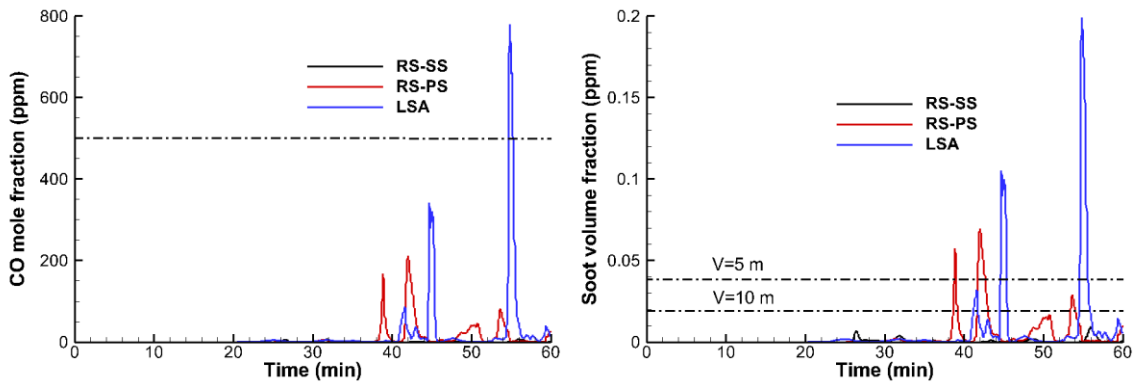

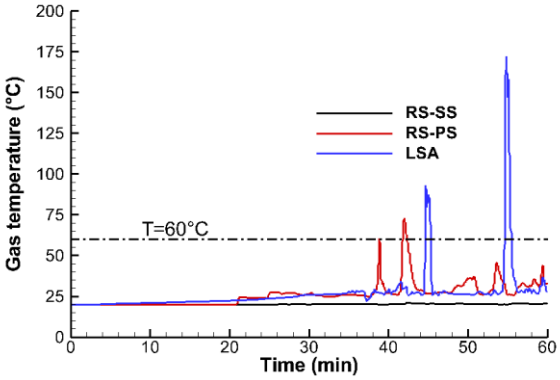

Figure 59: Scenario MS8: time evolutions of maximum CO mole fraction, gas temperature, and soot volume fraction at the monitored points in the LSA, RS and DR on both sides of the Magnolia Seaways.

Figure 60: Scenario MS8: 2D field of the incident radiative heat flux obtained at a height of 1.80 m in the LSA of the 1st house deck after 1 h of fire. Black areas correspond to areas where the radiative heat flux is greater than 2.5 kW/m².

SCENARIO MS9

Observations

As shown inTable 12, and from Figure 61 to Figure 63:

- Smoke detection occurs at 28 s in DZ4.
- Fire is out of control at 43 min 5 s in DZ3.
- ATSFR: 4 min due to excessive RHF.
- All the cargo in DZ2 and DZ3 is ignited in less than 52 min, as well as targets in just over 50 min. 61 trucks are ignited out of the 70 located in the upper deck. The structure is damaged in all drencher zones of this deck.
- No fire spread to upper deck due to external flames.
- Fire can spread to the weather deck through the uninsulated ceiling as the floor temperature exceeds locally 600°C, which is significantly higher than the ignition temperature of vehicle tires.
- RS and DR on the port side of the weather deck are safe for approximately the first 19 min of fire. After this time, tenability criteria are exceeded in these areas.

From 48 min of fire, the RS on the starboard side is exposed to an excessive incident RHF. After 1 h of fire, all areas likely to be used for evacuation are unusable (see for example, the RHF in Figure 63).

LSA on the 1st house deck are safe for approximately the first 7 min of fire. After this time, tenability criteria are largely exceeded.

Table 15: Scenario MS9: simulation results. SWI means Swift detection, LSA embarkation stations, DR disembarkation route, and RS rescue station. For consequences to human, the value in bold blue corresponds to the first tenability criterion that was exceeded in the areas of interest. Times are given in minutes and seconds (min's").

	DZ2	DZ3	DZ4	DZ5
Heat detection at 54°C	7'40"	5'34"	2'02"	4'47"
Heat detection at 78°C	10'15"	7'15"	2'31"	7'49"
Smoke detection	2'53"	1'39"	**0'28"**	1'33"
Structure damage	52'02"	41'10"	11'05"	42'01"
Target ignition	50'10"	25'34"	5'57"	30'23"
First truck ignition	40'22"	15'03"	0'00"	21'12"
Last truck ignition	51'42"	**43'05"**	-	-
no of trucks ignited	61/70			
Predicted/Prescribed total heat content (TJ)	1.121/1.150			

Consequences to human	DZ2	DZ3	DZ4	DZ5	RS-SS	RS and DR-PS	LSA	SWI
RHF	46'00"	25'00"	**7'00"**	30'00"	**48'00"**	25'00"	34'00"	**4'00"**
T60	28'34"	36'13""	32'57"	25'00"	-	29'29"	21'06"	32'54"
CO	28'08"	52'19"	33'23"	14'40"	-	38'10"	36'32"	33'01"
Visibility 5m	5'08"	16'28"	11'27"	4'33"	-	21'00"	8'50"	16'04"
Visibility 10m	**4'53"**	**6'29"**	10'21"	**4'16"**	-	**19'26"**	**7'18"**	15'20"

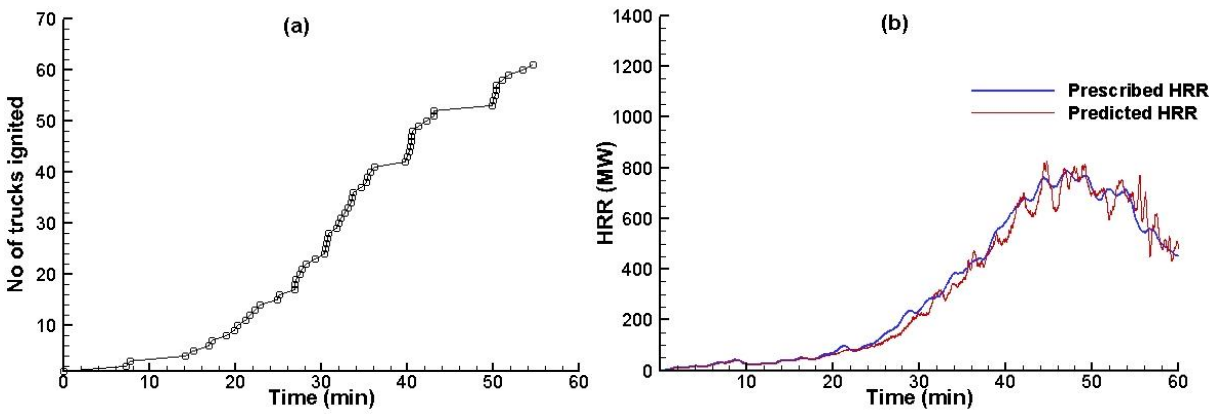

Figure 61: Scenario MS9: a) Number of truck ignited vs. time, and b) comparison between the time evolutions of the theoretical HRR (i.e., the total pyrolysis rate multiplied by the chemical heat of combustion) and effective HRR.

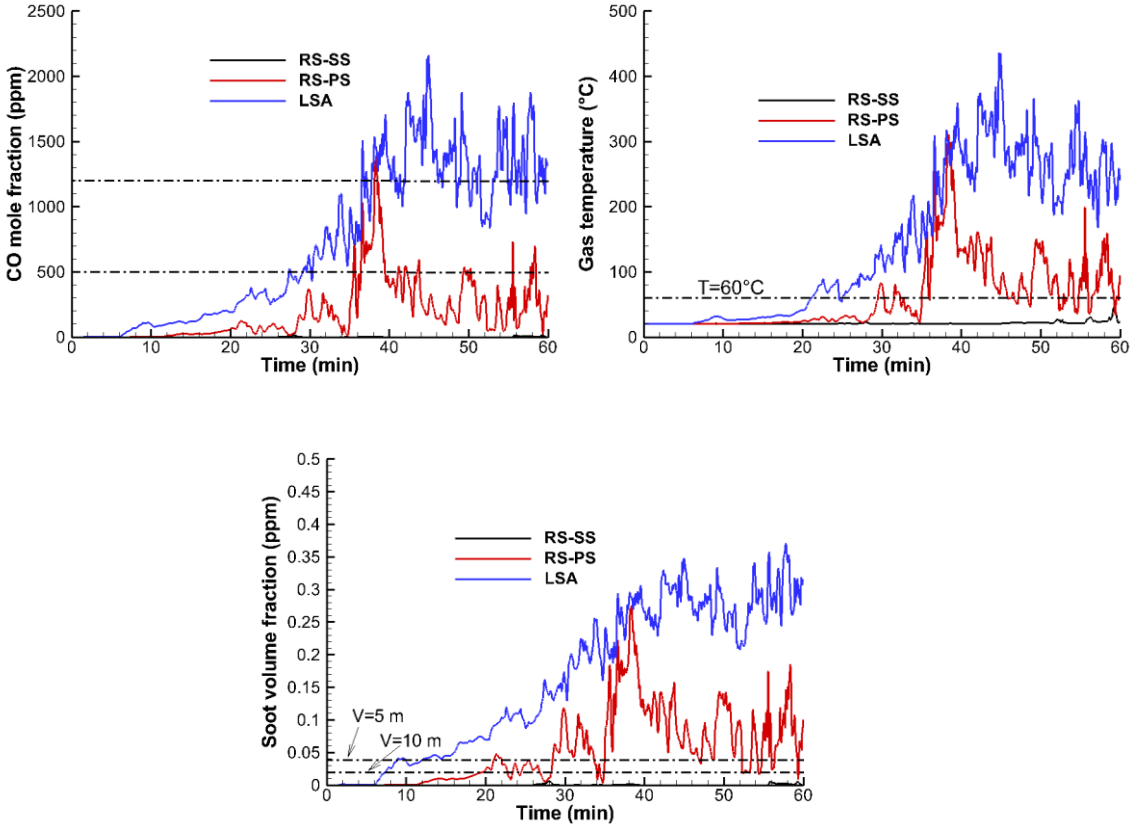

Figure 62: Scenario MS9: time evolutions of maximum CO mole fraction, gas temperature, and soot volume fraction at the monitored points in the LSA, RS and DR on both sides of the Magnolia Seaways.

Figure 63: Scenario MS9: 2D field of the incident radiative heat flux obtained at a height of 1.80 m in the LSA of the 1st house deck after 1 h of fire. Black areas correspond to areas where the radiative heat flux is greater than 2.5 kW/m².

SCENARIO MS10

Observations

As shown in Table 16, and from Figure 64 to Figure 66:

- Smoke detection occurs at 28 s in DZ4.
- Fire is out of control at 57 min 43 s in DZ3.
- ATSFR: 2 min 8 s due to degraded visibility.

- All the cargo in DZ3 is ignited in less than 58 min. Targets are ignited in all drencher zones of the upper deck, except in DZ2 due to under-ventilated conditions. 61 trucks are ignited out of the 70 located in the upper deck. The structure is damaged in DZ3 and DZ4 only.
- No fire spread to target cars on upper decks due to external flames.
- Fire can spread to the weather deck through the uninsulated ceiling as the floor temperature exceeds locally 571°C, which is significantly higher than the ignition temperature of vehicle tires.
- Regarding CO, gas temperature and soot concentration, the RS and DR are safe throughout the fire. In contrast, the 18-knot headwind pushes smoke toward the LSAs, making these areas unsafe as early as 6 min 32 s of fire.
- RS and DR on the PS of the weather deck remain safe for the first 19 min of fire; after this time, they are exposed to an excessive RHF.

Visibility is reduced to 10 m from 6 min 32 s in the LSA on the 1st house deck. Then, the LSA are exposed to excessive heat and smoke levels.

RS on the SS of the weather deck is always safe, but the route to get there could be exposed to excessive RHF.

Table 16: Scenario MS10: simulation results. SWI means Swift detection, LSA embarkation station, DR disembarkation route, and RS rescue station. For consequences to human, the value in bold blue corresponds to the first tenability criterion that was exceeded in the areas of interest. Times are given in minutes and seconds (min's").

	DZ2	DZ3	DZ4	DZ5
Heat detection at 54°C	10'23"	8'14"	1'38"	5'01"
Heat detection at 78°C	15'35"	11'33"	1'45"	5'53"
Smoke detection	2'26"	1'41"	**0'28"**	1'03"
Structure damage	-	36'05"	17'56"	-
Target ignition	-	17'35	6'19"	27'52"
First truck ignition	40'13"	8'30"	0'00"	19'28"
Last truck ignition	-	**57'43"**	-	-
no of trucks ignited	61/70			
Predicted/Prescribed total heat content (TJ)	0.932/1.027			

Consequences to human	DZ2	DZ3	DZ4	DZ5	RS-SS	RS and DR-PS	LSA	SWI
RHF	47'00"	18'00"	6'00"	28'00"	-	**19'00"**	20'00"	7'00"
T60	20'41"	21'43"	13'21"	20'04"	-	-	17'42"	10'59"
CO	13'47"	13'35"	19'05"	21'55"	-	-	30'00"	19'05"
Visibility 5m	5'24"	6'31"	5'04"	4'43"	-	-	8'08"	4'48"
Visibility 10m	**4'56"**	**5'30"**	**2'12"**	**4'00"**	-	-	**6'32"**	**2'08"**

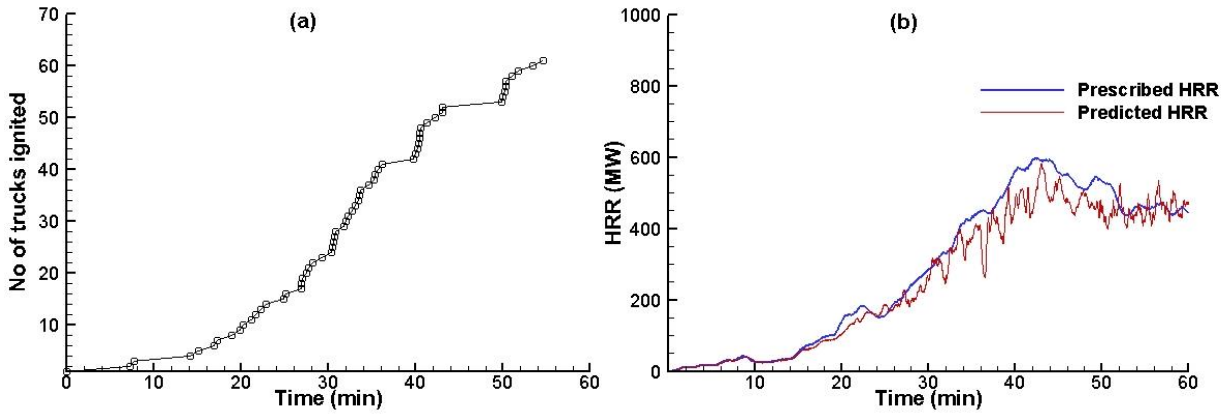

Figure 64: Scenario MS10: a) Number of truck ignited vs. time, and b) comparison between the time evolutions of the theoretical HRR (i.e., the total pyrolysis rate multiplied by the chemical heat of combustion) and effective HRR.

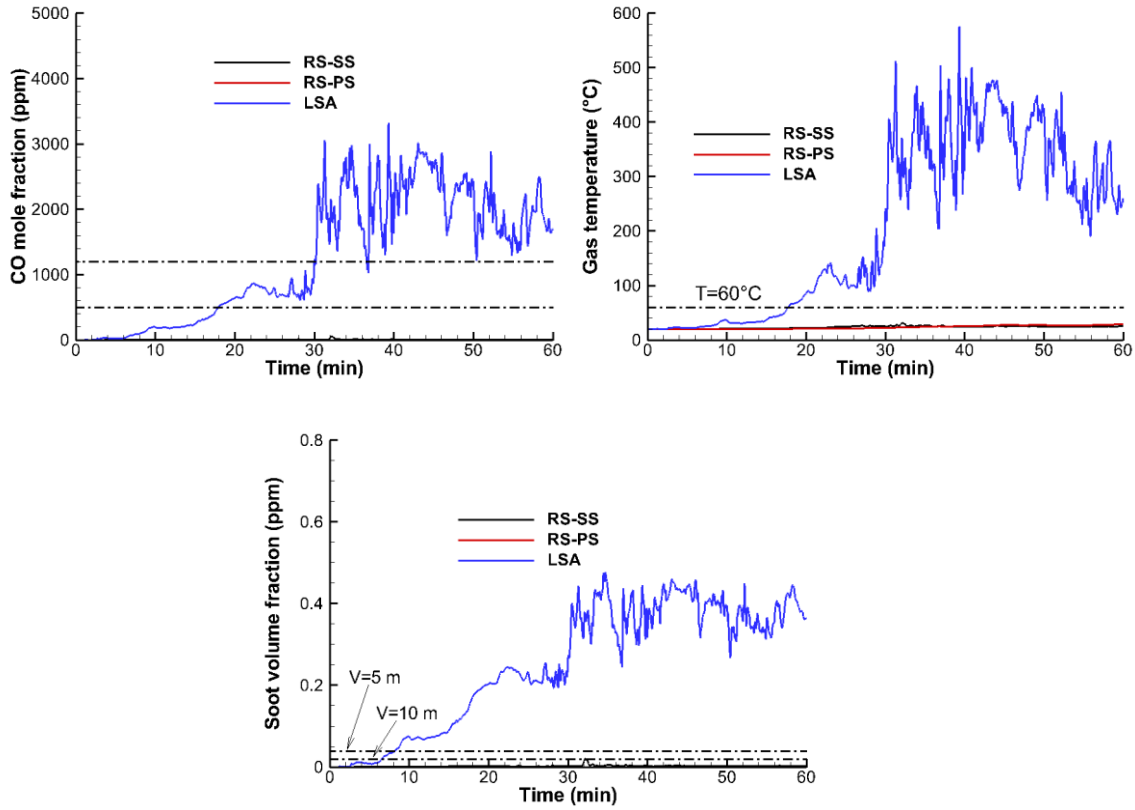

Figure 65: Scenario MS10: time evolutions of maximum CO mole fraction, gas temperature, and soot volume fraction at the monitored points in the LSA, RS and DR on both sides of the Magnolia Seaways.

Figure 66: Scenario MS10: 2D field of the incident radiative heat flux obtained at a height of 1.80 m in the LSA of the 1st house deck after 1 h of fire. Black areas correspond to areas where the radiative heat flux is greater than 2.5 kW/m².

SCENARIO MS11

Observations

As shown in Table 17, and from Figure 64 to Figure 66:

- Smoke detection occurs at 28 s.
- ATSFR: 4 min 2 s due to degraded visibility.
- Due to under-ventilated conditions, only 3 trucks out of the 20 in the lower hold are ignited and no structure damage is observed. Target ignition occurs in less than 6 min of fire.
- Fire can spread to the upper deck through the uninsulated ceiling as the floor temperature reaches locally 414°C, which is significantly higher than the ignition temperature of vehicle tires.
- Although not shown, the RS, LSA, and DR remain safe for 1 h of fire, and beyond.

Table 17: Scenario MS11: simulation results. SWI means Swift detection, LSA embarkation station, DR disembarkation route, and RS rescue station. For consequences to human, the value in bold blue corresponds to the first tenability criterion that was exceeded in the areas of interest. Times are given in minutes and seconds (min's").

	DZ12				
Heat detection at 54°C	1'48"				
Heat detection at 78°C	2'09"				
Smoke detection	**0'28"**				
Structure damage	-				
Target ignition	5'48"				
First truck ignition	0'00"				
Last truck ignition	-				
no of trucks ignited	3/20				
Predicted/Prescribed total heat content (TJ)	0.020/0.074				
Consequences to human	DZ12	RS-SS	RS and DR-PS	LSA	SWI
RHF	12'00"	-	-	-	-
T60	7'16"	-	-	-	10'37"
CO	7'23"	-	-	-	8'34"
Visibility 5m	3'17"	-	-	-	5'05"
Visibility 10m	**3'00"**	-	-	-	**4'02"**

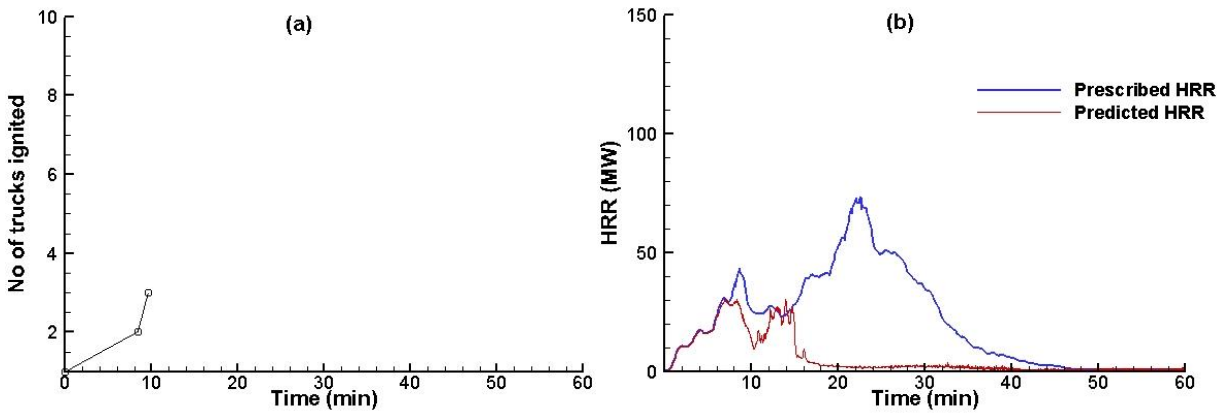

Figure 67: Scenario MS11: a) Number of truck ignited vs. time, and b) comparison between the time evolutions of the theoretical HRR (i.e., the total pyrolysis rate multiplied by the chemical heat of combustion) and effective HRR.